

UNCLASSIFIED

AD NUMBER: AD0476627

LIMITATION CHANGES

TO:

Approved for public release; distribution is unlimited.

FROM:

Distribution authorized to U.S. Gov't. agencies and their contractors; Administrative/Operational Use, 6 Aug 1965. Other requests shall be referred to Army Missile Command, Redstone Arsenal, AL 35809.

AUTHORITY

USAMC LTR 23 AUG 1971

118710

REPORT NO. 1026
COPY NO.



**DEVELOPMENT OF AN ALL FLUID
PNEUMATIC PRESSURE REGULATOR**

Monthly Progress Report

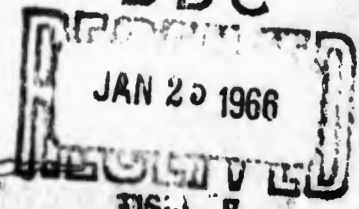
(Phase I Summary)

LIBRARY COPY

OCT 27 1965

LANGLEY RESEARCH CENTER
LIBRARY, NASA
LANGLEY STATION
HAMPTON, VIRGINIA

DDC



31614 E



RESEARCH LABORATORIES DIVISION
SOUTHFIELD, MICHIGAN

AD NO. 476627

DDC FILE COPY

28635

FOREWORD

This report was prepared by the Research Laboratories Division of The Bendix Corporation for the U. S. Army Missile Command under Contract DA 01-021-AMC-11905(Z). The project is under the technical direction of AMC Project Engineer, Mr. B. J. Clayton.

Bendix

ABSTRACT

→ The requirements of an all-fluid pneumatic pressure regulator have been investigated and recommendations for a design have been made. The three major pressure regulator subsystem functions are (1) throttling, (2) feedback signal transfer, (3) reference, or error detection. The primary recommendation is that the throttling function be performed by a vortex valve supplied from a dual volume storage bottle. This represents the ideal all-fluid approach. The alternate recommendation is that throttling be performed with a vortex-controlled mechanical element. This avoids the volume penalty associated with the dual volume tank. With either approach, the feedback function can be performed with a circuit using confined jet amplifiers which combine a high supply pressure recovery with a low control to supply pressure ratio. A reference circuit distinct from the feedback circuit may not be required. ↗

TABLE OF CONTENTS

	<u>Page</u>
SECTION 1 - INTRODUCTION	1-1
SECTION 2 - INVESTIGATION OF METHODS FOR ALL FLUID PRESSURE REGULATION	2-1
2.1 Requirement, Concept, and Subsystem Functions	2-1
2.1.1 AMC Technical Requirement No. 715 -- Summary	2-1
2.1.2 Concept and Subsystem Functions	2-1
2.1.3 Throttling	2-2
2.1.4 Feedback	2-3
2.1.5 Pressure Reference	2-4
2.2 Throttling Methods	2-4
2.2.1 General Description of Vortex Valves	2-4
2.2.2 Single-Stage Vortex Throttling Valve	2-7
2.2.3 Multiple-Stage Vortex Throttling Valve	2-14
2.2.4 Vortex Throttling Valve with Vortex Pilot Valve	2-19
2.2.5 Vortex Controlled Throttling Valve with Mechanically Variable Area	2-25
2.2.6 Dual Volume Gas Bottle	2-28
2.3 Feedback Methods	2-31
2.3.1 Performance of Confined-Jet Amplifiers	2-31
2.3.2 Confined-Jet Amplifiers with Vortex Control Valves	2-33
2.3.3 Parallel-Staged Confined-Jet Feedback Amplifiers	2-33
2.4 Reference Methods	2-41
2.4.1 Single Versus Multiple-Orifice Bridge	2-41
2.4.2 Reference Circuit Using Jet-on-Jet Amplifiers	2-45
2.4.3 Inherent Reference of Feedback Amplifiers	2-48
SECTION 3 - SUMMARY OF RESULTS, CONCLUSIONS, AND RECOMMENDATIONS	3-1
3.1 Summary of Results	3-1
3.1.1 Throttling Methods	3-1
3.1.2 Feedback Methods	3-2
3.1.3 Reference Methods	3-2

Bendix

	<u>Page</u>
3.2 Conclusions	3-2
3.3 Recommendations	3-3
APPENDIX A - NOTATION FOR SECTIONS 1 THROUGH 3	A-1
APPENDIX B - THEORETICAL ANALYSIS OF VORTEX VALVES	B-1
APPENDIX C - BREADBOARD COMPONENTS	C-1
APPENDIX D - FLOW CHARACTERISTICS OF n ORIFICES IN SERIES	D-1

LIST OF ILLUSTRATIONS

<u>Figure No.</u>	<u>Title</u>	<u>Page</u>
2-1	Regulator Concept and Subsystem Functions	2-2
2-2	Elementary Vortex Valve Configuration and Nomenclature	2-5
2-3	Static Performance Characteristics of Vortex Valves	2-6
2-4	Schematic Symbol for Vortex Valves	2-7
2-5	Single-Exit Valve Performance	2-8
2-6	Double-Exit Vortex Valve Performance	2-10
2-7	Single-Stage Vortex Throttling Element with Part of the Gas Supply Stored at Higher Pressure for Control Purposes	2-12
2-8	Single-Stage Vortex Throttling Element with Restriction in the Supply Line to Achieve Control from a Single Storage Bottle	2-12
2-9	Determination of Supply Pressure Requirements for Single-and-Multiple Orifice Restriction in the Supply Line of a Vortex Throttling Valve	2-13
2-10	Staging Analysis - Schematic and Notation	2-15
2-11	Normalized Flow-Pressure Characteristics	2-15
2-12	Output Configuration for Vortex Pilot Valve	2-19
2-13	Pilot Configuration of Cascaded Vortex Valve	2-20
2-14	Two-Stage Piloted Vortex Valve Performance	2-21
2-15	Two-Stage Piloted Vortex Valve Performance	2-22
2-16	Throttling Circuit Test	2-23
2-17	Two-Stage Piloted Vortex Valve Performance	2-23
2-18	Two-Stage Piloted Vortex Valve Performance (Positive Feedback)	2-24
2-19	Two-Stage Piloted Vortex Valve Performance (Positive Feedback)	2-24
2-20	Vortex Regulator Element	2-25
2-21	Dual Pressure Bottle System	2-29
2-22	Confined-Jet Amplifier Configuration and Schematic Symbol	2-31
2-23	Confined-Jet Amplifier Test and Receiver Configurations	2-32

Bendix

<u>Figure No.</u>	<u>Title</u>	<u>Page</u>
2-24	Confined-Jet Amplifier Performance - Receiver A	2-34
2-25	Confined-Jet Amplifier Performance - Receiver B	2-35
2-26	Confined-Jet Amplifier Performance - Receiver C	2-36
2-27	Confined-Jet Amplifier Performance - Receiver D	2-37
2-28	Confined-Jet Amplifier Performance - Receiver A	2-38
2-29	Single-Stage Feedback Amplifier Test Schematic	2-39
2-30	Single-Stage Feedback Amplifier Performance; No Feedback	2-39
2-31	Single-Stage Feedback Amplifier Performance; Positive Feedback	2-40
2-32	Parallel-Staged Feedback Amplifier Test-Two Stages	2-41
2-33	Two-Stage Feedback Amplifier Performance	2-42
2-34	Two-Stage Feedback Amplifier Interstage Pressures Corresponding to Figure 2-33	2-43
2-35	Two-Stage Feedback Amplifier Performance with Output Load	2-44
2-36	Flow Function for Orifices in Series	2-46
2-37	Single Versus Multiple Orifice Bridge	2-46
2-38	Reference Circuit Test Schematic	2-47
2-39	Reference Circuit Switching Characteristic	2-47
3-1	Schematic of System with Dual Volume Tank	3-4
3-2	Schematic of Pressure Regulator with Mechanical Element	3-4
B-1	Simple Vortex Chamber	B-1
B-2	Vortex Chamber Characteristic Curves with Regulated Supply	B-2
B-3	Vortex Chamber Characteristic Curves with Regulated Control	B-4
B-4	Vortex Chamber Maximum Flow Discharge Coefficient	B-4
B-5	Characteristic Curves of Vortex Chamber Center Pressure, P_1	B-6

<u>Figure No.</u>	<u>Title</u>	<u>Page</u>
B-6	Determination of $\frac{P_1}{P_e}$ from Weight Flow Characteristic Curves	B-6
B-7	Operation of Vortex Valve with Exit Hole. Flow Sonic	B-8
B-8	Vortex Tangential Velocity Distribution	B-10
B-9	Assumed Tangential Velocity Profile for Gases	B-11
B-10	Gas Flow Functions	B-14
B-11	Momentum Function - $f_3 \frac{P_o}{P_c}$	B-15
B-12	Theoretical-Experimental Correlation P_o/P_e	B-18
B-13	Maximum Tangential Mach Number Versus P_c/P_e	B-19
C-1	Typical Vortex Valve Components	C-3
C-2	Control Injector Plate	C-3
C-3	Throttling Circuit Assembly	C-4
C-4	Confined-Jet Amplifier Components	C-4
D-1	Orifice and Pressure Notation	D-1
D-2	Critical Pressure Ratio for Equal Orifices in Series as a Function of the Number of Orifices $k = 1.4$	D-4

Table No.

D-1	Nondimensional Effective Areas of Equal Orifices in Series for Various Pressure Ratios	D-5
-----	--	-----

Bendix

SECTION 1

INTRODUCTION

This is the fourth progress report prepared under Phase I of this project. Since this is the final progress report of Phase I, it has been written as a Phase I summary report and therefore supercedes the previous monthly progress reports, Bendix Research Laboratories Division reports 2942 (13 April 1965), 2963 (1 May 1965), and 3005 (11 June 1965).

Section 2 of this report reviews the pressure regulator requirements and describes the subsystem functions required to satisfy these requirements. Each of the subsystem requirements is then examined in detail and methods of performing the function are explored.

Section 3 summarizes the results of Phase I, exhibits the principal conclusions, and recommends the approach to be developed during Phase II. Two different approaches have been found to be feasible; the first, a primary recommendation, is based on a dual volume gas storage bottle; and the secondary, is based upon the use of a mechanical variable area element.

Appendix A gives the notation used in the main body of the report. Appendix B presents a somewhat more detailed analysis and description of the vortex valve. Appendix C describes the components used in the experimental portion of the work. Finally, Appendix D describes the pneumatic flow characteristics of a series of n identical orifices.

SECTION 2

INVESTIGATION OF METHODS FOR ALL FLUID PRESSURE REGULATION

2.1 REQUIREMENT, CONCEPT, AND SUBSYSTEM FUNCTIONS

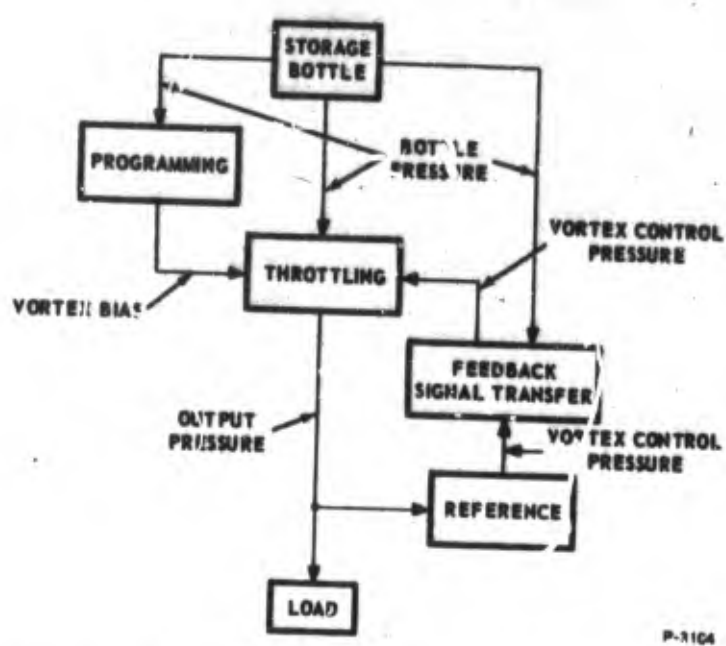
2.1.1 AMC Technical Requirement No. 715 -- Summary

The regulator concept being investigated is based upon the use of vortex type fluid elements to deliver a constant output pressure from a variable supply pressure. The objective of the investigation is to determine the feasibility of regulating the pressure of gas supplied to an all fluid missile control system from a pressurized gas storage bottle without the use of conventional mechanical regulators. The gas (air or nitrogen) is to be stored at 1000 psig. The function of the regulator is to deliver a constant pressure of 15 psig to a fixed load orifice of 0.02 in² while the supply pressure decreases from 1000 to 100 psig. A variation of plus or minus 1.5 psi is allowed, and the flow through the load orifice is sonic for all allowable output pressures.

2.1.2 Concept and Subsystem Functions

The three subsystem functions required to provide closed-loop regulation are: (1) throttling the flow of gas from the storage bottle. (2) reference or comparison of the output pressure with the desired output pressure, and (3) the transfer of feedback signals to exercise control of the throttling elements as a function of the deviation of the output pressure from the desired pressure. Although the term "regulator" implies the use of feedback, it is not necessary (at least in principle) to use feedback to satisfy the requirements of the regulator. An alternative approach is to program the effective area of the throttling element as a function of the storage bottle pressure. This concept uses the fact that, because the load orifice is sonic and the area is fixed, the regulator would ideally deliver a constant flow to the load. The effective area of the throttling element must, therefore, vary in inverse proportion to the bottle absolute pressure, and this variation could be programmed without feedback. This investigation is centered on the application of closed-loop control in anticipation of future AMC regulator requirements with variable

Bendix



P-1104

Figure 2-1 - Regulator Concept and Subsystem Functions

load conditions, but a combination of open-loop programming with feedback control is thought to offer the potential advantages of both approaches. The interconnection of subsystem functions in the regulator is represented in Figure 2-1.

2.1.3 Throttling

The required nominal load flow at 15 psig output pressure is

$$\begin{aligned}
 w_L^* &= (C_D C_2 / T^{1/2}) A_L P_R \\
 &= ((1)(0.532) / (530)^{1/2})(0.02)(29.7) \quad (2-1) \\
 &= 0.0138 \text{ lb/sec}
 \end{aligned}$$

where the coefficient of discharge for the load orifice is assumed to be one. The effective area of the throttling element must increase to 8.0 times its initial value, as the bottle pressure decreases from 1015 to

115 psia and the regulated pressure from 31.2 to 28.2 psia, to satisfy the equation

$$\begin{aligned}\dot{w}_T &= (C_D C_2/T^{1/2}) A_T P_S \\ &= \dot{w}_L^* \\ &= (C_D C_2/T^{1/2}) A_L P_R\end{aligned}\tag{2-2}$$

The extreme effective areas of the throttling element must be

$$A_T \Big|_{P_B = 1015} = \frac{A_L P_{R \max}}{P_B \max} = 0.000615 \text{ in}^2$$

and

$$A_T \Big|_{P_B = 115} = \frac{A_L P_{R \min}}{P_B \min} = 0.0049 \text{ in}^2$$

Taking a discharge coefficient of 0.8 for the effective throttling orifice gives an effective diameter range of 0.031 to 0.088 inch.

2.1.4 Feedback

The pressure signal output from the reference element must be capable of changing the impedance (or effective area) of the throttling element. Vortex valves require control pressures greater than the supply pressure so feedback signal transfer devices must operate at bias ratios (output/input) near 1000/20 - 50/1 when the bottle pressure is a maximum and the output of the pressure reference is 20 psia. This does not imply that the perturbation signal amplification must be 50; the amplification required for the feedback signal transfer will depend on the loop gain required for the regulator and the distribution of this gain between the reference, feedback, and throttling elements.

The output bias of the feedback amplifier must track the required throttling element control pressure to within its perturbation signal range. By feedback "amplifier" we mean all of the elements required to perform the function of feedback signal transfer from the reference element output pressure to the throttling element control pressure.

800-418

2.1.5 Pressure Reference

The deviation of the output pressure from the desired value must be sensed to provide an input to the feedback amplifier. The pressure reference may require separate devices for this function alone, or the reference function may be an intrinsic part of the characteristics of the first (low pressure) stage of the feedback amplifier. In either case, it is necessary to provide a means of manually adjusting the regulated pressure. The output pressure is a "gage" pressure so the reference function is relative to the regulator ambient pressure.

2.2 THROTTLING METHODS

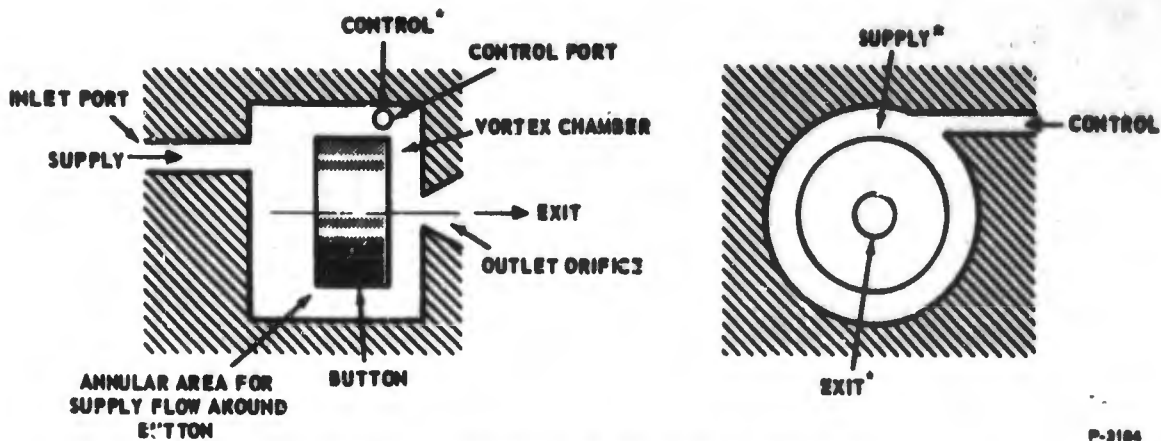
2.2.1 General Description of Vortex Valves

Vortex valves are the only all fluid devices that exhibit a variable and controlled impedance. The performance of vortex valves will, therefore, govern the feasibility of the throttling function required for the regulator.

The impedance of vortex valves is produced by a combination of the pressure-flow characteristics of orifices and the radial pressure distribution in a vortex flow; the variable impedance is induced by control of the tangential velocity of the vortex field. A detailed analysis of the valve operation is given in Appendix B. In this section, only the salient characteristics that determine the effectiveness of vortex valves in the regulator throttling application are described from the viewpoint of input-output characteristics. The geometry and nomenclature of Bendix' vortex valves will be introduced as these characteristics are described.

The elementary vortex valve configuration is shown in Figure 2-2. The supply flow enters the valve inlet port and is routed to the vortex chamber through the annular space around the valve "button." In the absence of control flow, the flow is radial from the outer wall of the chamber toward the outlet orifice; then, because the pressure drop is small through the relatively large passages between the valve inlet and the outlet orifice, the flow through the valve is determined by the supply pressure, exit pressure, and the area of the outlet orifice in the equation

$$\dot{w}_o = (C_D C_2 / T^{1/2}) A_e P_S f_1(P_e / P_S) \quad (2-3)$$



* THESE FLOWS ARE NORMAL TO THE PLANE OF THE PAPER

P-3184

Figure 2-2 - Elementary Vortex Valve Configuration and Nomenclature

When the control port pressure is higher than the pressure at the outer wall of the vortex chamber, a control flow enters the chamber tangentially and produces a vortex flow. The vorticity of the combined supply and control flows is determined by their relative momenta and the geometrical effectiveness of the valve design. The radial pressure distribution in the vortex chamber (and hence the pressure at the radius of the outlet orifice) is determined by the centrifugal forces on the individual elements of fluid in the vortex chamber. The flow through the valve is a function of the pressure at the radius of the outlet orifice. Therefore, the flow for a given supply pressure is determined by the control pressure through its influence on the vortex field.

The static performance characteristics of vortex valves are conveniently represented by a family of curves of flow versus supply pressure with fixed control pressure (Figure 2-3). The upper envelope of the curves of constant control pressure is the orifice flow characteristic for the outlet orifice; when $P_C < P_S$, there is no control flow or pressure drop from the outer wall of the vortex chamber to the radius of the outlet orifice. The lower bound on the curves of constant control pressure are points at which the supply flow is shut off completely and the flow through the outlet orifice of the valve is equal to the control flow. The "turndown ratio" of the vortex valve is defined as

$$\text{Turndown Ratio} = \frac{\dot{w}_o \left| P_C \leq P_S \right.}{\dot{w}_o \left| P_C \geq P_{CSC} \right.} \Bigg| P_S = \text{constant}$$

Bendix

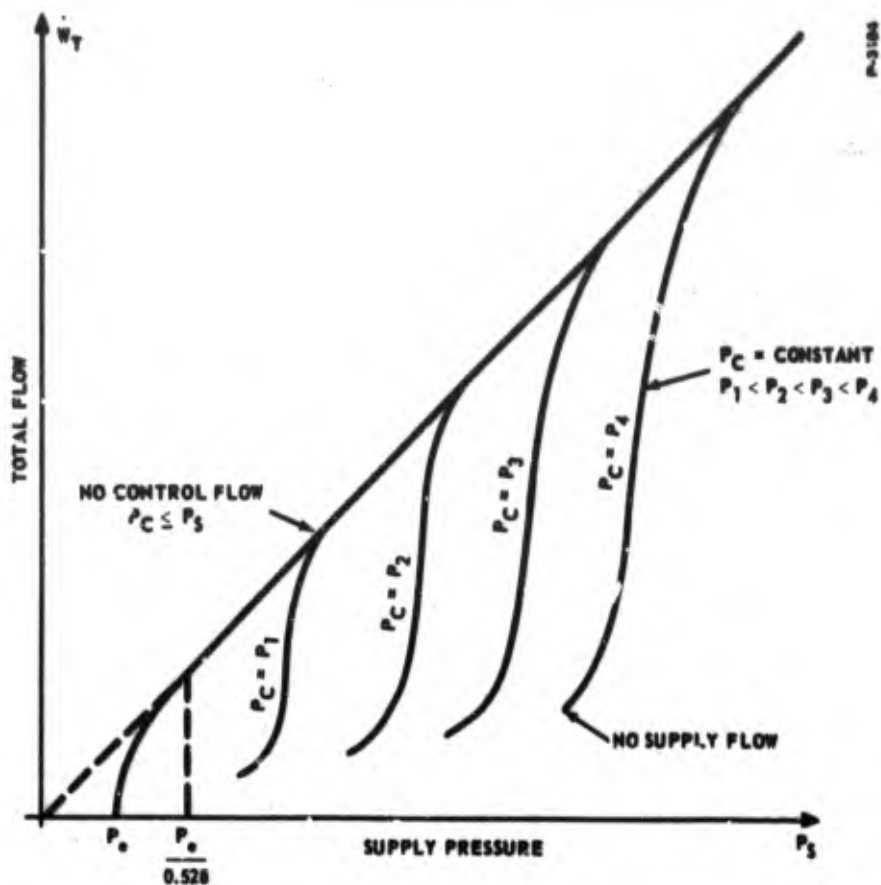
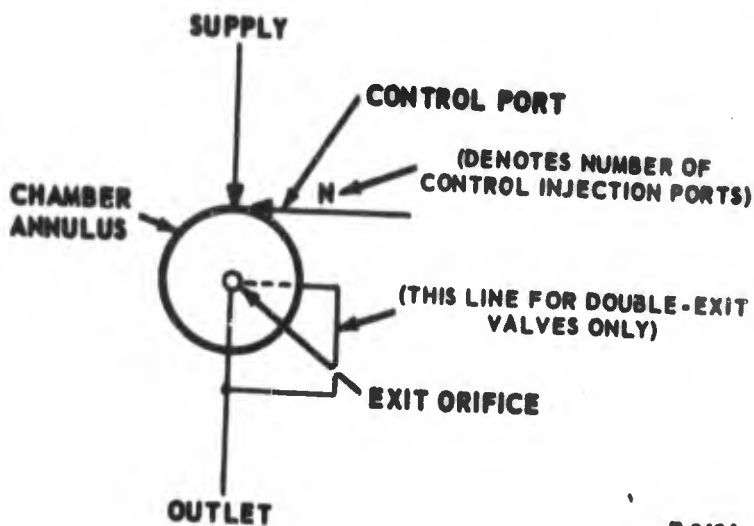


Figure 2-3 - Static Performance Characteristics of Vortex Valves

where P_{CSC} is the control pressure for supply flow cutoff at the given supply pressure. The turndown ratio is nearly independent of P_S for $P_S \gg P_e$.

The schematic symbol for vortex valves is given in Figure 2-4. The valve configurations represented by this symbol are generally more complex than that shown in Figure 2-2, but the use of multiple control ports and double-exit valves does not alter the fundamental concept of the vortex valve.



P-3184

Figure 2-4 - Schematic Symbol for Vortex Valves

2.2.2 Single-Stage Vortex Throttling Valve

Single-Exit Valve Performance -- The performance of a single-exit valve is shown in Figure 2-5. The characteristics of valves are obtained experimentally by plotting the pressure upstream of a load orifice; in Figure 2-2 the load area is equal to the required regulator load area. The pressure downstream of the load orifice is nearly atmospheric so the load flow is given approximately by $(0.014)(P_O + 15)/30$ where P_O is in psig and P_O is greater than 15. For P_O less than 15, the expression for the load flow is multiplied by $f_1(15/(P_O + 15))$. This valve has an exit orifice diameter of 0.08 inches, less than the 0.088 inches required to deliver the desired load flow at a supply pressure of 100 psig, but its performance characteristics are useful in studying the throttling function. We see that the valve will deliver the required load flow for supply pressures between 650 and 150 psig. The absolute supply pressure ratio $665/165 = 4.0$ is the same as the turndown ratio for the valve; the turndown ratio, evaluated at $P_S = 650$ psig, is $(103 + 15)/30 = 3.94$. It is evident that the supply flow must be cut off when $P_S = 650$ psig, and that a control pressure of $P_C = 750$ psig is required.

Double-Exit Valve Performance -- By adding an additional exit hole in the vortex valve button, the maximum flow capacity of the valve can be increased without a proportional increase in the control

Bendix

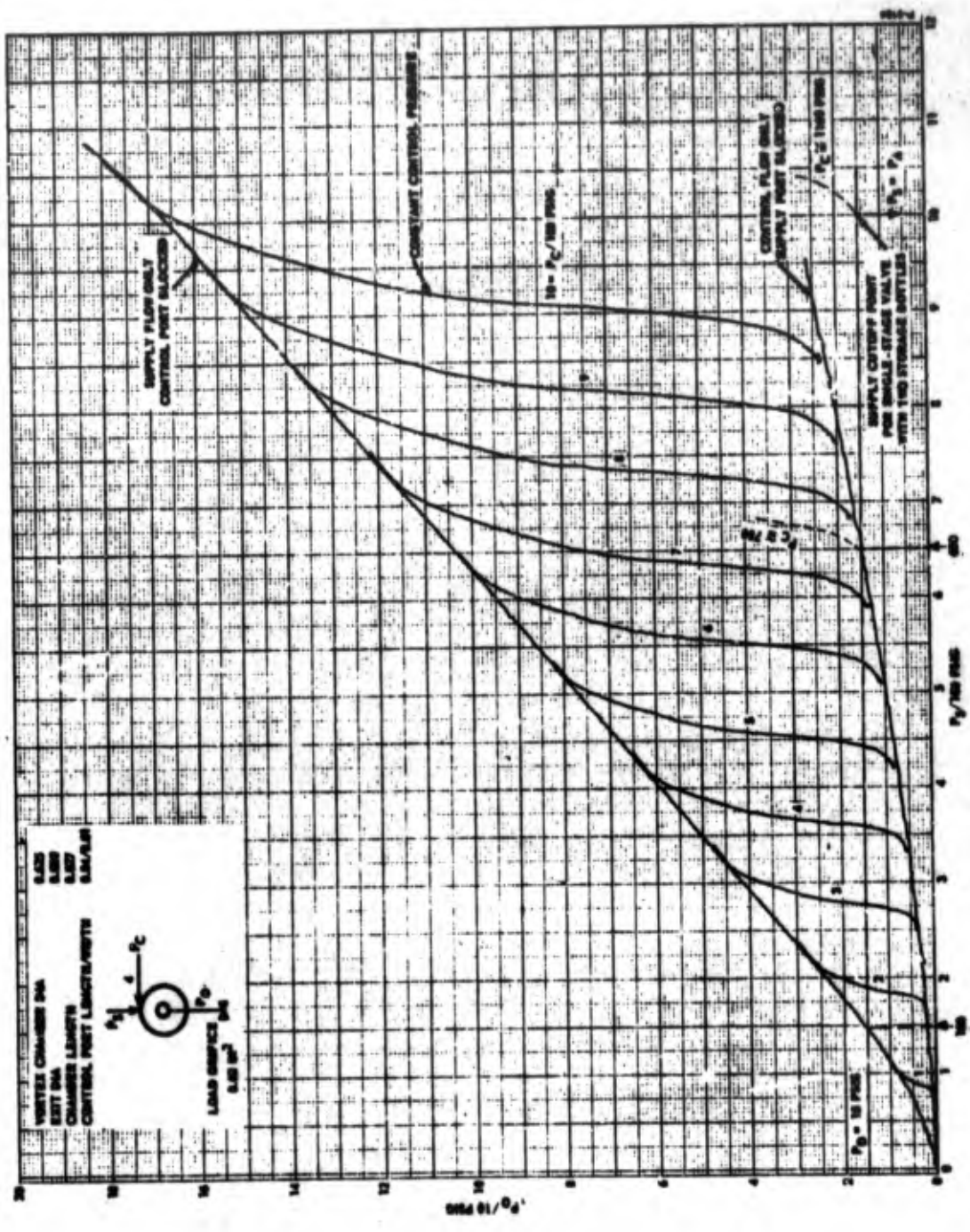


Figure 2-5 - Single-Exit Valve Performance

flow required to achieve full turndown. Figure 2-6 shows the performance of the valve with the characteristics in Figure 2-5 after conversion to a double-exit configuration. This makes the valve too large for the present application; it now delivers the required load flow between supply pressures of 425 and 50 psig. But the increased effectiveness of the double-exit configuration is demonstrated by the range of supply pressure over which the valve will deliver twice the required flow. The absolute supply pressure ratio is now $680/115 = 5.9$ which is a 50 percent improvement in supply pressure range over the single-exit configuration.

The full advantage of double-exit valves is not demonstrated in the above comparison because the modified valve did not realize the improvement in turndown capability that was expected. The turndown ratio evaluated at $P_S = 640$ psig in Figure 2-6 is 4.6 which is to be compared with the turndown of 3.9 for the single-exit valve. The slight improvement in turndown in this case is attributed to the loss of control port effectiveness that resulted when the annular clearance around the button was increased without a corresponding change in the control port. Another double-exit valve has demonstrated an 8.1/1 turndown ratio at a supply pressure of 80 psig, and there should be no change in its turndown ratio at higher pressures (no such change has been experienced in other valves). The 8.1/1 turndown ratio of this valve was confirmed prior to making the modifications in the original single-exit valve button.

Control -- To control the valve along the line of $P_O = 15$ psig in Figure 2-5, the control pressure must at least equal the supply pressure. The control pressure ratio $P_C/P_S = 1.15$ when $P_S = 650$ and decreases to 1.0 as the supply pressure decreases to 150 psig.

The simplest control scheme would be to store part of the gas at higher pressure for control purposes as illustrated in Figure 2-7. P_{BC} must be greater than P_B if the programming, reference, and feedback elements are to provide the control pressure P_C required along the line $P_R = 15$ psig in Figure 2-5. Extending this line to the right, beyond the range of the single-exit valve, we estimate the control pressure required for supply flow cutoff would be 1160 psig when the storage bottle pressure P_B is 1000 psig. If the feedback amplifier can then deliver a P_C up to about 80 percent of P_{BC} , a storage pressure of 1500 psig would be enough for the supply cutoff point at $P_B = 1000$ psig in Figure 2-5. We see that a valve with turndown ratio $181/30 = 6.0$ would provide the throttling range from $P_B = 1000$ to 150 psig. The dual storage bottle concept will be discussed further in Section 2.2.6.

Bendix

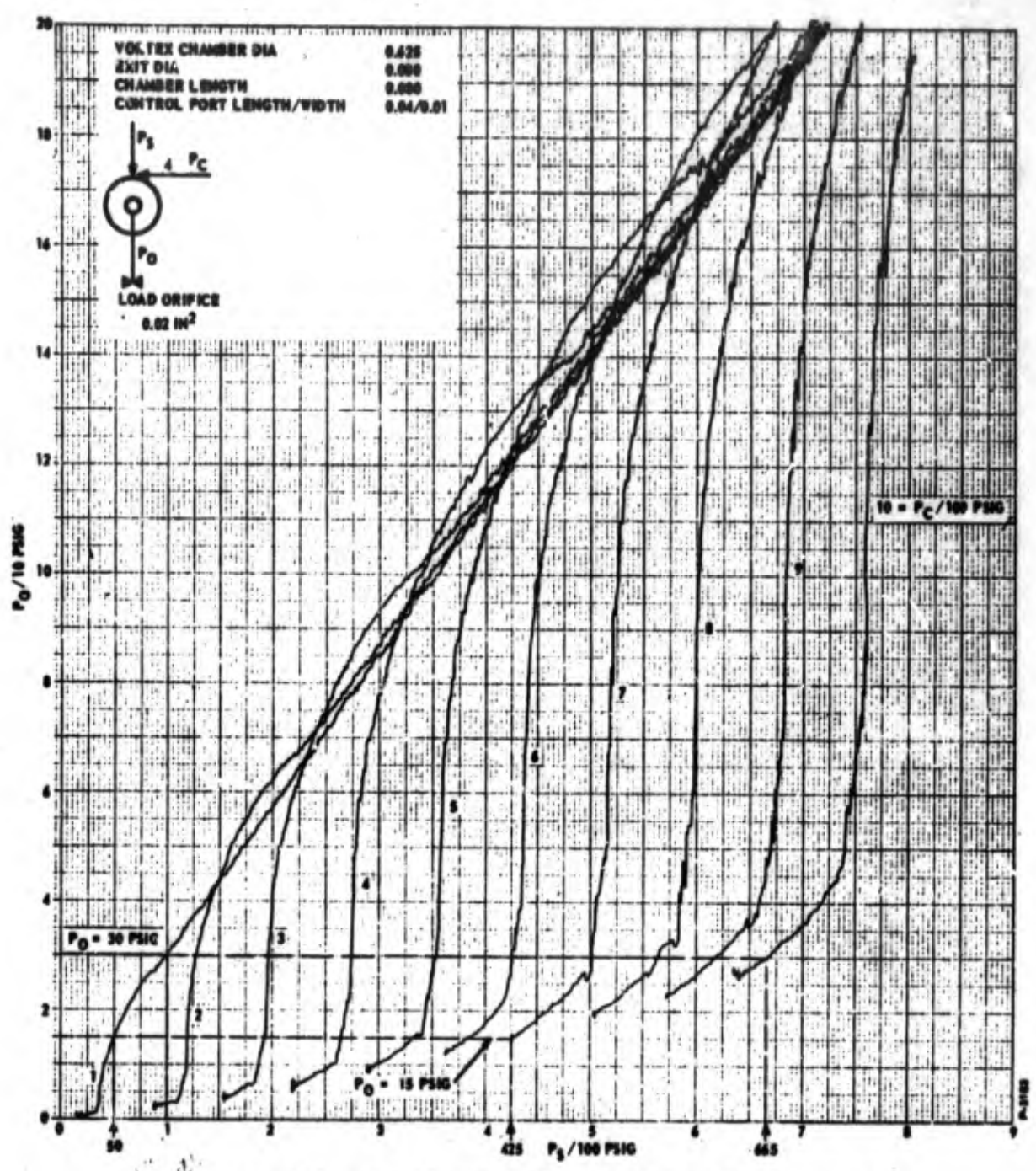


Figure 2-6 - Double-Exit Vortex Valve Performance

Another potential method of obtaining the P_C/P_S ratio required to shut off the throttling vortex valve at the higher levels of P_B would be to use a pressure dropping orifice in the supply line of the vortex valve. However, this approach can be eliminated from consideration for this application by the following analysis.

In Figure 2-8, the restriction in the supply line is represented by A_S . If the restriction is a single orifice, the supply flow is given by

$$\dot{w}_S = (C_D C_2/T^{1/2}) A_S P_B f_1 (P_S/P_B) \quad (2-4)$$

When the bottle pressure P_B is at its minimum value, the vortex valve should provide minimum impedance. This means $P_C < P_S$ so there would be no control flow \dot{w}_C at the minimum P_B . The smallest A_S that can be used must deliver the required load flow \dot{w}_L^* when $P_B = 115$ psia and the valve is "open" enough to drop P_S below the critical pressure for sonic flow through A_S . For this condition

$$\dot{w}_L^* = (C_D C_2/T^{1/2}) A_S (115) f_1 (<0.532) \quad (2-5)$$

Combining (2-4) and (2-5) gives

$$\dot{w}_S/\dot{w}_L^* = (P_B/115) f_1 (P_S/P_B) \quad (2-6)$$

This equation is plotted in Figure 2-9 to show the P_S required at higher bottle pressures to keep the supply flow $\dot{w}_S = \dot{w}_L^*$. The actual P_S required will be greater than this because, when the valve is turned down, nearly all of the flow through the valve is control flow. It is clear from Figure 2-9 that a single-orifice restriction sized to deliver the required load flow at the minimum bottle pressure would itself require a pressure ratio $P_S/P_B = 0.99$ when the bottle pressure is five times its minimum value ($P_B = 560$ psig). The pressure recovery of the output stage of practical feedback devices is less than about 80 percent of the supply pressure and $P_S/P_C < 0.8$ is required for full turndown of the vortex valve, so this method of control is restricted to applications where the inlet pressure does not drop more than about three percent of its initial value. In other words, a single-orifice restriction A_S sized to provide $P_S/P_B = 0.64$ at the maximum P_B , must become sonic when P_B decreases to 97 percent of its initial value. This is shown in Figure 2-9.

Bendix

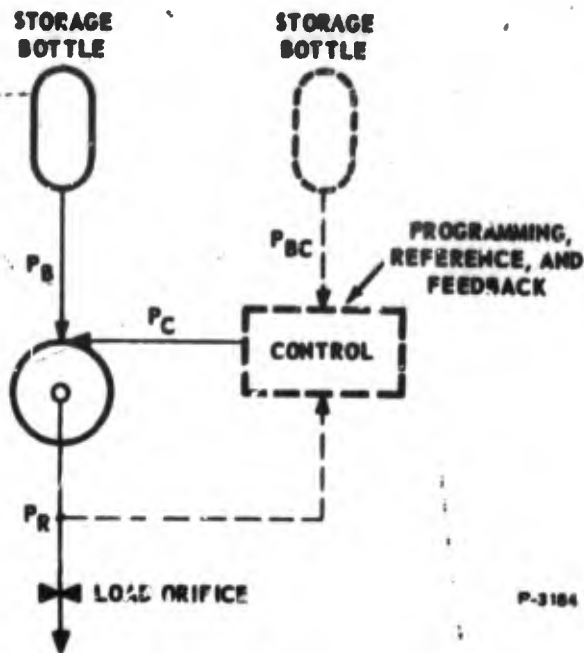


Figure 2-7 - Single-Stage Vortex Throttling Element with Part of the Gas Supply Stored at Higher Pressure for Control Purposes

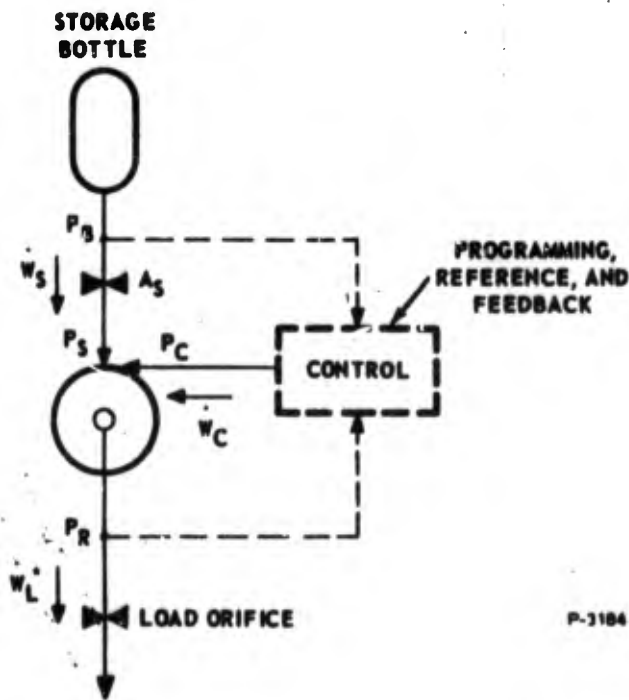


Figure 2-8 - Single-Stage Vortex Throttling Element with Restriction in the Supply Line to Achieve Control from a Single Storage Bottle

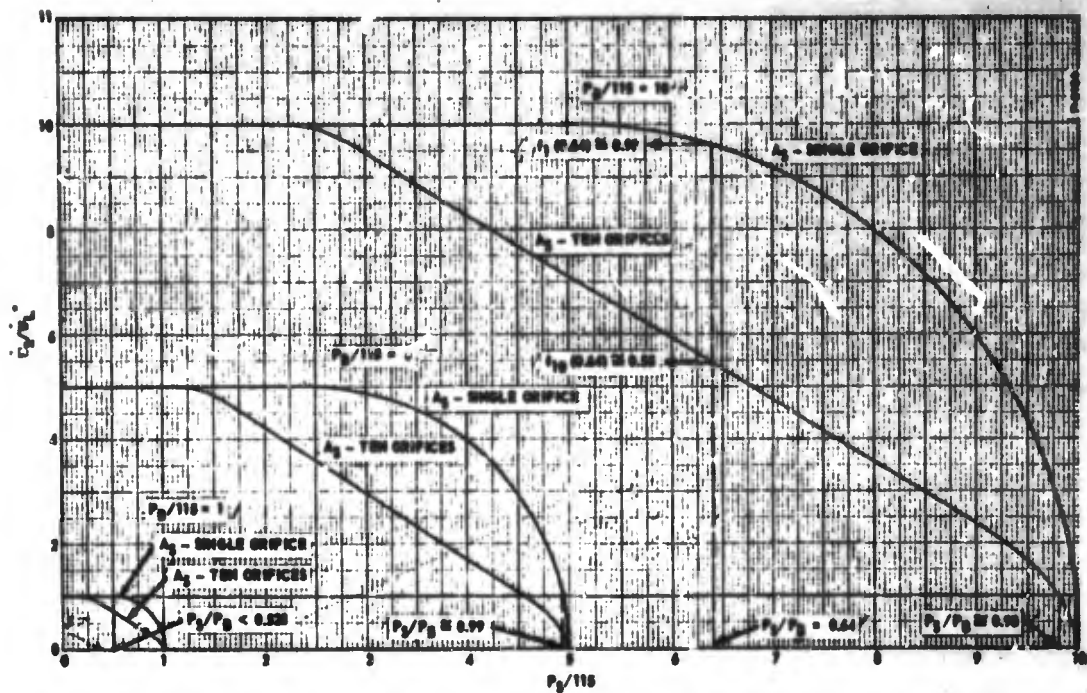


Figure 2-9 - Determination of Supply Pressure Requirements for Single-and-Multiple Orifice Restriction in the Supply Line of a Vortex Throttling Valve

Some improvement in operating range is obtained by using a series of orifices in place of a single orifice for the restriction. This is a consequence of the fact that the critical pressure ratio of a series of orifices is less than that of a single orifice. This is discussed in Appendix D. The effect of the multiple orifices can be analyzed by determining the function of P_S/P_B corresponding to $f_1 (P_S/P_B)$ used in the preceding discussion. The advantage of increasing the number of orifices n decreases rapidly for $n > 10$ so we have approximated $f_{10}(P_S/P_B)$ in Figure 2-9 to illustrate the control range obtained by using ten orifices in series. If the series of orifices is sized for an initial $P_S/P_B = 0.64$, the inlet pressure can drop to about one half of its initial value before the series of orifices begin to limit the supply flow. To obtain the throttling range required for the regulator, the pressure ratio across the series of orifices must be $P_S/P_B \approx 0.98$ when P_B is ten times its minimum value.

Although there is some advantage in using a series of orifices instead of a single orifice, a restriction in the vortex valve supply line can not be used to drop the supply pressure to the valve for control purposes in this application.

Bendix

2.2.3 Multiple-Stage Vortex Throttling Valve

The problem of providing adequate control-to-supply pressure ratios $P_C/P_S \geq 1.25$ for the throttling valve by use of a restriction in the valve's supply line was approached by allowing the restriction to be variable in the form of another vortex valve. This suggests the possibility of one or more vortex valves acting as variable impedances, and turned the investigation toward the more general question of how to stage or combine vortex valves to realize throttling performance that cannot be achieved in a single valve alone.

Figure 2-10 shows a circuit consisting of two vortex valves connected in series and indicates the pressure and flow notation. The last subscript "i" refers to the initial conditions and the last subscript "f" refers to final conditions.

Figure 2-11 gives a representation of the normalized flow-pressure characteristics of a variable pneumatic impedance. The upper curve AC represents the device "turned on," with the impedance a minimum. The lower curve BD represents the device "shut off" with the impedance a maximum.

The curves are plotted as \dot{w}_o/\dot{w}_N versus P_u/P_d where P_u/P_d is the pressure ratio, \dot{w}_o is the outlet flow, and:

$$\dot{w}_N = \frac{\Delta C_2 C_d A_e P_d}{\sqrt{T}} \quad (2-7)$$

where

$$C_2 = \sqrt{\frac{gk}{R \left(\frac{k+1}{2} \right)^{(k+1)/(k-1)}}} \quad (2-8)$$

The equation of the straight line segment A is:

$$\frac{\dot{w}_o}{\dot{w}_N} = \frac{P_u}{P_d} \quad (2-9)$$

The equation of the straight line segment B is:

$$\frac{R_t \dot{w}_o}{\dot{w}_N} = \frac{P_u}{P_d} \quad (2-10)$$

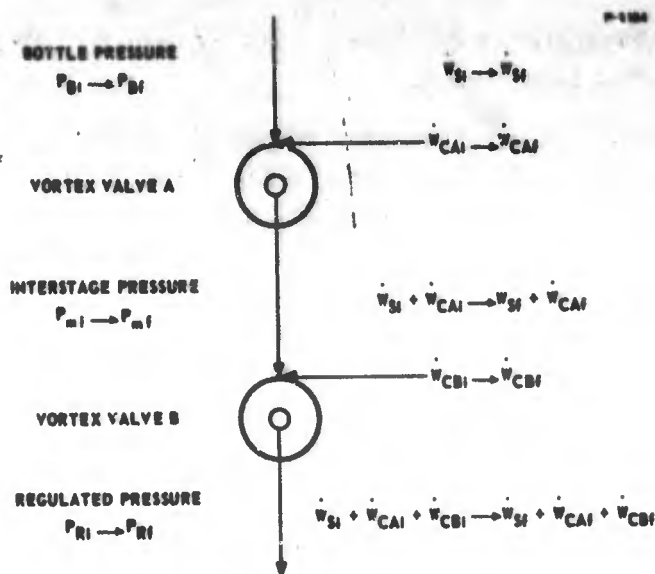


Figure 2-10 - Staging Analysis - Schematic and Notation

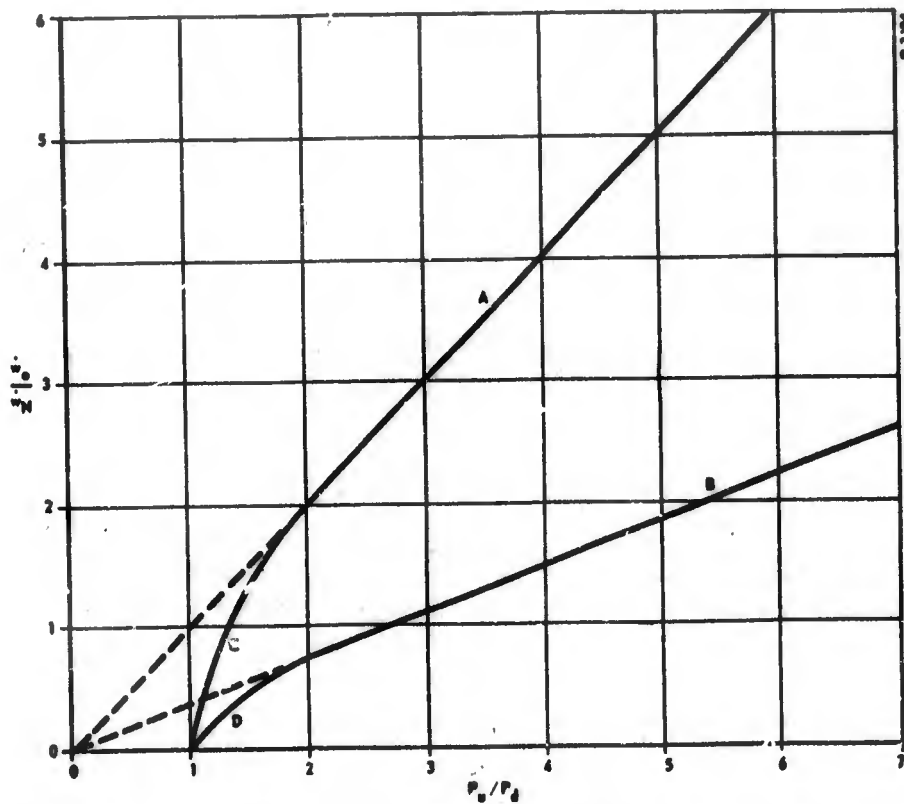


Figure 2-11 - Normalized Flow-Pressure Characteristics

Bendix

where R_t is the turndown ratio (maximum impedance divided by minimum impedance) of the device.

A rigorous description of the curved line segments C and D would be based upon the equation for the flow of a compressible fluid through an orifice or nozzle. However, it is sufficiently accurate and much more convenient to use the elliptical approximation to the compressible flow equation credited to Fleigner.* Based on this approximation, the equation for the curved line segment C is:

$$1 + \frac{1}{4} \left(\frac{w_o}{w_N} \right)^2 = \frac{P_u}{P_d} \quad (2-11)$$

Similarly the approximate equation for the curved line segment D is:

$$1 + \frac{1}{4} \left(\frac{R_t \dot{w}_o}{\dot{w}_N} \right)^2 = \frac{P_u}{P_d} \quad (2-12)$$

Equation (2-12) is only an approximate description of a vortex valve in the full turned down condition which will have a critical pressure ratio significantly greater than 2. However, the equation will be sufficiently accurate for use in the region $1 < P_u/P_d < 2$.

If the staged vortex valves of Figure 2-10 are part of a perfect pressure regulator supplying a fixed load we can say:

$$\dot{w}_{Si} + \dot{w}_{CAi} + \dot{w}_{CBi} = \dot{w}_{CAf} + \dot{w}_{CBf} + \dot{w}_{Sf} \quad (2-13)$$

$$P_{Ri} = P_{Rf} = P_R \quad (2-14)$$

If the downstream vortex valve B is to exercise any control over the flow through the staged impedances, the upstream vortex valve A must operate in a range of pressure ratios such that changes in the interstage pressure P_m will affect the flow through the vortex valve A. If the vortex

* "Thermodynamics," J. E. Emswiler, F. L. Schwartz, McGraw-Hill Book Company, Inc., New York and London, p. 302, 1943.

valve A was an orifice, this would be approximately defined by $1 \leq P_B/P_m \leq 2$. Since a wide open vortex valve is an orifice and since $P_{B1}/P_{m1} < P_{Bf}/P_{mf}$ we can say that $1 \leq P_B/P_m \leq 2$. That is, vortex valve A must operate in the region described by equations (2-11) and (2-12). For convenience we can assume that vortex valve B is described by equations (2-9) and (2-10).

If vortex valve A is in the fully turned down condition $\dot{w}_S = 0$ and the control flow \dot{w}_{CA} will be the full flow through the valve. It will be impossible to operate vortex valve B in the fully turned down condition unless $\dot{w}_{CA} = 0$.

If we let R_{tA} be the turndown ratio of vortex valve A and R_{tB} be the turndown ratio of vortex valve B, we can write the following equations from equations (2-9) through (2-14) noting that the initial impedances must be a maximum if P_R and $\dot{w}_S + \dot{w}_{CA} + \dot{w}_{CB}$ are to be constant. This implies that $\dot{w}_{S1} = \dot{w}_{CA1} = \dot{w}_{CB1} = 0$.

$$R_{tB} (\dot{w}_{CA1} + \dot{w}_{CB1}) = \frac{C_2 C_d A_B P_{m1}}{\sqrt{T}} \quad (2-15)$$

$$\dot{w}_{Sf} = \frac{C_2 C_d A_B}{\sqrt{T}} P_{mf} \quad (2-16)$$

$$R_{tA} \dot{w}_{CA1} = \frac{2 C_2 C_d A_A P_{m1}}{\sqrt{T}} \sqrt{\left(\frac{P_{B1}}{P_{m1}}\right)^{-1}} \quad (2-17)$$

$$\dot{w}_{Sf} = \frac{2 C_2 C_d A_A P_{mf}}{\sqrt{T}} \sqrt{\left(\frac{P_{Bf}}{P_{mf}}\right)^{-1}} \quad (2-18)$$

We will define a parameter ψ :

$$\psi = \frac{\dot{w}_{CA1}}{\dot{w}_{CA1} + \dot{w}_{CB1}} = \frac{\dot{w}_{CA1}}{\dot{w}_{Sf}} \quad (2-19)$$

Bendix

Equations (2-7) and (2-15) through (2-19) may be combined to give:

$$\left(\frac{\psi R_{tA}^2}{R_{tB}}\right) = \frac{\left(\frac{P_{Bi} - 1}{P_{mi}}\right)}{\left(\frac{P_{Bf} - 1}{P_{mf}}\right)} \quad (2-20)$$

We will define an overall turndown ratio for the staged vortex valves

$$R_{to} = \frac{P_{Bi}}{P_{Bf}} \quad (2-21)$$

From equations (2-15) and (2-16) it can be seen that:

$$R_{tB} = \frac{P_{mi}}{P_{mf}} \quad (2-22)$$

Combining equations (2-20) through (2-22) gives:

$$R_{to} = \left(\frac{P_{mf}}{P_{Bf}}\right) \left(\frac{R_{tB}^2 - \psi^2 R_{tA}^2}{R_{tB}}\right) + \left(\frac{\psi^2 R_{tA}^2}{R_{tB}}\right) \quad (2-23)$$

The limiting case are:

$$\text{If } \frac{P_{mf}}{P_{Bf}} = 1, R_{to} = R_{tB} \quad (2-24)$$

$$\text{If } \frac{P_{mf}}{P_{Bf}} = \frac{1}{2}, R_{to} = \frac{R_{tB}^2 - \psi^2 R_{tA}^2}{2 R_{tB}} \quad (2-25)$$

From the above equation, it can be seen that unless $\psi R_{tA} > R_{tB}$, $R_{to} < R_{tB}$. Furthermore, it will be impossible to operate vortex valve B in the fully turned down condition, since provision must be made for the flow \dot{w}_{CA} .

Thus the value for R_{tB} in the staged configuration will be less than the maximum R_{tB} possible. Permitting even small amounts of supply flow to enter a vortex valve significantly decreases turndown ratio.

Since the overall turndown ratio of the two vortex valves connected in series will in general be less than the turndown ratios of the individual valves and since the effective turndown ratios of the individual valves will be less than the maximum possible value, it may be concluded that staging valves will give no improvement in turndown. In certain cases, there will be an improvement in the value of P_C/P_S required to obtain a given turndown. This will be discussed in the next section.

2.2.4 Vortex Throttling Valve with Vortex Pilot Valve

Combined-Valve Performance - Another method of cascading vortex valves is to use a "pilot" valve (Figure 2-12) which feeds the control and supply ports of a second valve as shown in Figure 2-13. The characteristics of valves connected in this way were determined experimentally and the effect of the pickoff location was investigated over a range of 0.25 to 1.75 outlet hole diameters. When the pickoff is 0.25 diameters from the outlet hole, the valve combination requires a minimum P_C/P_S for full turndown, but the throttling can not be controlled over the complete throttling range. A jump phenomenon with hysteresis occurs at the most sensitive operating point until the pickoff is moved to about 1.25 diameters from the outlet hole. When the pickoff is more than 1.25 diameters from the outlet hole the turndown ratio is reduced. Performance characteristics for the pilot configuration of cascaded valves, with what appears to be the best location for the pickoff, are shown in Figures 2-14 and 2-15. From Figure 2-14, the inlet pressure range where the combined valves will satisfy the regulator throttling requirement is from 900 to 200 psig.

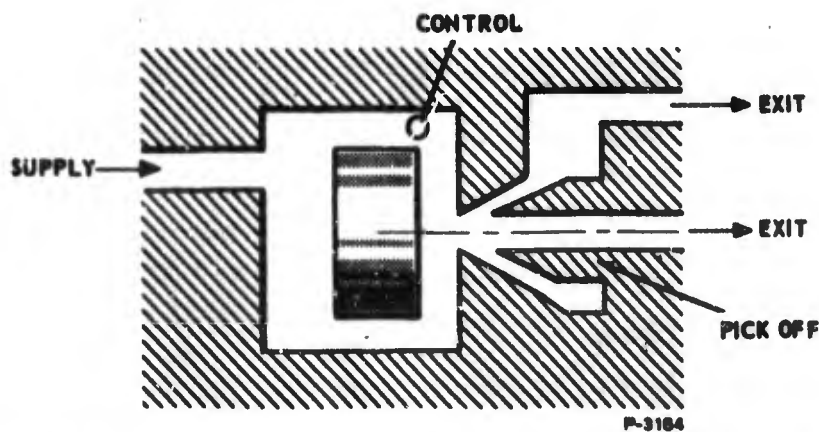


Figure 2-12 - Output Configuration for Vortex Pilot Valve

Bendix

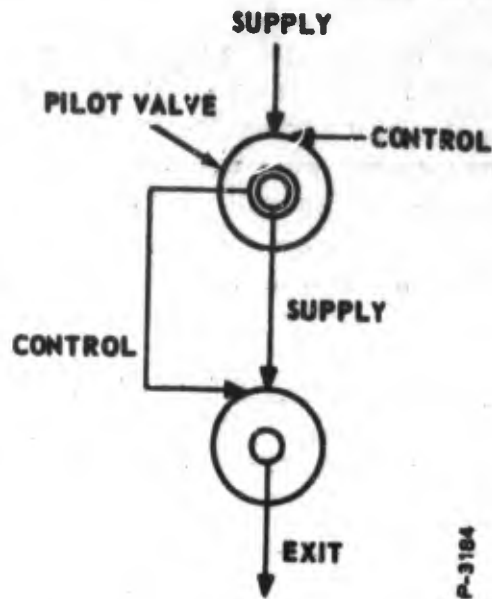


Figure 2-13 - Pilot Configuration of Cascaded Vortex Valve

Control - The pilot configuration provides a reduction in the ratio P_C/P_S required for maximum impedance sensitivity and full turndown, but putting a restriction in the supply line of the pilot valve to obtain even this P_C/P_S requirement is still impractical.

From Figure 2-15 $P_C > 1120$ psig is required for full turndown when $P_S = 1000$ psig. We must provide a pressure source greater than the supply pressure to obtain effective throttling control. For the throttling tests shown in Figure 2-16, P_{S_3} was set at $1.5P_{S_1}$ psig. The throttling performance with A_{F_2} (positive feedback path) closed is shown in Figure 2-17. The circuit will not throttle to the required load flow above $P_{S_1} = 700$ psig, but the operating line $P_0 = 21$ psig shows that a properly sized valve would operate to a minimum inlet pressure of about 225 psig.

It is not necessary to size the valve perfectly, however, because the positive feedback path A_{F_2} can be used to lower the throttling saturation for $P_{S_1} > 700$ psig as shown in Figure 2-18 and 2-19. The positive feedback reduces the control pressure P_{F_3} required to throttle the load flow to the required value without significantly increasing the minimum inlet pressure.

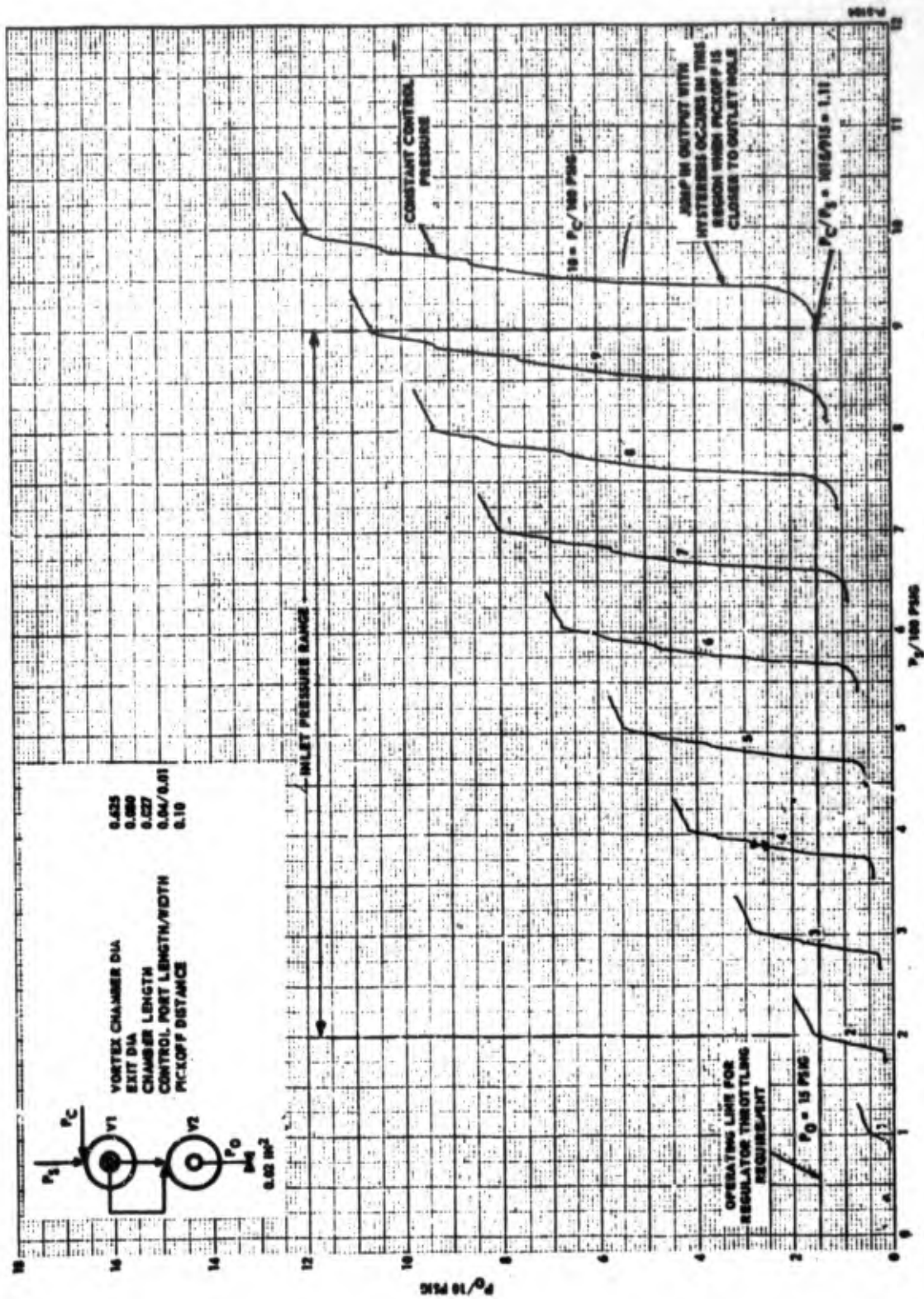


Figure 2-14 - Two-Stage Piloted Vortex Valve Performance

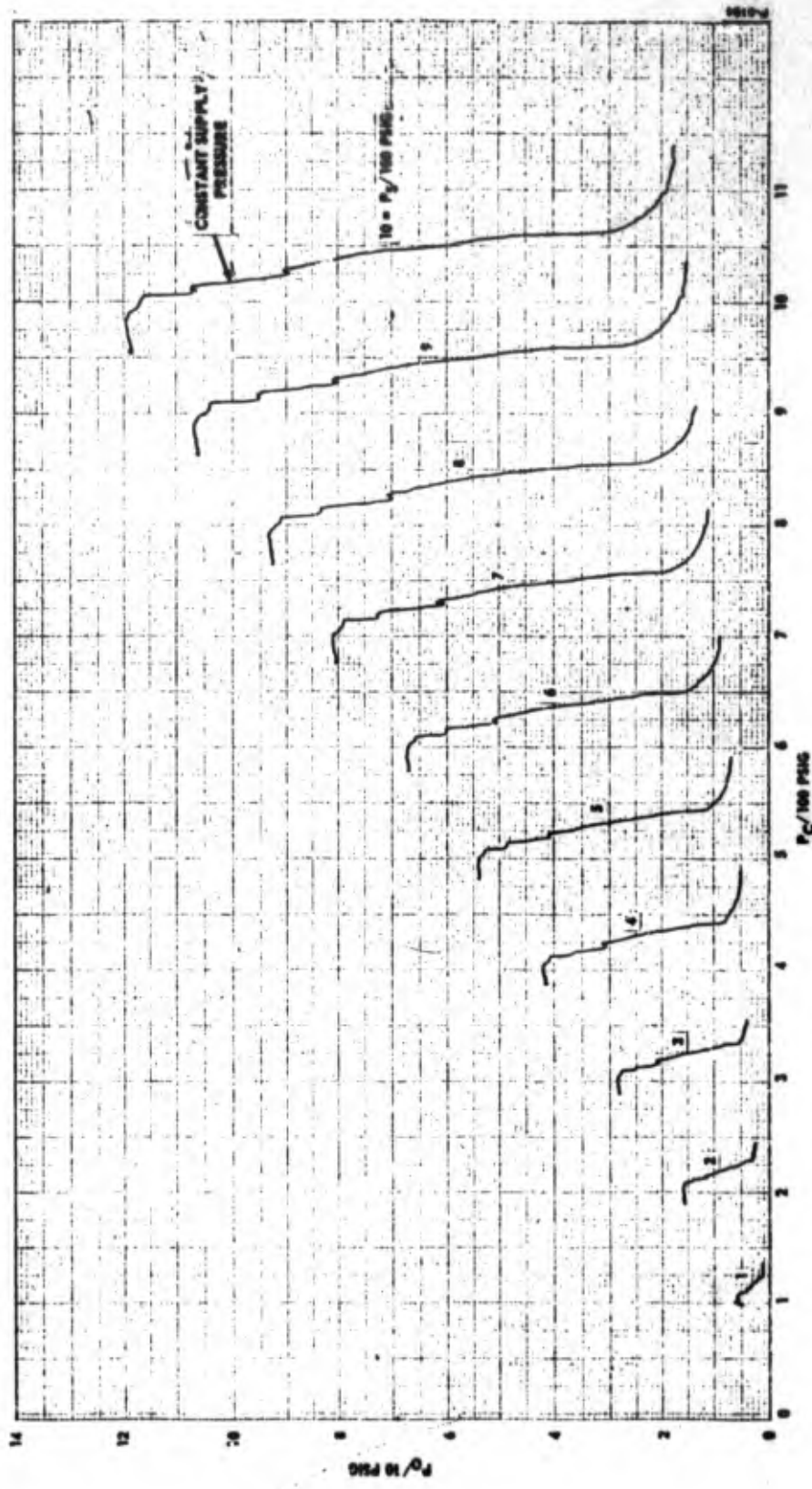


Figure 2-15 - Two-Stage Piloted Vortex Valve Performance

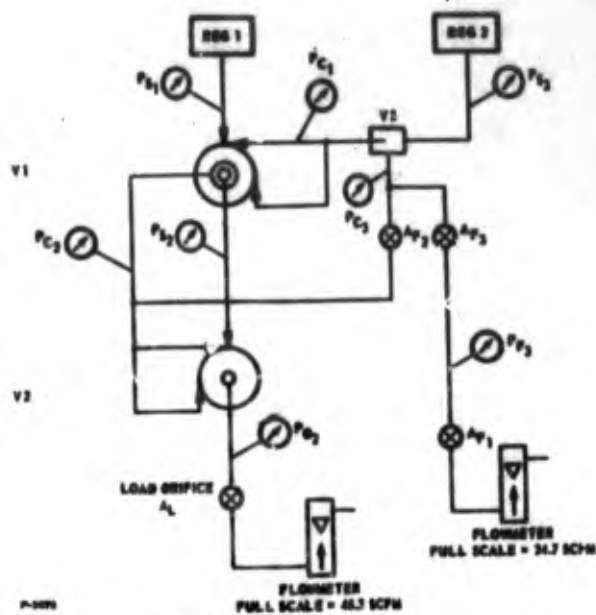


Figure 2-16 - Throttling Circuit Test

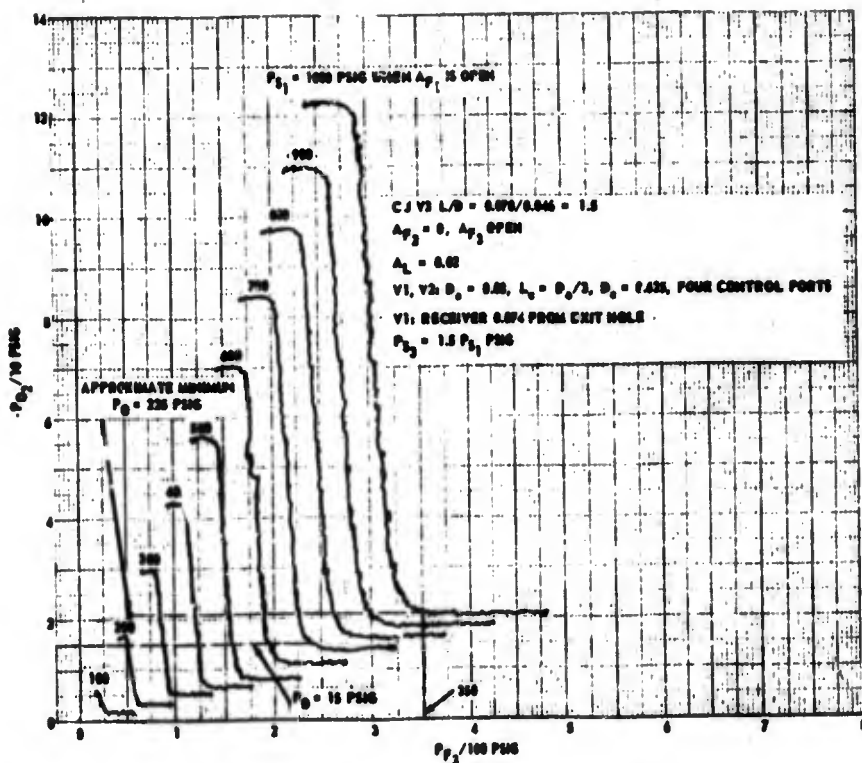


Figure 2-17 - Two-Stage Piloted Vortex Valve Performance

Bendix

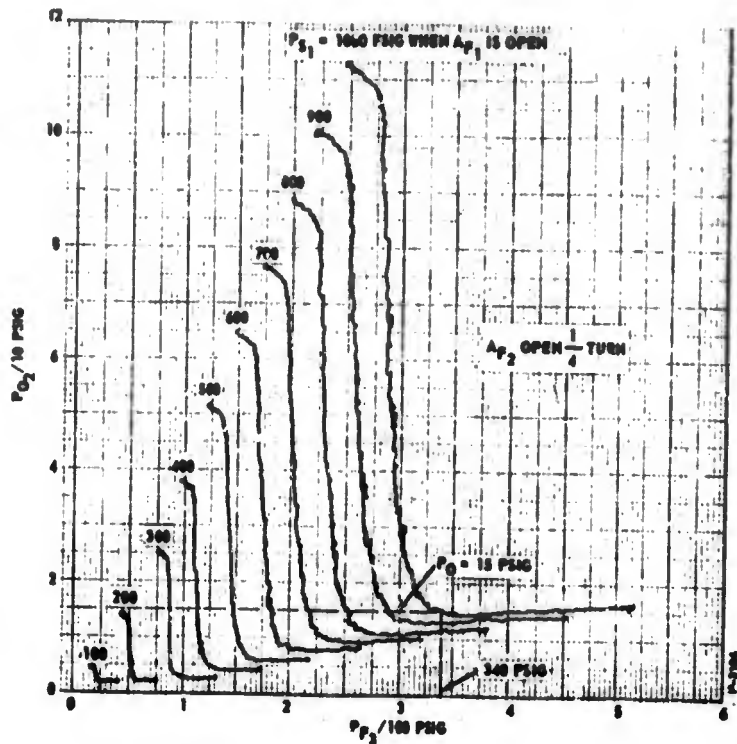


Figure 2-18 - Two-Stage Piloted Vortex Valve Performance (Positive Feedback)

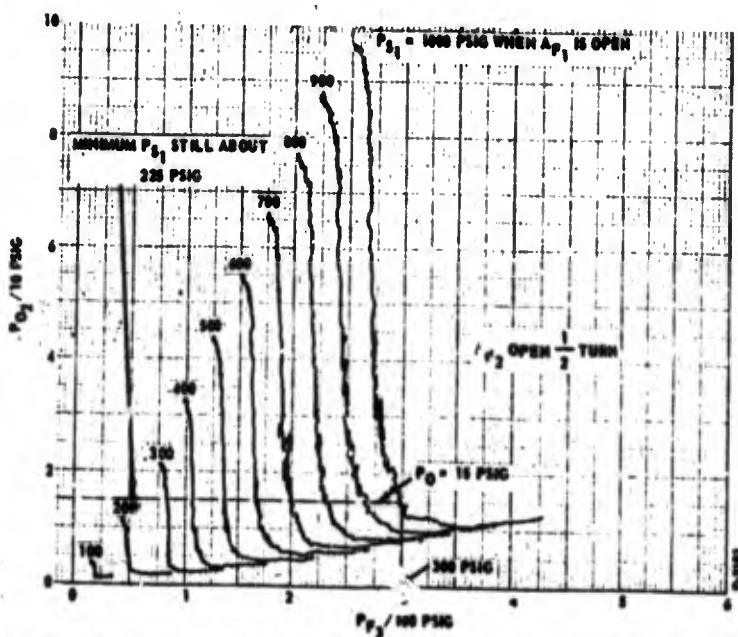


Figure 2-19 - Two-Stage Piloted Vortex Valve Performance (Positive Feedback)

2.2.5 Vortex Controlled Throttling Valves with Mechanically Variable Area

One approach which avoids the limitations imposed by the use of a fixed-area pressure dropping orifice at the outlet of the gas storage bottle is to use a mechanically variable area as the primary pressure dropping element. The use of a variable area deviates from the idealized goal of having an all-fluid system with no moving parts. However, the scheme which has been investigated appears to represent an extremely practical solution to the problem of producing the required pressure regulator performance with a minimum of moving parts while retaining the high reliability and other desirable characteristics of a completely all-fluid system.

Figure 2-20 shows a possible layout of a vortex regulator element with a mechanically variable area. This is basically a vortex

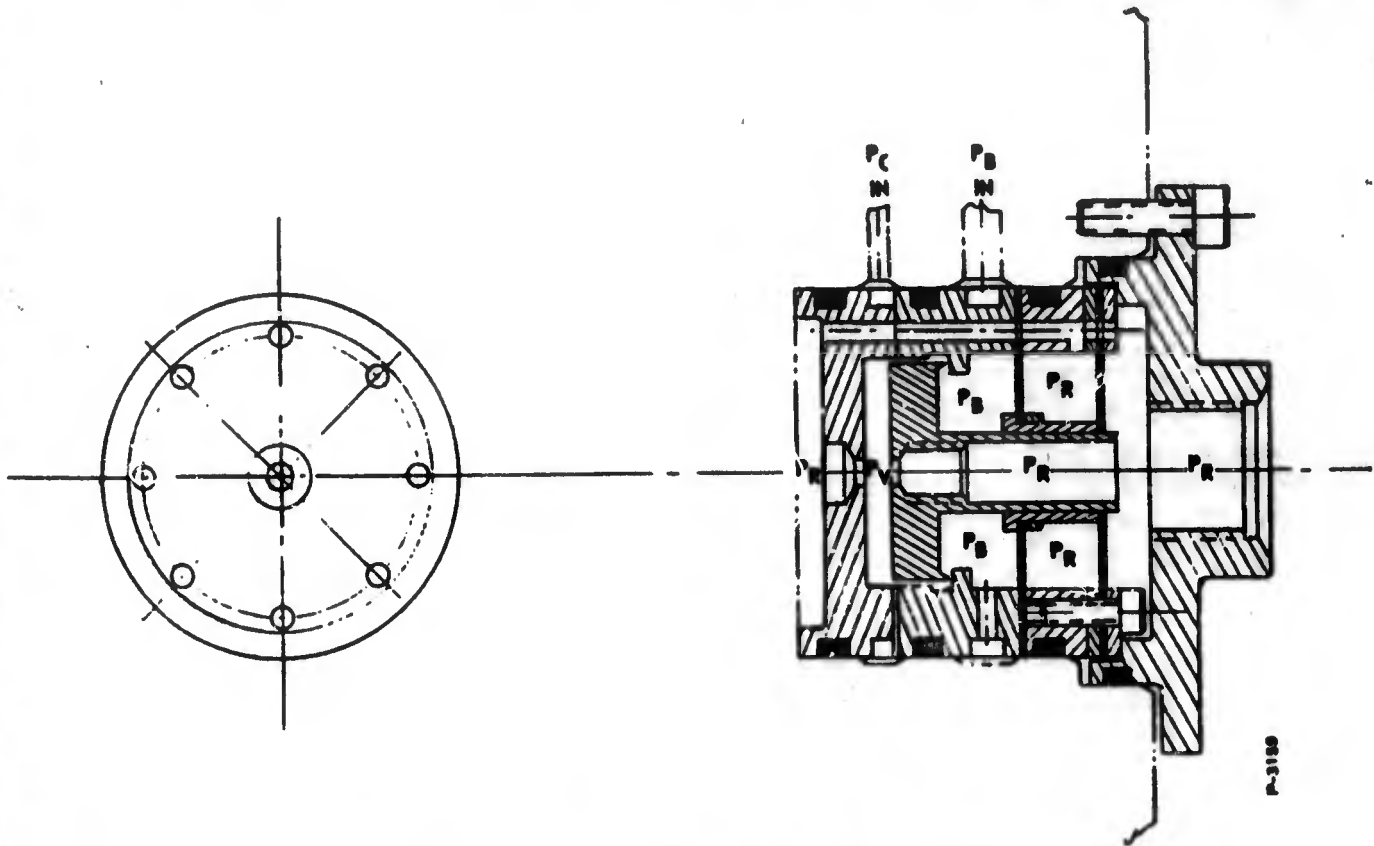


Figure 2-20 - Vortex Regulator Element

Bendix

valve with a moving button. The upstream edge of the button meters the supply gas flow. Schematically the device can be represented as a vortex valve in series with a mechanical valve. The control pressure is designated as P_C ; the bottle pressure, as P_B ; the mean vortex chamber pressure, as P_V ; and the regulated pressure as P_R . As can be seen from the drawing, the button position is defined by the force balance of the difference between the pressure forces across the button and a diaphragm acting against a spring force produced by the diaphragm and a Belleville spring. A shim placed underneath the Belleville washer determines the maximum button travel:

With the maximum pressure applied to the control ports, the mean pressure underneath the button is high enough to close the metering element and the flow is governed by the control port area. With no control pressure, the flow through the metering element is a maximum. Thus, by properly modulating control pressure as a function of bottle pressure and load demand, a constant regulated pressure can be maintained.

The force balance on the button is given by:

$$A_B (P_B - P_V) - A_d (P_B - P_R) + F_d = 0 \quad (2-26)$$

where A_B and A_d are the button and diaphragm areas and F_d is the spring force.

It is assumed that the control pressure, P_C , is derived from P_B . A conservative recovery for a confined jet amplifier driving a flowing load is 65%. Thus, if the maximum value of P_B has a nominal value of 1000 psia, the maximum value of $P_C = 650$ psia. A realistic P_C/P_S value to shut off a vortex valve is 1.3. Hence, if the vortex valve is in the shutoff condition with $P_C = 650$ psia, it may be assumed that the vortex chamber pressure at the outer wall is 500 psia.

The turndown of a double exit vortex valve will be somewhat in excess of 8 for high pressure air. Thus the equivalent pressure at the exit hole will be approximately 60 psia.

The definition of these pressures and the assumption of a nominal flow of 0.014 lbs/sec of air defines the geometry of the vortex valve. For the values derived here, the diameter of the exit hole is 0.087 in. the button diameter is 0.700 in.

With $P_B = 1000$ psia, the valve element is closed and all flow passes through the control ports. With $P_B = 100$ psia all flow passes through the metering element. If a constant nominal flow of 0.014 lb/sec of air is to be maintained, the pressure at the exit hole must remain at 60 psia. With no swirl in the vortex chamber, this pressure will extend back to the downstream side of the metering edge. It can then be calculated that the metering element must have a travel of 0.0037 in. to maintain the desired flow at $P_B = 100$ psia.

From equation (2-26) it can be seen that the minimum value of F_d corresponds to the case in which the metering element is open. If a minimum value of F_d is assumed, equation (2-26) may be solved for A_d , using the known values of P_B , P_V , P_R , and A_B for the open metering element. The same equation may then be used to solve for the maximum value of F_d , using the previously established value of A_d , and the known values of P_R , P_V , and P_B for the closed metering element. For this part of the calculation, test data shows that the effective value of P_V is approximately equal to the pressure at the outer wall of the vortex chamber. Once the maximum and minimum values of F_d have been established, the required diaphragm spring rate may be computed from the previously established metering edge travel.

The following results have been obtained and bracket the required diaphragm and Belleville spring characteristics.

$F_{dmin} = 0$	$A_d = 0.220 \text{ in}^2$
	$F_{dmax} = 21 \text{ lbs}$
	Rate = 5700 lb/in
$F_{dmin} = 5 \text{ lb}$	$A_d = 0.292 \text{ in}^2$
	$F_{dmax} = 90 \text{ lbs}$
	Rate = 23000 lb/in

Preliminary analysis indicates that a practical diaphragm and spring will lie within the bounds defined by the above range of required diaphragm characteristics.

Bendix

The resonant frequency of the mechanical element may be approximated by the equation for the frequency of a simple spring-mass system.

$$f_n = \frac{1}{2\pi} \sqrt{\frac{k}{m}} \quad (2-27)$$

If the button is assumed to be stainless steel its weight will be approximately 0.05 pounds. Substituting this into equation (2-27) along with the minimum diaphragm spring rate of 5700 lb/in gives an undamped natural frequency, $f_n = 1060$ cps. The element will thus be quite stiff and insensitive to vibration.

2.2.6 Dual Volume Gas Bottle

In Section 2.2.2, an approach to the throttling element was discussed which involved the use of a dual volume gas storage bottle. One of these gas volumes is pressurized to a higher level than the other and serves as a source of control pressure for the throttling of the flow from the lower pressure bottle. The discussion in Section 2.2.2 was concerned with the throttling element requirements; the discussion here will be primarily concerned with gas storage requirements.

It can easily be shown that for single compartment spherical pressure vessels or for single compartment cylindrical pressure vessels having spherical ends and identical L/D ratios, the pressure vessel weight for a given factor of safety and weight of gas is theoretically independent of the storage pressure. Although practical constraints may alter this conclusion somewhat in certain applications, it can generally be considered to hold in the real case.

Storage volume, on the other hand, decreases inversely as initial storage pressure. Ullage is also reduced. As a result, as pressure vessel technology improves, the trend has been for gas storage bottle pressures to increase, especially in military and aeronautical applications.

In view of the above, the necessity of having to store the pressurizing gas at two different levels must be counted a disadvantage. Furthermore, the possibility of leakage disturbing the required balance between the weights of gas stored in the two volumes must be considered. On the other hand, the dual volume approach has the outstanding advantage of producing an all fluid system of the purest form. Since this corresponds to the goal of this project, the dual volume approach thus deserves investigation.

One of the first questions which occurs during such an investigation is to determine the ratio of the volumes of the two tanks. This may be approached by the following reasoning:

Consider the dual bottle system indicated in Figure 2-21. At the initial conditions the vortex valve will be shut off and the flow from the low pressure bottle will be zero. At the final conditions, it may be assumed that the low pressure bottle supplies the total demand of the load and the reference circuit. In other words:

$$\dot{w}_{Bi} = 0 \quad (2-28)$$

$$\dot{w}_{Bf} = \dot{w}_L^* + \dot{w}_R \quad (2-29)$$

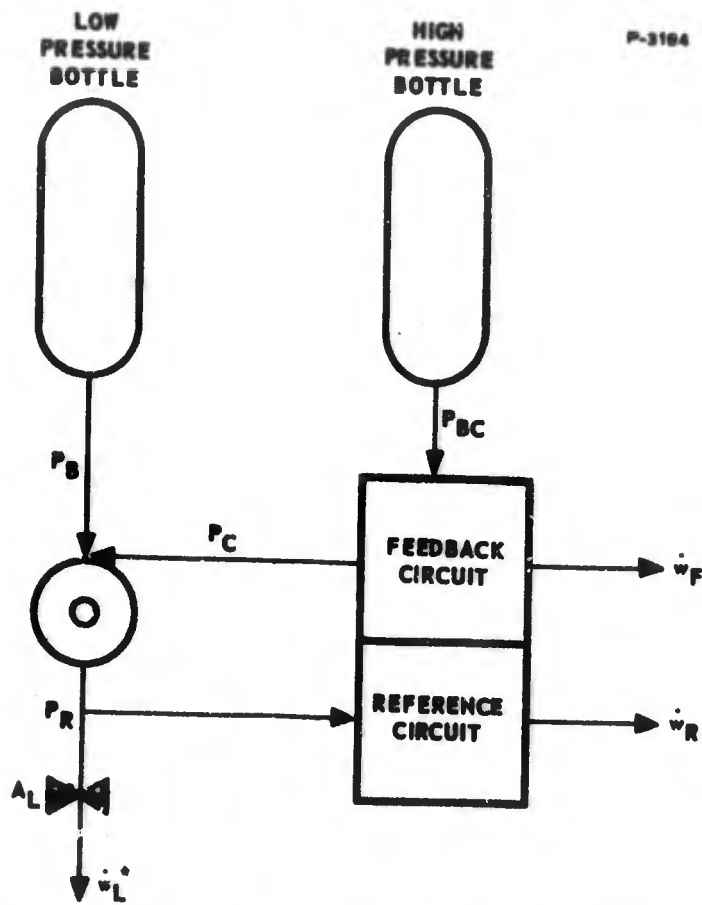


Figure 2-21 - Dual Pressure Bottle System

Bendix

Assuming that pressure P_B decays as a linear function of time, we can say:

$$W_B = \left(\frac{\dot{w}_L^* + \dot{w}_R}{2} \right) t_o \quad (2-30)$$

At the initial conditions, the high pressure bottle will supply the total flow demand of the system. It may be assumed that all flow from the high pressure bottle passes through confined jet amplifiers which, viewed from the input, act as sonic orifices. Therefore if $P_{BCi}/P_{BCi} = 0.1$, we can say:

$$\dot{w}_{BCi} = \dot{w}_L^* + \dot{w}_R + \dot{w}_{Fi} \quad (2-31)$$

$$\dot{w}_{BCi} = \frac{\dot{w}_L^* + \dot{w}_R + \dot{w}_{Fi}}{10} \quad (2-32)$$

We will also assume that P_{BC} decays as a linear function of time:

$$W_{BC} = 0.55 (\dot{w}_L^* + \dot{w}_R + \dot{w}_{Fi}) t_o \quad (2-33)$$

Defining the efficiency of the feedback circuit as $\eta_F = 1 - \dot{w}_{Fi} / (\dot{w}_L^* + \dot{w}_R + \dot{w}_{Fi})$ and dividing equation (2-33) by equation (2-30) gives:

$$\frac{W_{BC}}{W_B} = \frac{1.1}{\eta_F} \quad (2-34)$$

The volumes of the two tanks are:

$$\frac{V_{BC}}{V_B} = \frac{1.1 P_{Bi}}{\eta_F P_{BCi}} \quad (2-35)$$

The P_C/P_B ratio required to shut off the vortex valve will range from perhaps 1.1 to 1.4, depending upon the final configuration selected. The pressure recovery of a confined jet amplifier supply a flowing load will be approximately 70 percent. Thus the ratio $P_{BCi}/P_{Bi} = 1.6$ to 2.0. The feedback efficiency η_F is not expected to be greater than 50 percent. Then equation (2-35) shows that the volumes of the two tanks will be approximately equal with the high pressure tank being possibly the larger.

If the two volumes are equal and $P_{BCi} / P_{Bi} = 2$ the volume of the two tanks will be 33-1/3 percent greater than the volume of a single tank initially at pressure P_{BCi} and holding the same weight of gas.

One approach to a dual compartment pressure vessel which might have merit in this application is described in "Chrysler-Type Oxygen Pressure Vessel Calculation, Design, and Testing" by H. R. Greenlee, WADD Technical Report 60-365 May 1960. This describes a pressure vessel concept consisting of a continuously wound high-pressure tube fitted and brazed to the inside of a cylindrical shell. The tube reinforces the cylinder and permits the use of a thinner cylindrical wall. However, this saving depends upon the two volumes being in the proper proportion, which does not necessarily hold in this application.

2.3 FEEDBACK METHODS

2.3.1 Performance of Confined-Jet Amplifiers

The feedback amplifier must operate with output bias pressure higher than the input bias pressure. The confined-jet amplifier shown in Figure 2-22 is the only available element with characteristics that satisfy this requirement, so the performance of individual confined-jet amplifiers must be well understood before an attempt is made to combine them in a staged feedback amplifier.

The test schematic diagram and the confined-jet receiver configurations that have been investigated are shown in Figure 2-23.

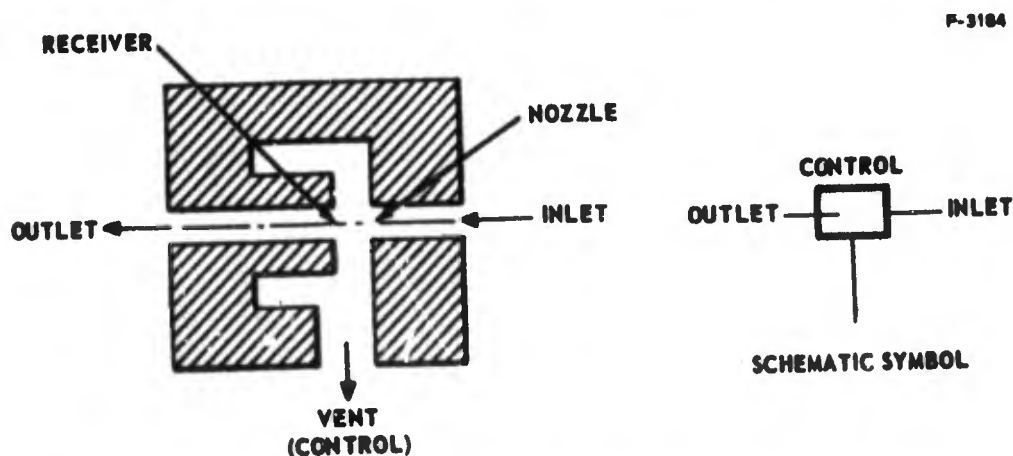
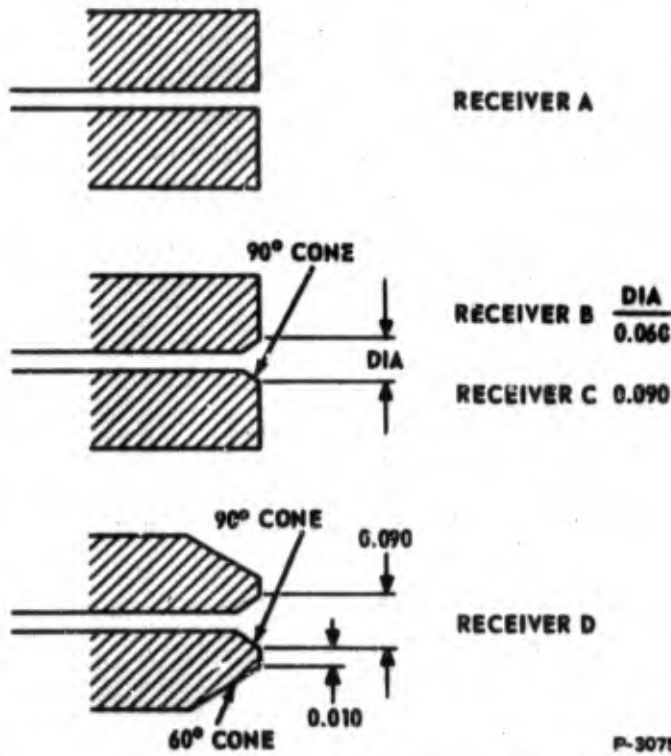
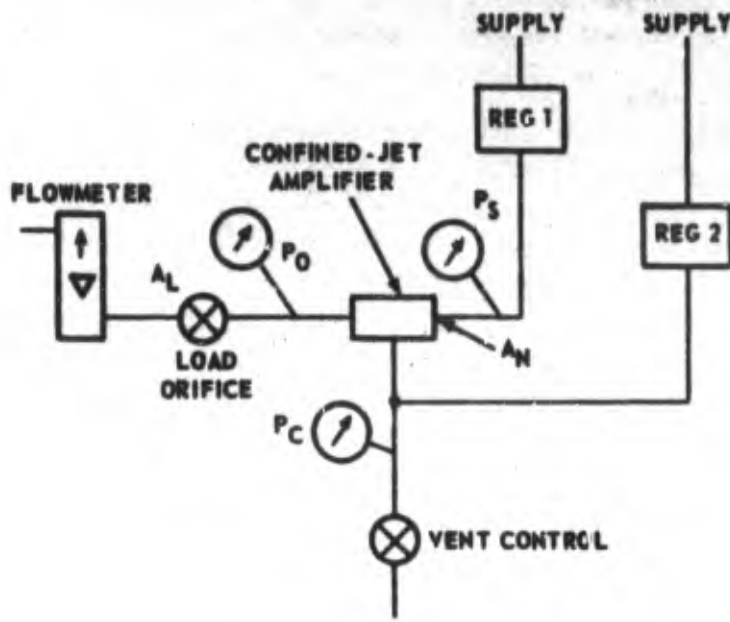


Figure 2-22 - Confined-Jet Amplifier Configuration and Schematic Symbol

Pendix



P-3075

Figure 2-23 - Confined-Jet Amplifier Test and Receiver Configurations

Figures 2-24 to 2-27 show the output pressure versus control pressure with various constant supply pressures. For these tests the receiver was positioned two nozzle diameters from the nozzle and load orifice area was one-half of the nozzle area. Note that the noisy operation in the high gain region of receiver A is reduced by the internal cone of receiver B. The noise is further reduced by the coned configurations of receivers C and D. Forty variations of receiver spacing from $L/D = 0.5$ to 3 were investigated using the four receiver configurations. Of these, the performances of receiver B and C (Figures 2-24 and 2-25) offer the highest incremental gain and operating range with comparatively low noise. The useful operation appears to be in the range $P_C/P_S = 0.15$ to 0.25, and the maximum output pressure is about 70 percent of the supply pressure.

An interesting, and possibly useful property of confined-jet amplifiers is illustrated in the test results shown in Figure 2-28. For this test a type-A receiver was used with $L/D = 1.4$ and the load area was equal to the nozzle area. We observe that, if the control pressure is held at 55 psig, the output pressure is very nearly independent of the supply pressure for $300 < P_S < 500$. This property, a result of the overlapping characteristics for different supply pressures, seems to hold for the type-A receiver more than the others, and the range of the supply pressure independence seems to increase with the load area. The output pressure recovery falls off with increasing load area, so there is a limit to the supply pressure range that can be obtained by loading.

2.3.2 Confined-Jet Amplifiers with Vortex Control Valves

A single-stage feedback amplifier is formed by using a vortex valve to control the vent flow (or pressure) of the confined-jet amplifier as shown in Figure 2-29. The output pressure recovery of the confined-jet amplifier is greater than the control pressure required for the vortex valve, so the output can be used directly to provide either positive or negative feedback around the amplifier. The performance of this circuit is shown in Figure 2-30 and 2-31. The use of positive feedback increases the output pressure recovery and reduces the control pressure required to deliver the maximum output pressure.

2.3.3 Parallel-Staged Confined-Jet Feedback Amplifiers

The parallel-staged feedback amplifier configuration is shown in Figure 2-32. The input-output characteristics of this amplifier are shown in Figure 2-33 and the corresponding interstage pressures are

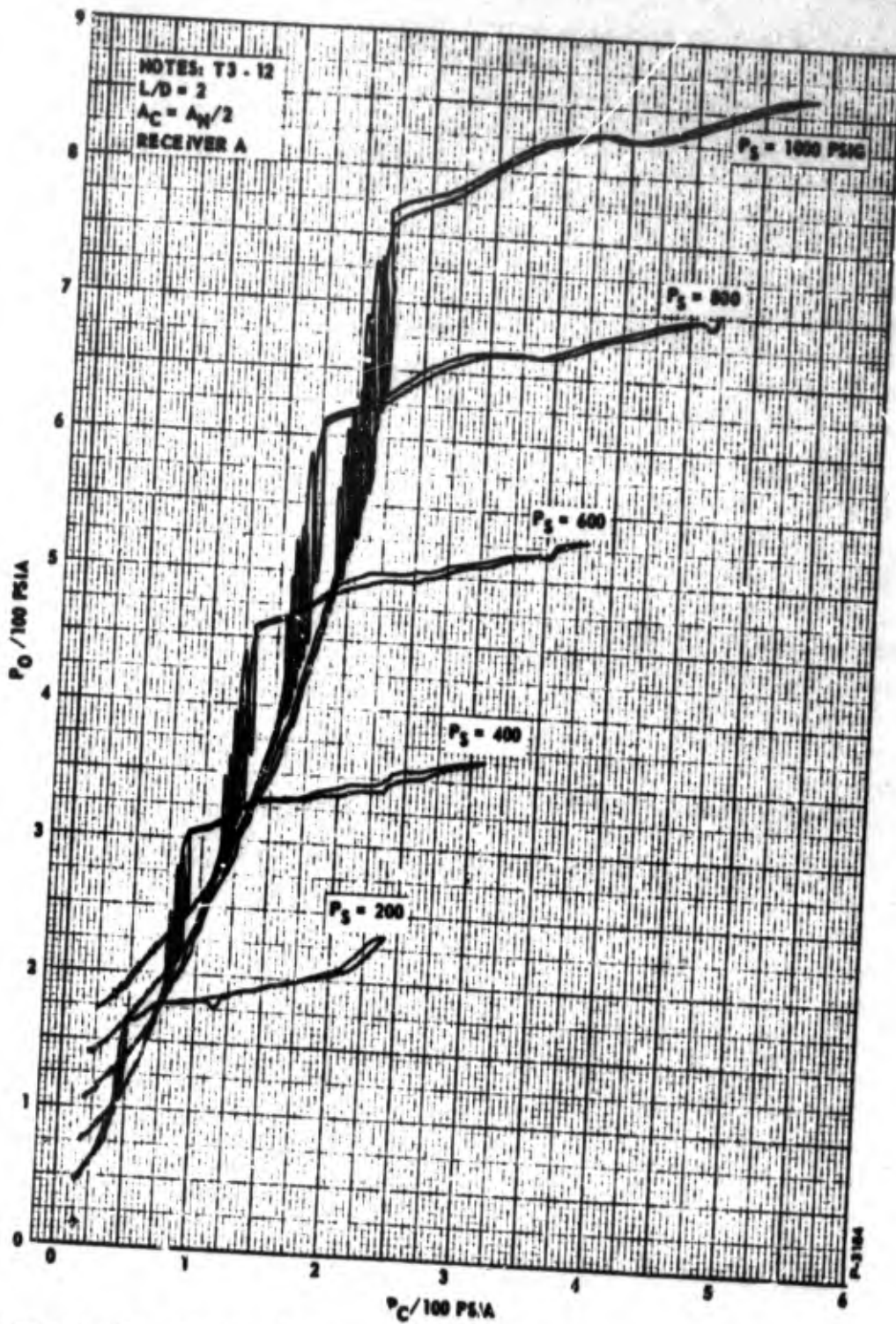


Figure 2-24 - Confined-Jet Amplifier Performance-Receiver A

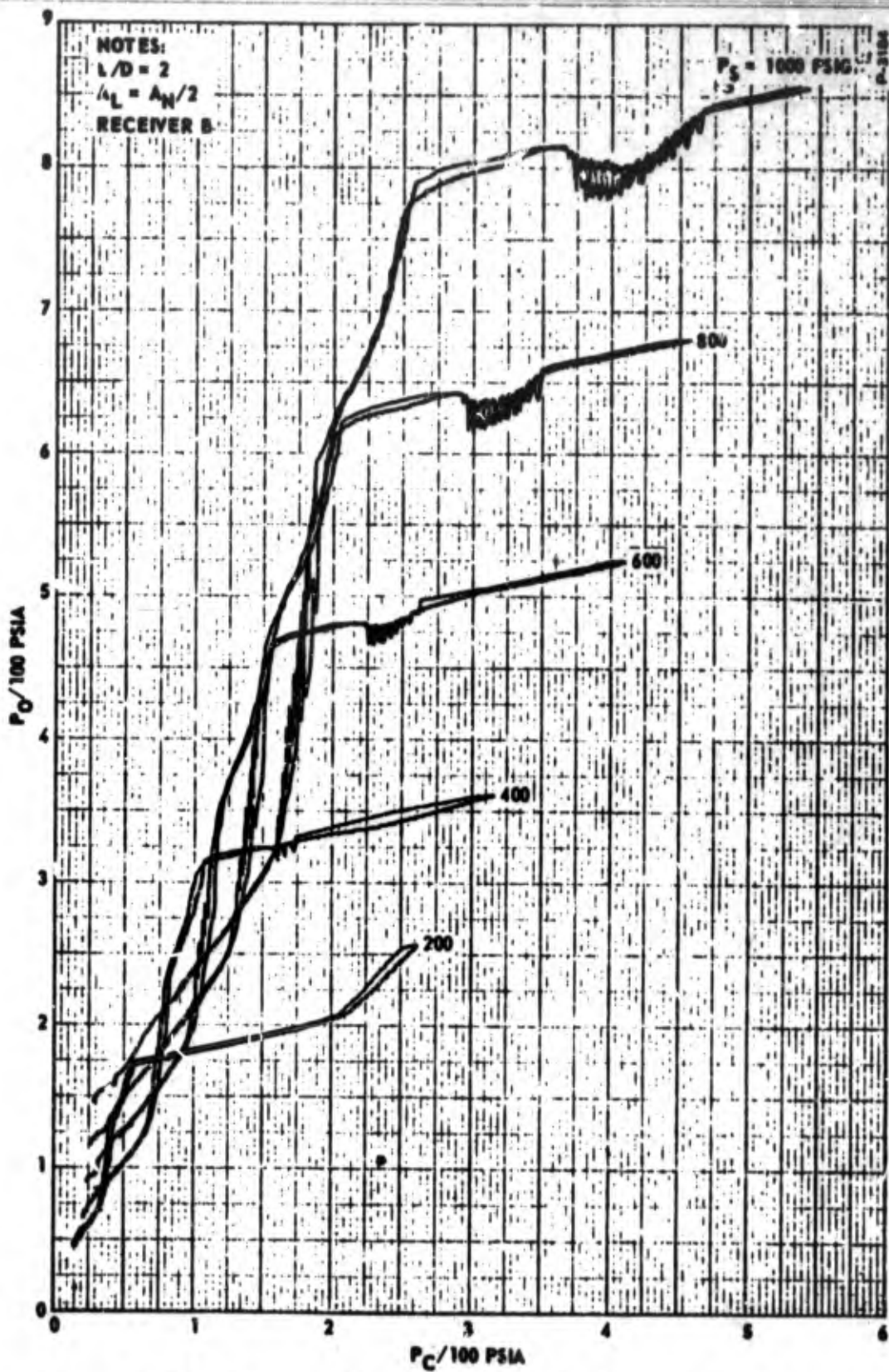


Figure 2-25 - Confined-Jet Amplifier Performance - Receiver B

Bendix

Bendix

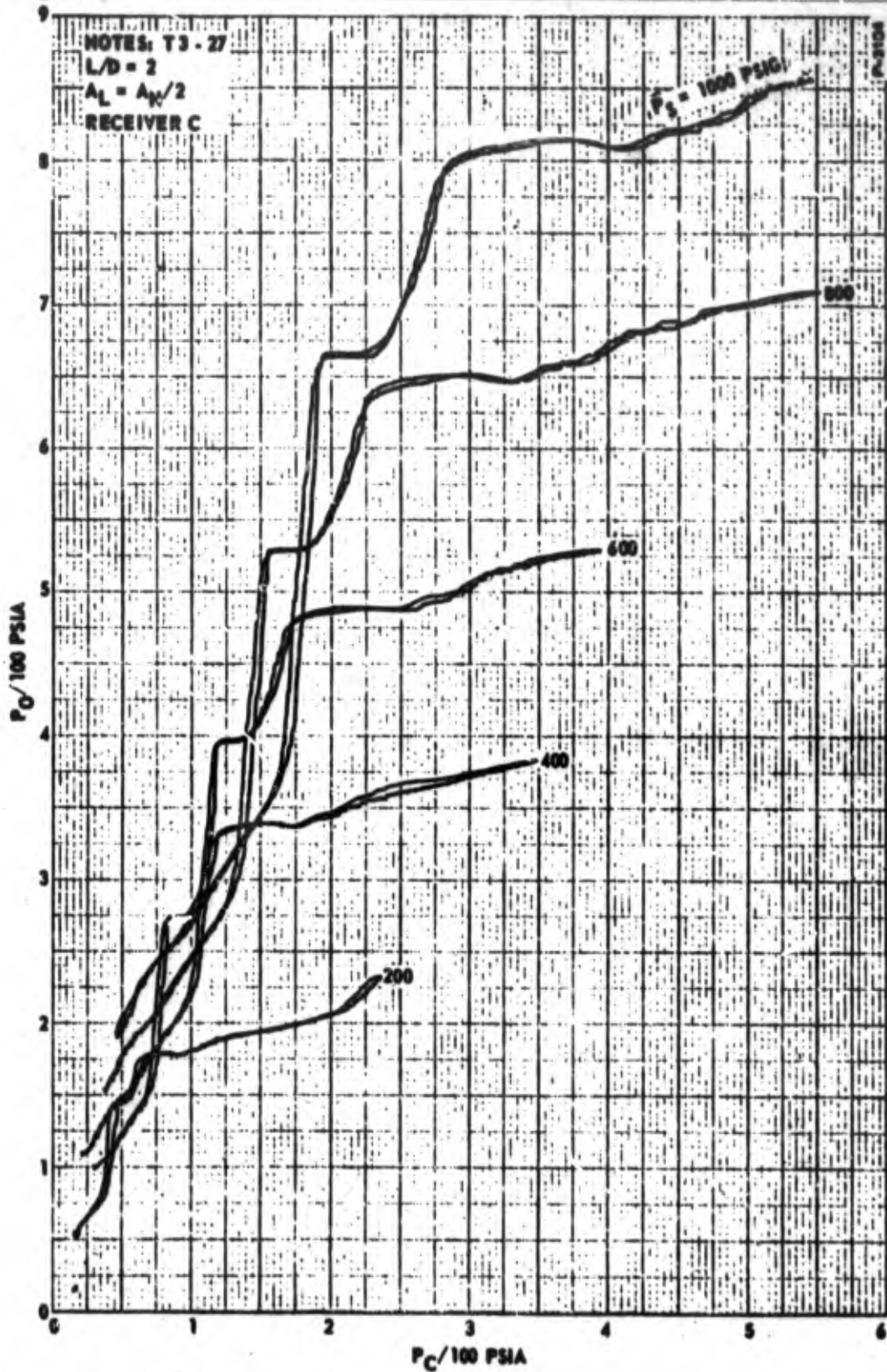


Figure 2-26 - Confined-Jet Amplifier Performance - Receiver C

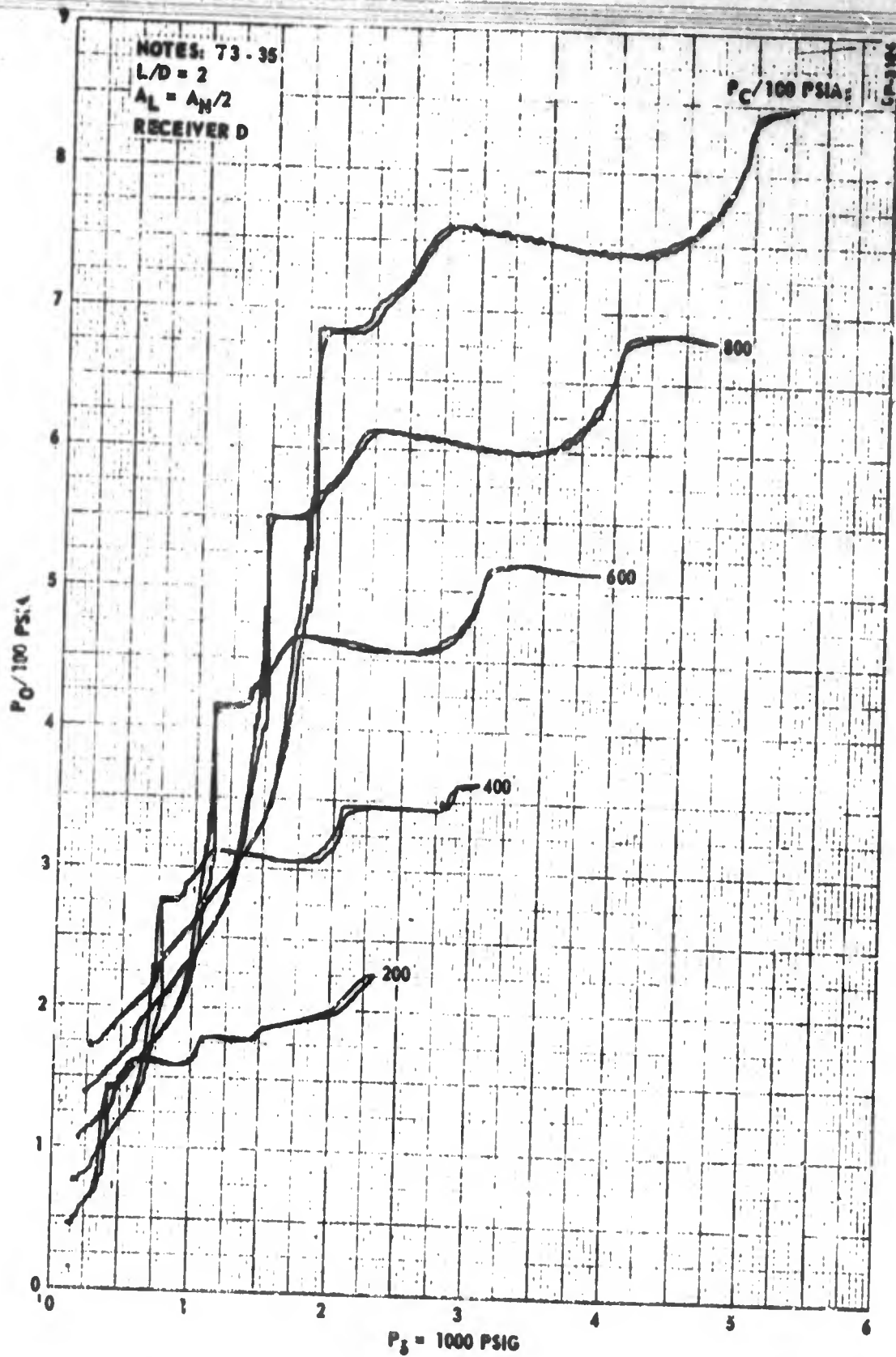


Figure 2-27 - Confined-Jet Amplifier Performance - Receiver D

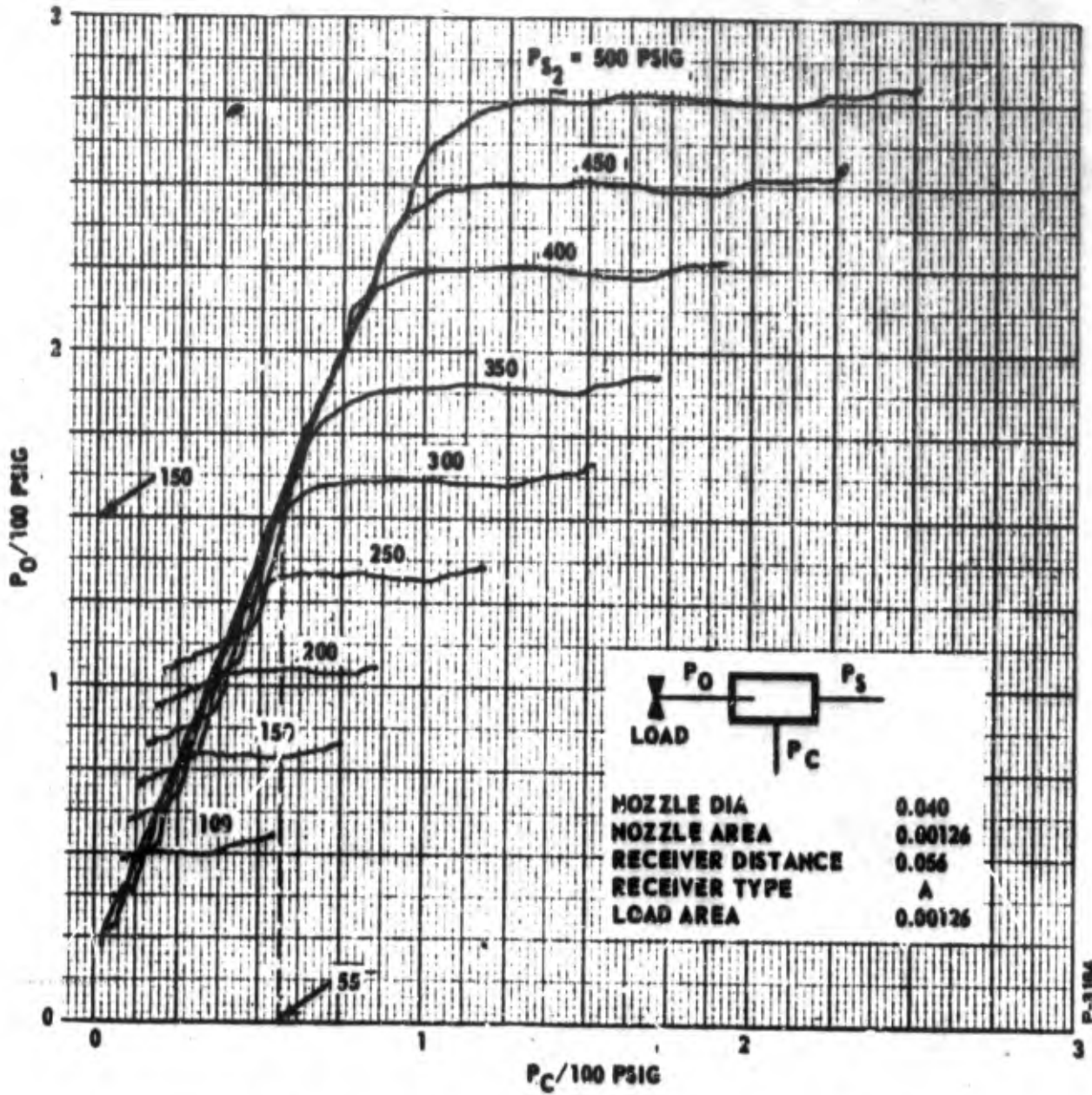
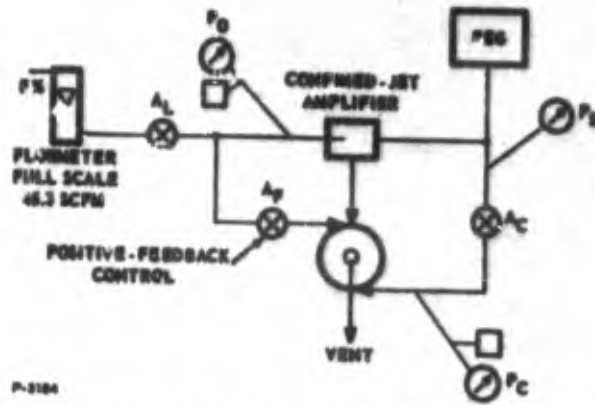


Figure 2-28 - Confined-Jet Amplifier Performance - Receiver A



P-2184

Figure 2-29 - Single-Stage Feedback Amplifier Test Schematic

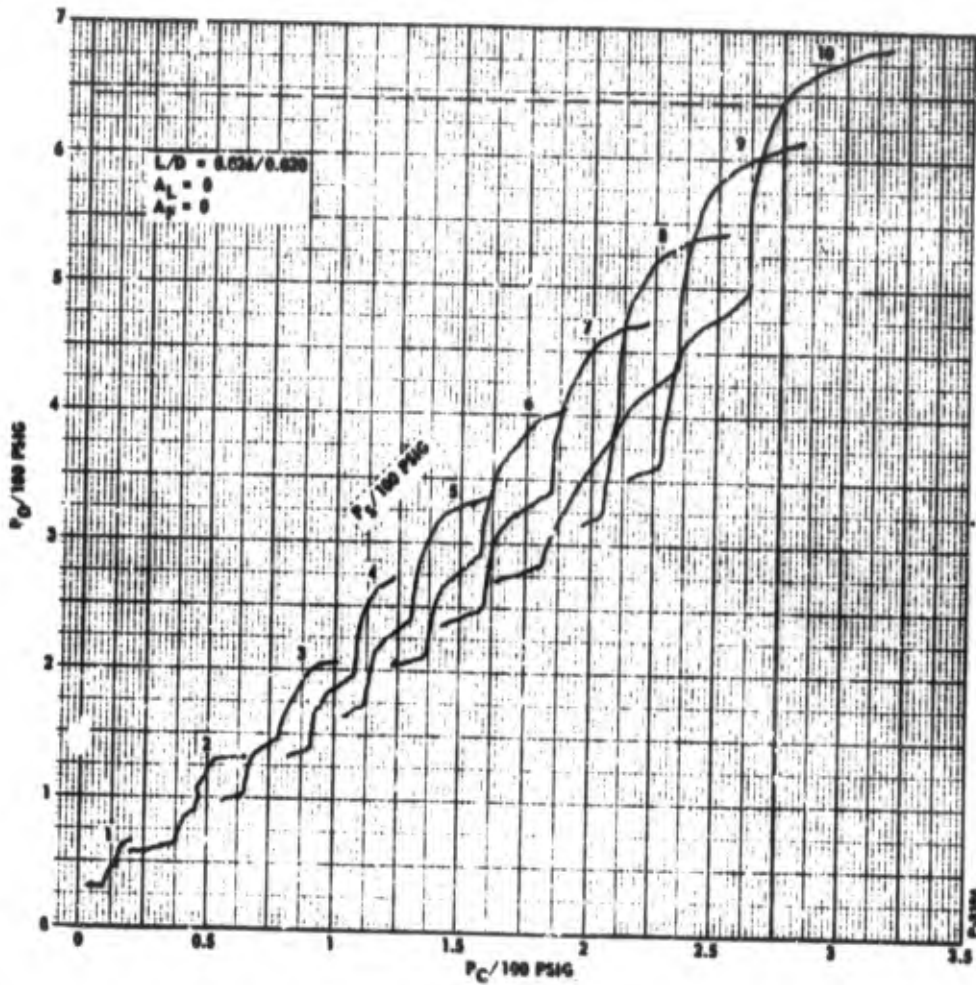


Figure 2-30 - Single-Stage Feedback Amplifier Performance; No Feedback

Bond

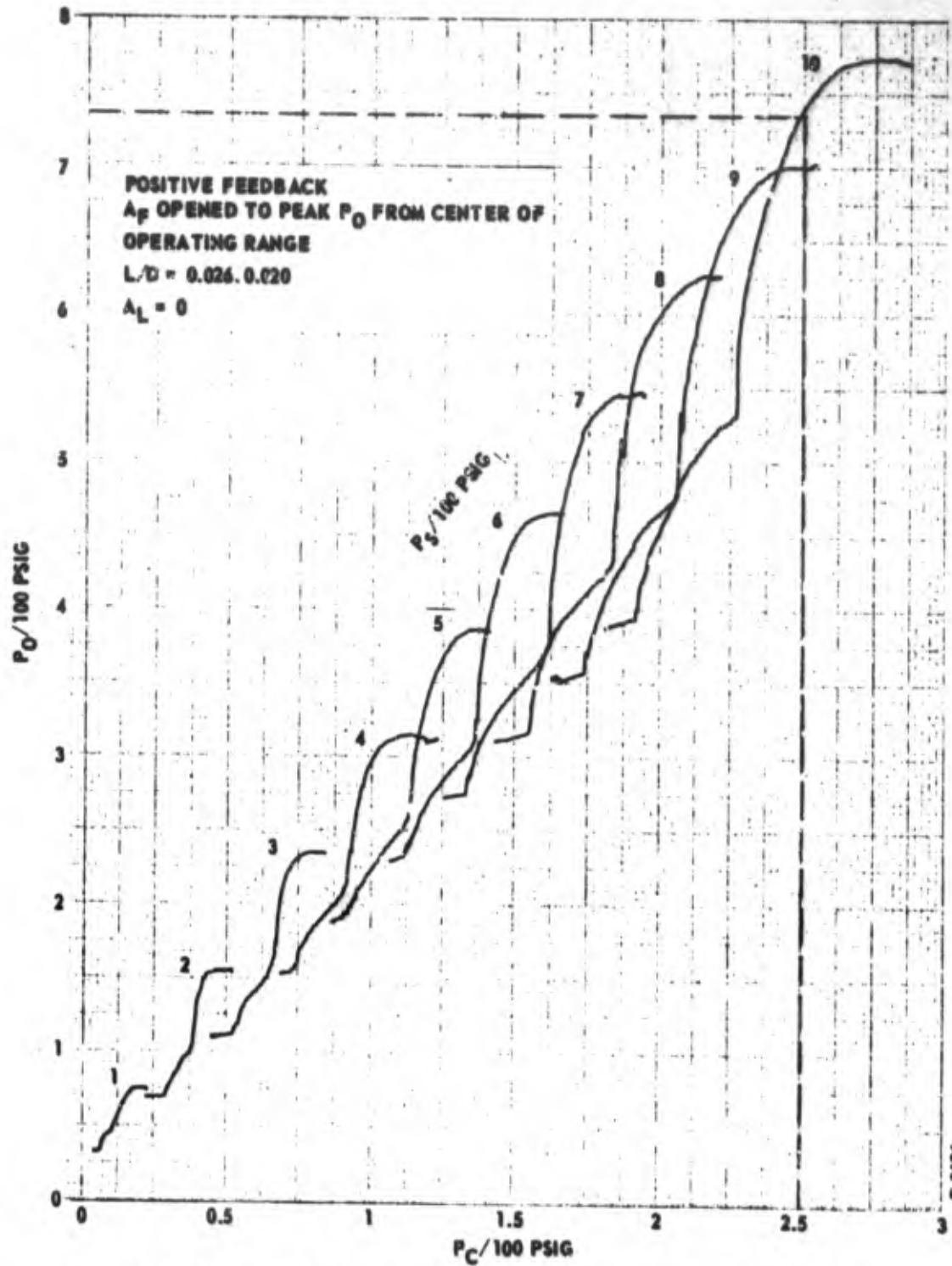
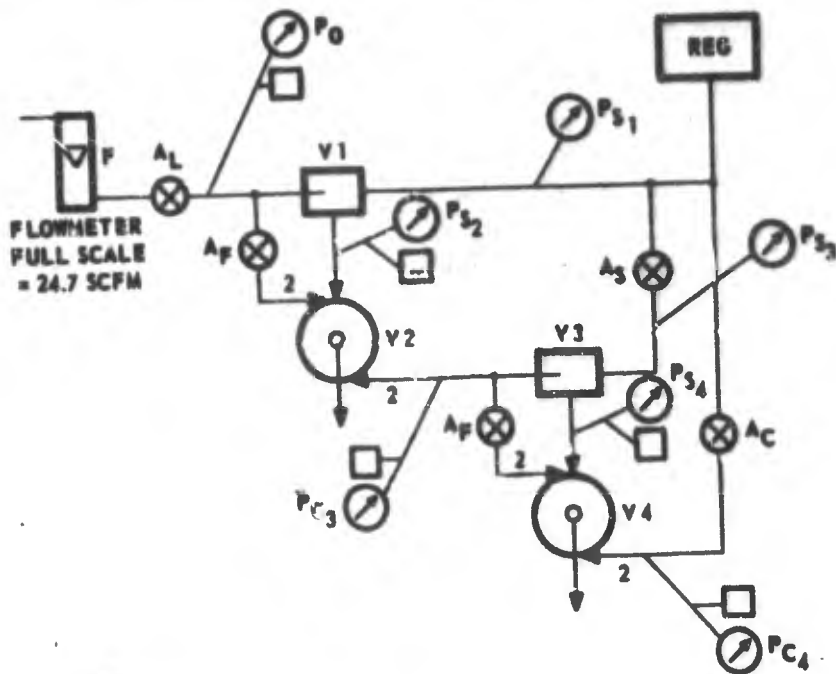


Figure 2-31 - Single-Stage Feedback Amplifier Performance; Positive Feedback



17-3184

Figure 2-32 . Parallel-Staged Feedback Amplifier Test-Two Stages

shown in Figure 2-34. These characteristics were obtained without positive feedback around either stage; it does not appear that positive feedback will be required to get high incremental gain. The characteristics with the load area set to produce output pressure saturation at about 70 percent of the supply pressure are shown in Figure 2-35.

2.4 REFERENCE METHODS

2.4.1 Single Versus Multiple-Orifice Bridge

The pneumatic flow characteristics of a series of equal area orifices have been developed in Appendix D; these results can be normalized by means of the following equation.

$$g\left(\frac{P_d}{P_u}\right) = \frac{\left(\frac{A_m}{A_l}\right)\left(\frac{P_d}{F_u}\right)^{1/k} \sqrt{1 - \left(\frac{P_d}{P_u}\right)^{(k-1)/k}}}{\left(\frac{A_m}{A_l}\right)\left(\frac{P_d}{P_u}\right)^{1/k} \sqrt{1 - \left(\frac{P_d}{P_u}\right)^{(k-1)/k}}} \quad (2-36)$$

max

Endix

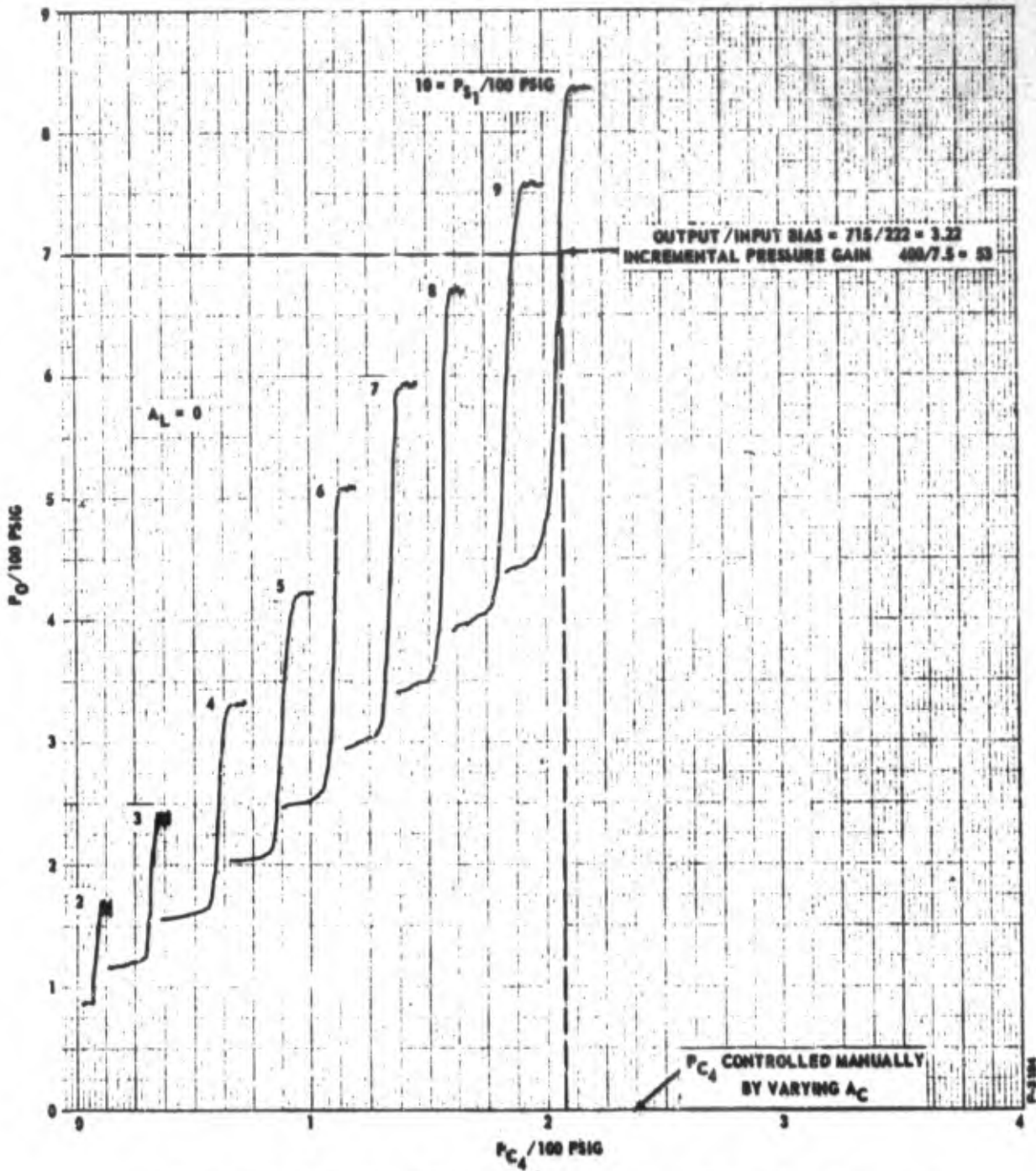


Figure 2-33 - Two-Stage Feedback Amplifier Performance

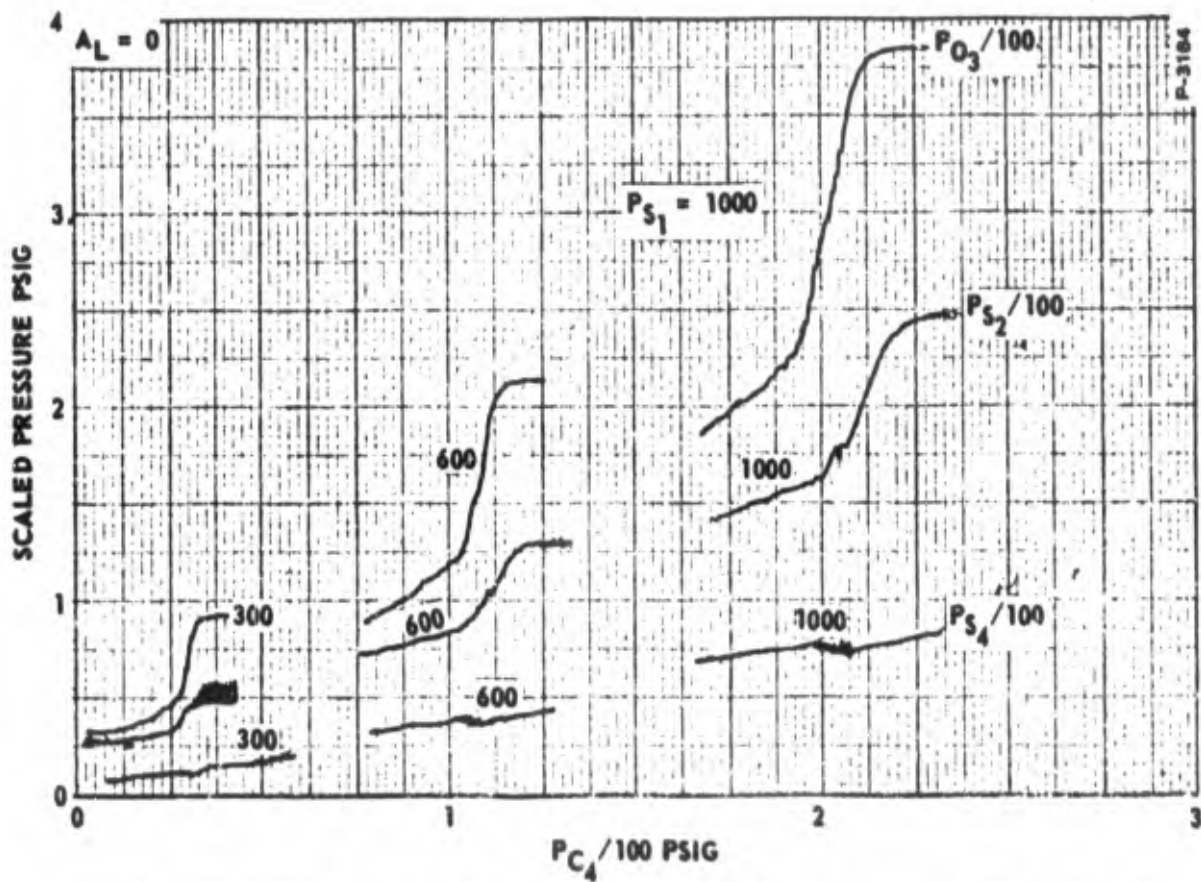


Figure 2-34 - Two-Stage Feedback Amplifier Interstage Pressures Corresponding to Figure 2-33

Bendix

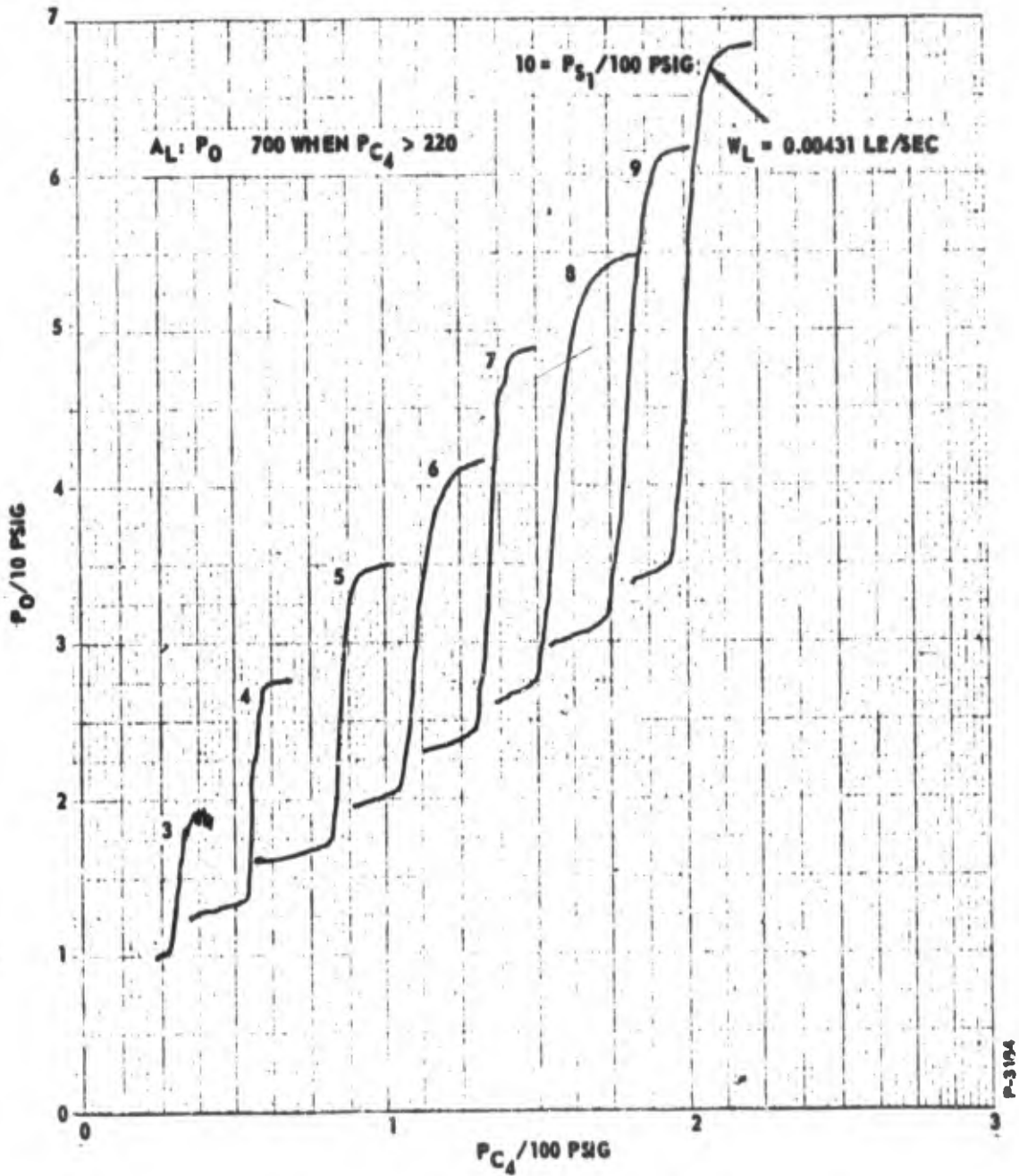


Figure 2-35 - Two-Stage Feedback Amplifier Performance with Output Load

If $n=1$, the above equation gives the f_1 function which is frequently used to calculate the flow of gases through restrictions. The function $g(P_d/P_u)$ is plotted in Figure 2-36 for $n = 1, 2, 5,$ and 10 and $k = 1.4$.

As can be seen from the Figure 2-36, increasing the number of orifices makes $g(P_d/P_u)$ a more nearly linear function of P_d/P_u and also decreases the critical pressure ratio. For $n = 10$, the critical pressure ratio is approximately 0.250 compared 0.528 when $n = 1$.

This change in shape of the flow function curve as pressure ratio changes appears to have application as a method of measuring changes in regulated pressure. If a series of n orifices is flowed in parallel with a single orifice, the relative quantities of flow in each branch will be a function of pressure ratio across them. The changes in flow in the two branches may be detected if the branches are in the supply and control lines of a vortex pressure amplifier as is indicated in Figure 2-37.

One restriction is that the outlet orifice of the vortex pressure amplifier must be flowing at a nonsonic pressure ratio. This is a consequence of the fact, as is shown in Appendix D, that setting the pressure ratio across an orifice sets the pressure ratio across any other orifice in series with it. If the outlet orifice of the vortex pressure amplifier is at a sonic pressure ratio, its pressure ratio will be effectively independent of changes in the sensed pressure. As a consequence, the pressure ratio across the parallel orifice branches will be fixed and the relative flows through the branches will be fixed, locking the operating point of the pressure amplifier.

In all fluid state systems, it is important that the various components be properly matched. Thus, the pressure amplifier must be capable of supplying flow to the components it controls. The ability of a pressure amplifier to deliver flow decreases as its gain increases. Furthermore, the output of the pressure amplifier is at a lower level than the sensed pressure. These factors impose restrictions upon this approach which will require further investigation.

2.4.2 Reference Circuit Using Jet-on-Jet Amplifiers

The use of a sonic versus subsonic-orifice bridge circuit has been demonstrated using jet-on-jet amplification as shown in Figure 2-38. In this circuit, orifice R4 is sonic and R1 is subsonic at the quiescent operating pressures indicated on the figure. The pressures

Bendix

Bentley

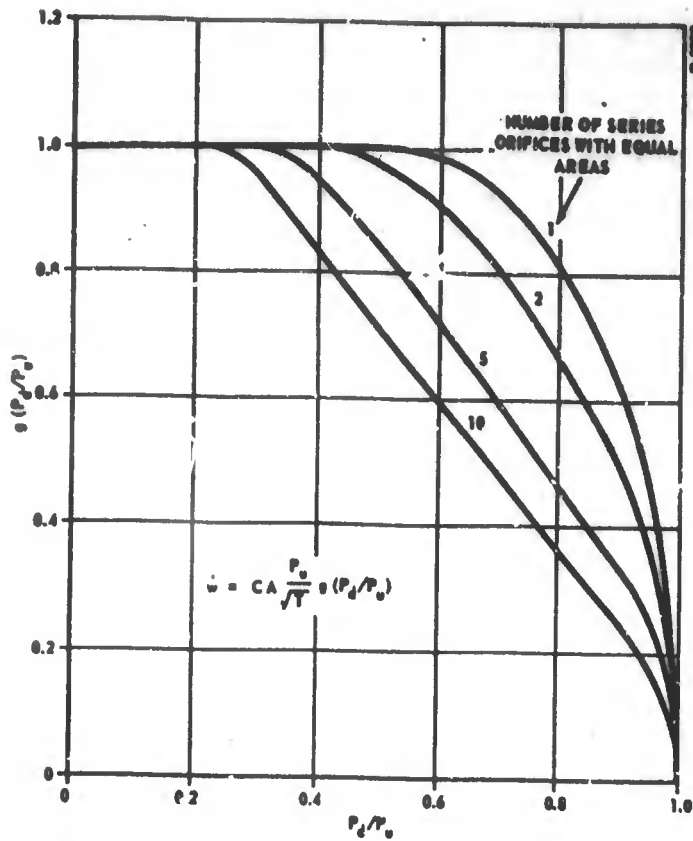


Figure 2-36 - Flow Function for Orifices in Series

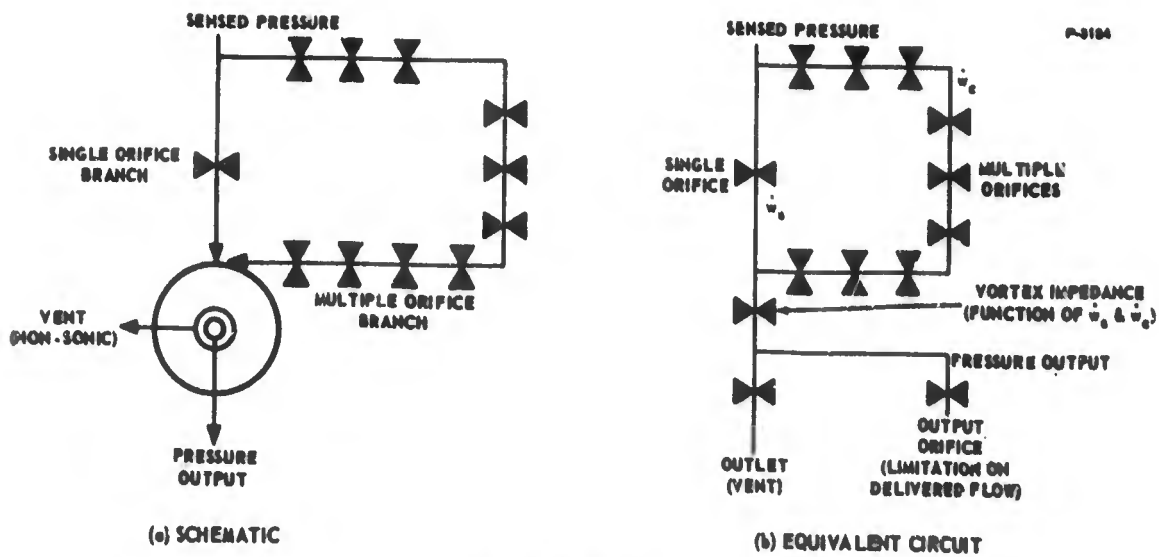


Figure 2-37 - Single Versus Multiple Orifice Bridge

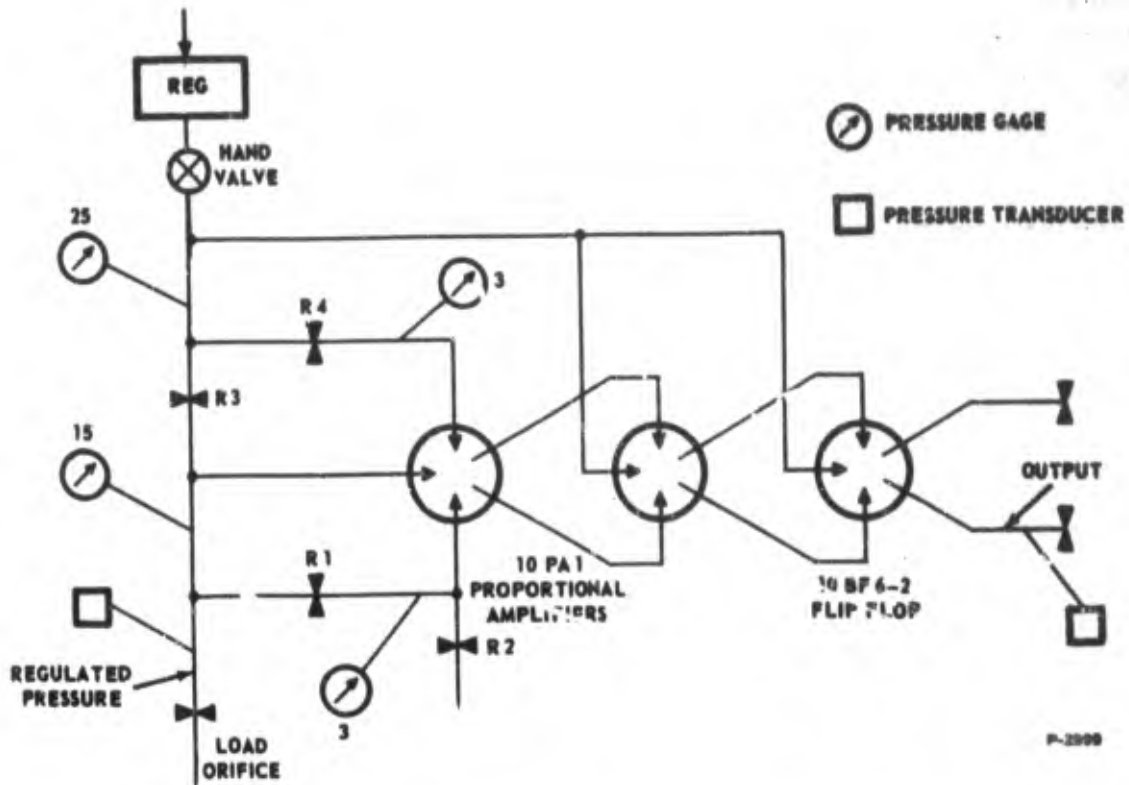


Figure 2-38 - Reference Circuit Test Schematic

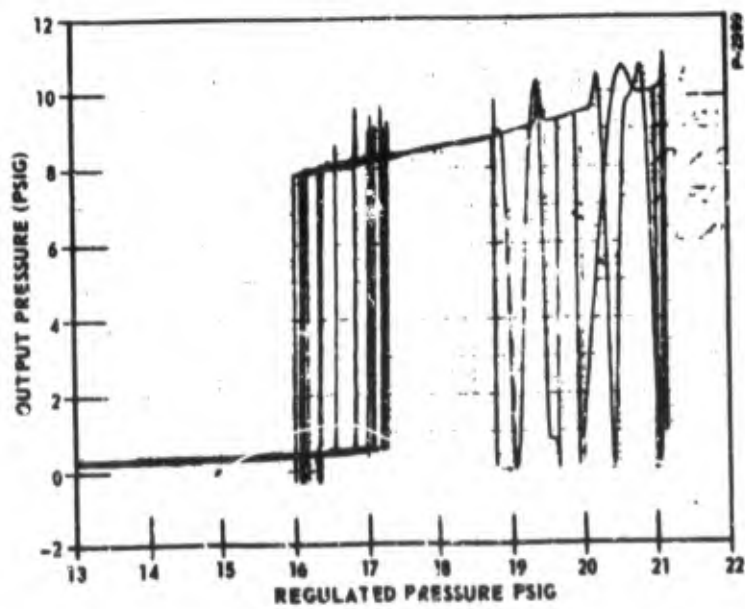


Figure 2-39 - Reference Circuit Switching Characteristic

downstream of orifices R1 and R4 are set equal at quiescent conditions so there is zero differential output from the proportional amplifiers; these pressures do not change symmetrically with small variations of the throttling valve (hand valve) so a differential input signal is applied to the control ports of the first proportional amplifier when the regulated pressure changes as a result of a change in the throttling valve flow. The input differential pressure signal is amplified by the proportional amplifiers to drive a flip-flop output device.

The performance of this reference circuit is shown in Figure 2-39 where several traverses of regulated pressure were made to examine repeatability. The maximum total hysteresis is less than 1.5 psi, but there is some erratic switching at regulated pressures above 19 psig. This test was intended only to demonstrate the feasibility of orifice reference bridges and not the method of reference signal amplification.

2.4.3 Inherent Reference of Feedback Amplifiers

The two preceding reference schemes have been based upon the detection of shifts in the regulated pressure by means of orifice bridge circuits and the amplification of the output of the bridge by means of fluid amplifiers. The output of the reference circuit is then further amplified in the feedback circuit to furnish a signal which is capable of controlling the throttling element.

Since the feedback circuit is required to amplify the output of the reference circuit in any event, the question arises as to the need for amplification in the reference circuit. Elimination of the reference circuit amplifiers has one desirable feature, the drop in pressure across the reference circuit is eliminated, reducing the magnitude of the pressure ratio across the feedback circuit.

Elimination of a separate reference circuit implies that the difference between atmospheric pressure and the regulated pressure will be applied directly to the input of the feedback circuit. Selection of this approach will be made if it can be shown that operating the feedback circuit with a higher gain and lower pressure ratio is an easier task than operating it with a lower gain and a higher pressure ratio.

SECTION 3
SUMMARY OF RESULTS, CONCLUSIONS,
AND RECOMMENDATIONS

3.1 SUMMARY OF RESULTS

The following results were obtained during Phase I of this project.

3.1.1 Throttling Methods

Vortex valves are variable impedance fluid state devices. Operation of vortex valves requires that a control pressure greater than the supply pressure be available. The turndown ratio which can be obtained and the P_C/P_S ratio required depend upon the exact configuration. The double exit valve can deliver turndown ratios of greater than 8 to 1 with high pressure nitrogen gas.

It can be demonstrated that the use of a fixed area orifice to drop the vortex valve supply pressure below the bottle storage pressure in order to obtain the necessary P_C/P_S ratio is impractical. This is a consequence of the fact that the pressure dropping orifice becomes sonic during bottle blowdown and becomes incapable of being controlled by the downstream vortex valve when the bottle pressure has decreased only slightly.

It can be shown that no significant increase in turndown will result from connecting vortex valves in series. However, a significant decrease in the maximum P_C/P_S ratio required to achieve maximum turndown of a vortex valve will be realized by connecting it in series with a vortex pilot valve.

The problem of obtaining a control pressure higher than the supply pressure can be solved either by using a mechanically variable area at the outlet of the pressure bottle or by using a pressure bottle with two compartments charged to different pressure levels. The first approach has a moving part in the system and hence is not strictly a fluid state device. While the weight of the dual volume tank is not appreciably greater than a single volume tank for the same weight of gas, it will occupy a greater volume.

3.1.2 Feedback Methods

The confined jet amplifier is a fluid state device which permits a low pressure source to control a high pressure source. By varying the geometry and spacing of the nozzle and receiver several gain characteristics can be achieved. Useful operation in the range of $P_C/P_S = 0.15$ has been obtained. Output pressure recoveries up to 70% of the supply pressure have been achieved with a flowing load. One highly useful property of the device is that it can be designed so that output pressure is insensitive to supply pressure changes over a wide range. Control of a confined jet amplifier by means of a vortex valve which throttles the confined jet amplifier vent has been demonstrated.

3.1.3 Reference Methods

Changes in the regulated pressure can be detected and amplified by means of orifice bridge circuits and either jet-on-jet or vortex pressure amplifiers. Although the change in regulated pressure is amplified, the level of the output is lower than the regulated pressure. Use of reference amplification will depend upon whether it is more difficult to obtain gain or pressure ratio in the feedback circuit.

3.2 CONCLUSIONS

The following conclusions have been drawn from the results:

- (1) No fixed area orifice having any appreciable pressure drop can be placed in the main flow path if the pressure regulator is to throttle flow over a wide range.
- (2) No fluid state device, other than the vortex valve, is capable of throttling a flow with acceptable efficiency. The vortex valve requires a source of control pressure higher than the supply pressure.
- (3) Conclusions (1) and (2) jointly lead to the conclusion that either a mechanically variable orifice or a dual volume pressure bottle are required to implement a throttling pressure regulator.
- (4) The feedback amplification circuit must be based on the confined jet amplifier. No other fluid state component has the high pressure recovery and low P_C/P_S ratio associated with this device.

3.3 RECOMMENDATIONS

On the basis of the above conclusions, it is evident that either a system based on the dual volume tank or a mechanically variable orifice must be recommended for development during Phase II. The dual volume tank approach has the advantage of not requiring a moving part and thus satisfies the original project goal. The dual compartment tank will require a greater volume than a single volume tank. The mechanically variable area approach will allow the use of a single volume tank and may be more efficient with a variable load.

In view of the fact that the use of a moving part deviates from the ideal of the fluid state system, the dual tank approach is considered as the primary recommendation. A schematic of this system is shown in Figure 3-1.

In this system, the throttling element will be a dual exit vortex valve connected in series with a pilot vortex valve to reduce the P_C/P_S ratio for shut-off. The feedback amplifier circuit will consist of confined jet amplifiers controlled by vortex valves. Since confined jet amplifiers can operate at $P_C/P_S < .250$, three confined jet amplifiers should be sufficient to elevate the P_R pressure to a level sufficiently high to control the supply at pressure P_{BC} . It is assumed that no reference circuit as such will be needed; the regulated pressure will serve as a direct input to the feedback amplifier circuit. An adjustable orifice located at the outlet of the lowest level vortex valve in the feedback circuit will serve as a fine adjustment for the regulated pressure. Coarse adjustments in the regulated pressure will require changes in the geometry of the confined jet amplifiers. The final system design should provide for the convenient replacement of the confined jet amplifier nozzles and receivers and changing of the spacing.

The alternate recommendation is that the pressure regulator incorporate a mechanical element similar to that described in Section 2.2.5. The over-all schematic for this approach is shown in Figure 3-2. The feedback amplifier circuit will be similar to that used with the dual bottle approach.

A final choice of system for future development is left to the Army Missile Command. There are considerations in making a final choice which are not completely known to the responsible Bendix technical personnel. Both approaches suggested should provide a pressure regulation system compatible with the application.

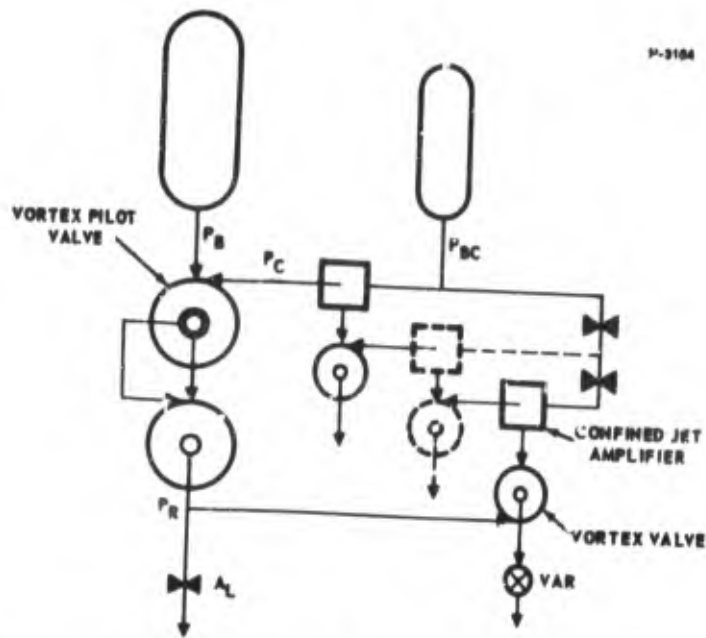


Figure 3-1 - Schematic of System with Dual Volume Tank

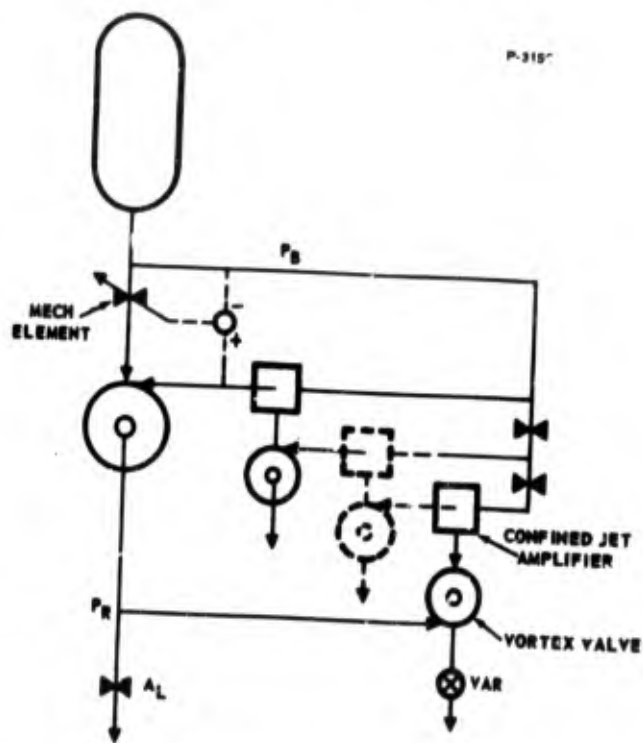


Figure 3-2 - Schematic of Pressure Regulator with Mechanical Element

APPENDIX A

NOTATION FOR SECTIONS 1 THROUGH 3

NOTE: Pressures will be in absolute units (psia) unless otherwise specified in text.

- A = Flow area - in²
- A_A = Exit hole area of vortex valve A - in²
- A_B = Exit hole area of vortex valve B, also cross-sectional area of button - in²
- A_d = Mean effective area of diaphragm - in²
- A_e = Exit hole area - in²
- A_F = Feedback orifice area - in²
- A_L = Load orifice area - in²
- A_m = Effective area of a series of orifices - in²
- A_N = Confined jet amplifier nozzle area - in²
- A_S = Supply orifice area - in²
- C_d = Orifice discharge coefficient - dimensionless
- C_2 = Characteristic gas coefficient - $\sqrt{^\circ R}/\text{sec}$
- D = Diameter - in.
- F_d = Diaphragm spring force - lbs
- f_n = Natural frequency - cps
- g = Standard sea level acceleration of gravity = 386 in/sec²
- k = Ratio of specific heats of gas - dimensionless
- K = Spring rate - lbs/in.
- L = Length - in.
- m = Mass - lb-sec²/in.

- n = Number of orifices in series - dimensionless
- P = Pressure - psia or psig
- P_B = Bottle pressure - psia or psig
- P_{BC} = Control bottle pressure - psia or psig
- P_C = Control pressure - psia or psig
- P_{CSC} = Control pressure for supply flow cutoff - psia or psig
- P_d = Pressure downstream of a pneumatic component - psia or psig
- P_e = Exit pressure - psia or psig
- P_F = Feedback pressure - psia or psig
- P_m = Interstage pressure - psia or psig
- P_R = Regulated pressure - psia or psig
- P_S = Supply pressure - psia or psig
- P_u = Pressure upstream of pneumatic component - psia or psig
- P_V = Mean vortex chamber pressure - psia or psig
- P_O = Inlet pressure to a series of orifices (Used in Appendix D), also outlet pressure - psia or psig
- P_1 through P_n = Pressure downstream of first through nth orifices in a series of orifices - psia or psig
- R = Ideal gas constant - lb-in/lb^oR
- R_t = Turndown ratio of a valve - dimensionless
- R_{tA} = Turndown ratio of valve A - dimensionless
- R_{tB} = Turndown ratio of valve B - dimensionless
- R_{to} = Overall turndown ratio - dimensionless
- T = Absolute temperature of gas at zero velocity - ^oR
- t_o = Total operating time - sec
- \dot{w} = Weight flow of gas - lbs/sec
- \dot{w}_B = Flow from bottle at pressure P_B - lb/sec

- \dot{w}_{BC} = Flow from bottle at pressure P_{BC} - lbs/sec
 \dot{w}_C = Control flow - lbs/sec
 \dot{w}_{CA} = Control flow for vortex valve A - lbs/sec
 \dot{w}_{CB} = Control flow for vortex valve B - lbs/sec
 \dot{w}_F = Vent flow of feedback circuit - lb/sec
 \dot{w}_L^* = Flow through load - lb/sec
 \dot{w}_N = Normalizing flow - lb/sec
 \dot{w}_O = Outlet flow - lb/sec
 \dot{w}_R = Vent flow of reference circuit - lb/sec
 \dot{w}_S = Supply flow - lbs/sec
 \dot{w}_T = Flow through throttling element - lbs/sec
 W_B = Weight of gas initially stored at pressure P_B - lbs
 W_{BC} = Weight of gas initially stored at pressure P_{BC} - lbs
 V_B = Volume of W_B lbs of gas - in³
 V_{BC} = Volume of W_{BC} lbs of gas - in³
 η_F = Feedback system efficiency expressed as a fraction - dimensionless

Subscripts

- 1 through n - Refers to first through nth orifices in a series of orifices
 i - Refers to initial conditions
 f - Refers to final conditions
 j - Refers to jth orifice in a series of n orifices
 min - Refers to minimum value
 max - Refers to maximum value

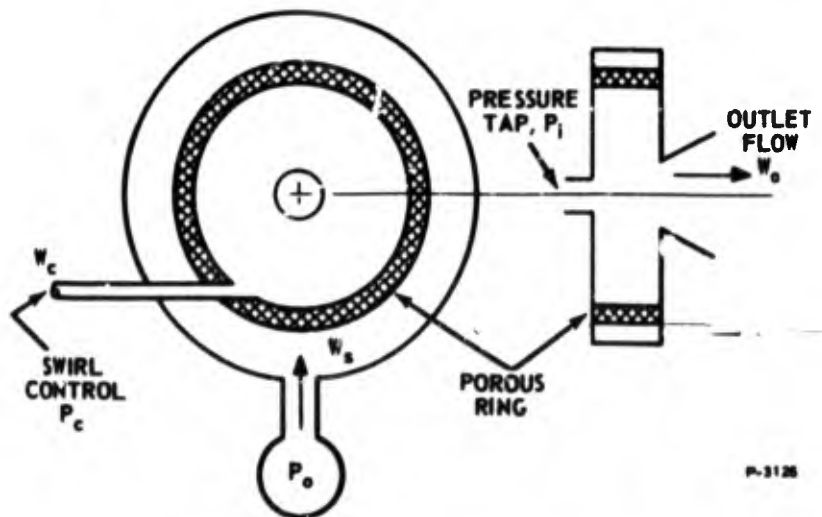
Bendix

APPENDIX B
THEORETICAL ANALYSIS OF VORTEX VALVES

This appendix provides a summary of an analysis accomplished for the purpose of describing vortex valve performance. It has been abstracted from "Phenomenology of Vortex Flow and Its Application to Signal Amplification" by L. B. Taplin and presented at Pennsylvania State University; Summer Engineering Seminars, Fluid Control Systems; July 6-16, 1965.

B.1 EXPERIMENTAL OBSERVATIONS OF PANCAKE VORTEX CHAMBERS

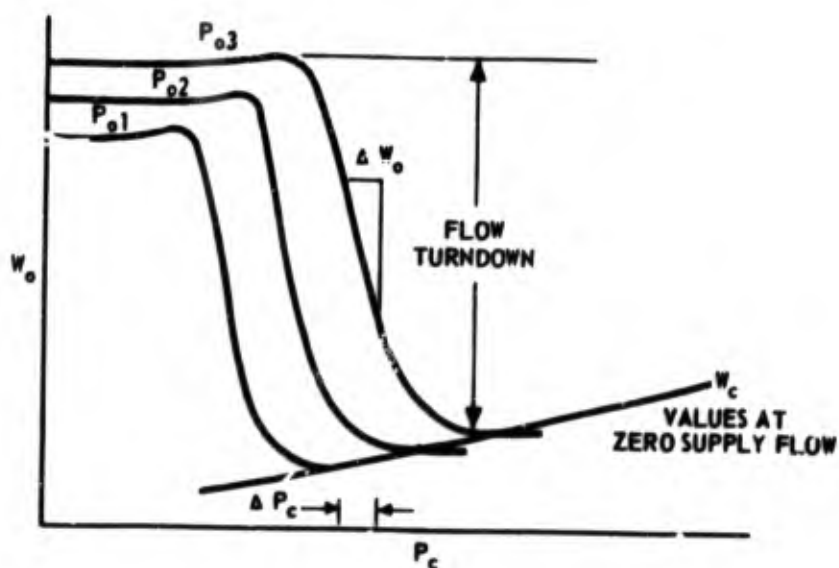
If a simple chamber is constructed as shown in the schematic, Figure B-1, some simple experiments will easily show the various amplifying properties which the vortex flow field possesses. The chamber is constructed so that the supplied radial flow component enters the chamber as uniformly as possible. One method, as shown, for accomplishing uniform radial chamber flow utilizes a porous ring pressurized externally by the supply pressure, P_o . To excite vortex flow, a tangential control port is used which introduces a tangential flow component



B-1 - Simple Vortex Chamber

Bendix

just at the inner edge of the porous ring. A number of tangential ports may be used to again achieve a high degree of uniformity in the flow field. The combined flows move towards the exit hole and in observing this fluid motion it is readily apparent that the radial velocity of the fluid must increase as the fluid approaches the exit. In addition, if the tangential velocity of a particle of fluid is observed, it will be noted that its tangential velocity increases as it moves towards the exit. This increase in tangential velocity must result if angular momentum of the fluid flow is to be conserved. Here, then, are two velocity amplifying properties of the vortex flow field. The tangential velocity amplification or gain is of particular importance as it is this gain that is primarily responsible for most of the unique vortex amplifier and sensing devices which are in use today. In particular, the tangential velocity increase leads to a centrifugal pressure buildup across the vortex chamber in a radial direction between the exit hole and the outer wall of the chamber. If such a centrifugal pressure buildup exists, then the chamber should present more resistance to flow as the chamber swirl or control flow component is increased. In order to examine this property of centrifugal pressure drop in its purest form it is necessary that the porous ring and supply plenum be designed to present a very small resistance to flow in comparison to the exit hole resistance. With the chamber designed in this manner, and operating the chamber with a regulated supply source, P_o , curves of weight flow as a function of control pressure or control flow may be plotted. These characteristic curves have the form shown in Figure B-2.



P-3126

Figure B-2 - Vortex Chamber Characteristic Curves with Regulated Supply

When the supply pressure is regulated, if there is a centrifugal pressure drop across the flow field, less pressure should be available at the exit hole to expel the fluid and the device should throttle flow as demonstrated by the experiment. A number of things are, of course, of immediate interest when one examines the experimental curves. Probably first, is the question of what controls the throttling range or turndown ratio. Looking at the minimum flow point, if the flow at the supply port is measured, it is found that this flow is zero or perhaps slightly reversed. The wall pressure has built-up to the extent that the supply flow is cut off; i.e., there is a value of control flow which causes supply cutoff. The turndown ratio for a given supply pressure is the ratio of maximum flow before throttling starts to the control flow which causes supply cutoff. If centrifugal pressure forces cause this throttling to take place, then tangential velocity of the flow field plays an important role in setting up a wall pressure to cause cutoff. Obviously, if the tangential velocity is high at the outer wall of the chamber and therefore throughout the chamber, the centrifugal pressure buildup should be large. Since the tangential velocity at the outer wall is a function of conserved angular momentum, then higher wall velocities should imply a higher control influx momentum. Writing the expression for outer wall velocity:

$$V_{to} = \frac{W_c v_c}{W_c + W_o}$$

It is noted that V_{to} is larger when the momentum rate, $W_c v_c$, is larger. Now, it is obvious that turndown ratio can be improved if for a given wall velocity, control velocity, v_c , is increased and therefore the control mass flow, W_c , is decreased. The higher control velocity requires a higher control pressure which in some applications may be a disadvantage.

Also, of interest is the flow gain -- another amplifying property -- of the device, $\Delta W_o / \Delta W_c$. It might be expected that this gain goes hand in hand with the turndown ratio and therefore higher flow gains are achieved if high control velocities are used.

The curves may be plotted in another way as shown in Figure B-3. Here the control pressure has been regulated and supply flow is varied to obtain the plots of W_o versus P_o . The upper curve in Figure B-3 defines the maximum flow of the chamber versus supply pressure with no control flow. The upper curve is essentially that of an orifice --

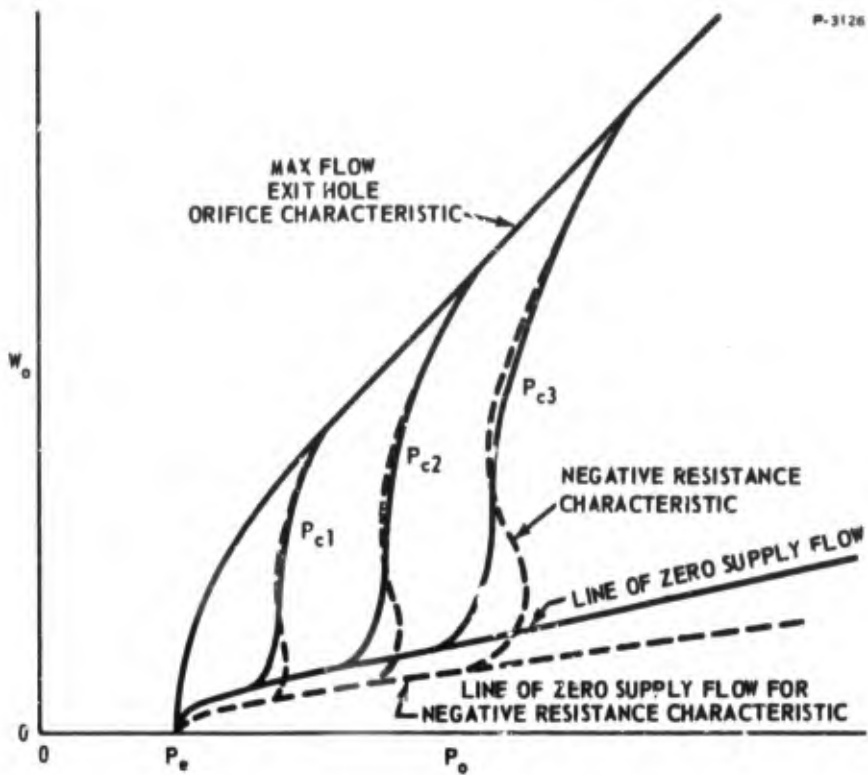


Figure B-3 - Vortex Chamber Characteristic Curves with Regulated Control

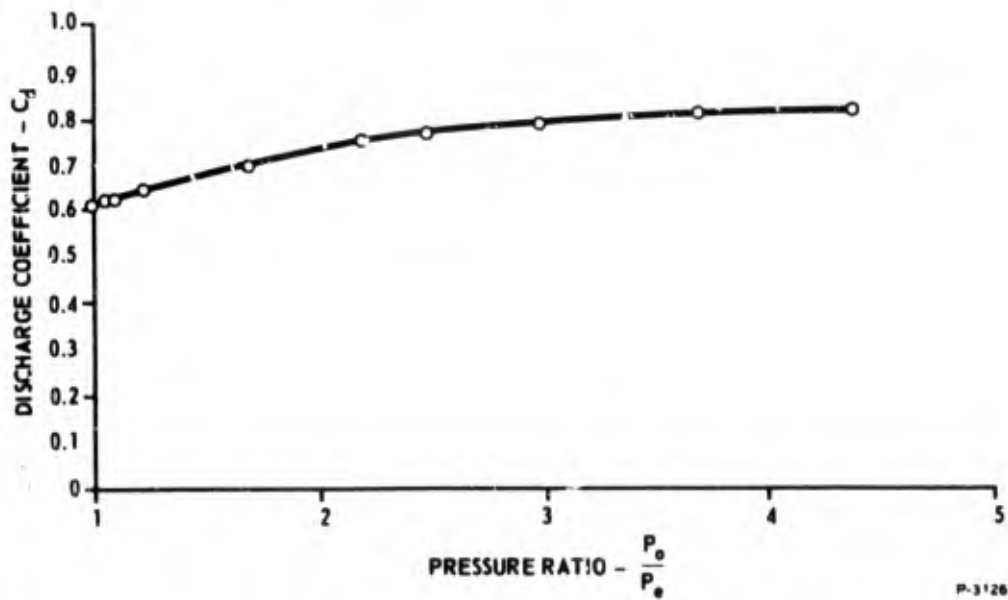


Figure B-4 - Vortex Chamber Maximum Flow Discharge Coefficient

the exit hole -- characteristic with a discharge coefficient that varies with supply to exit pressure ratio as shown in Figure B-4. This discharge coefficient curve was obtained for a particular chamber and values do change somewhat with geometry of the chamber. The trend in coefficient change is in general correct for most pancake shaped chambers.

Returning to Figure B-3 the locus of points defining the minimum flow through the chamber constitute that characteristic flow curve obtained for control flow alone with supply flow zero. In examining the flow data in Figure B-3, it is interesting to note that the constant control pressure characteristic curves are nearly equally spaced across the map in the direction of increasing control and supply pressure. The equal spacing indicates that a proportional relationship between P_c and P_o exists.

Another interesting observation in testing some chambers is that multivalued flows can exist for a given supply pressure; i.e., the characteristic curves exhibit a region of negative resistance. These negative resistance curves are indicated by the dashed lines in Figure B-3. In general, these negative resistance characteristics show up when the vortex chamber thickness is relatively large and the supply plenum resistance is low in comparison to the exit hole resistance.

Another interesting experiment involves monitoring the pressure, P_i , at the center of the vortex chamber wall as flow changes; see Figure B-1. A plot of this pressure, P_i versus supply pressure for regulated control pressure has a form very similar to the weight flow characteristic curve; see Figure B-5. In fact, if the hole for measuring P_i is properly sized the pressure measured is virtually that average pressure which acts on the exit hole of the vortex device to expel the fluid. Further, as will be discussed later, this pressure is very closely related to the calculated pressure which occurs at the rim of the chamber exit hole.

A close indication of the value of P_i can be found directly from the weight flow characteristic curves if the discharge coefficient for the exit hole is reasonably independent of the degree of chamber swirl or control flow.

This determination of P_i , as demonstrated in Figure B-6, where for a given set of quiescent operating pressures, and weight flow -- the circled point -- a dashed line constructed horizontally across the graph

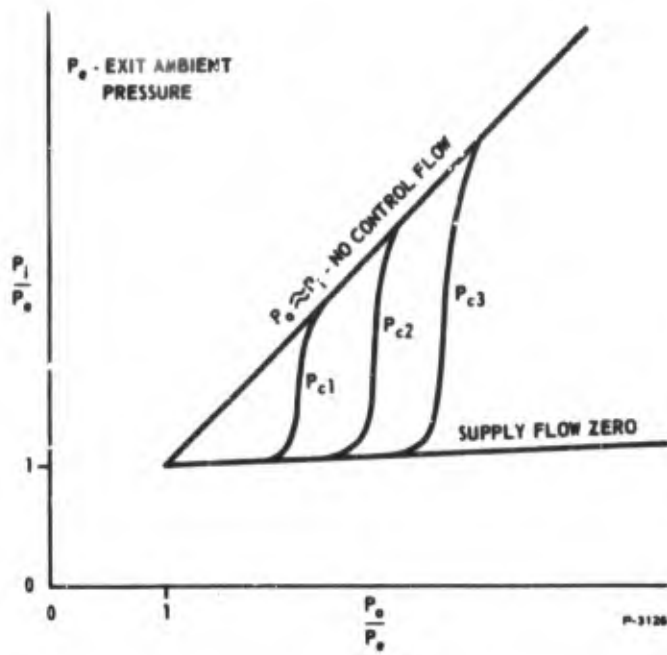


Figure B-5 - Characteristic Curves of Vortex Chamber Center Pressure, P_i

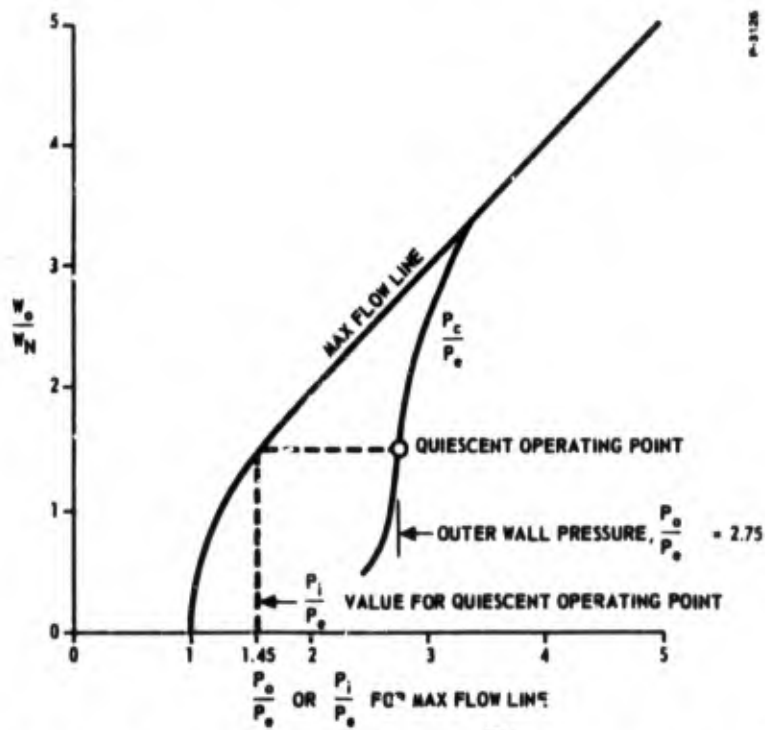


Figure B-6 - Determination of $\frac{P_i}{P_e}$ from Weight Flow Characteristic Curves

to the maximum flow line and then down to the P_0/P_e axis gives the value of P_i/P_e if the discharge coefficient is independent of swirl. The curves shown in Figure B-6 have been normalized with respect to the ambient or back pressure, P_e , on the exit hole of the valve and a normalizing weight flow, W_N , which is given by:

$$W_N = \frac{C_d C_A P_e}{\sqrt{T}}$$

This flow parameter, W_N , is then representative of the exit hole size, operating gas media, and gas temperature. This normalization will be used in developing a mathematical model for the vortex chamber.

The pressure ratio across the vortex flow field in the radial direction is given by P_0/P_i or, for the example in Figure B-6, $P_0/P_i = 2.75/1.45$. It is interesting to note that when the exit hole is flowing sonically, $P_i/P_e > 2$, the pressure ratio across the chamber, P_0/P_e , can be much larger than critical. When the exit hole is flowing sonically, back pressure cannot affect the flow through the chamber for a given supply and control pressure. In the normalized plot a change in P_e causes a shift in the operating point, but W_N and P_c/P_e change in a manner so that the actual weight flow, W_0 , remains constant. An example of how the pressure ratios and weight ratio change for shifting back pressures is shown in Figure B-7 where P_0 , P_c , and W_0 are all constant. With a starting quiescent point at $P_0/P_e = 8$, with the control port sized so that $P_c/P_e = 10$ and $W_0/W_N = 4$, if the back pressure is doubled the new operating point will be at $P_c/P_e = 5$ with P_0/P_e at 4 and $W_0/W_N = 2$. Since W_N is doubled if P_e is doubled, W_0 is the same value as before. This operation provides some insight into the nature of the vortex valve. It can be looked upon in general as an adjustable set of orifices in which the ratio of P_c/P_0 defines the apparent size and number of orifices. For the case where the exit hole is known to be sonic, a single orifice can be found to exhibit the same flow relationship versus P_0/P_e .

The normalization selected has some interesting characteristics. The maximum flow line above a P_0/P_e of 2 is a straight line of unity slope; i.e., W_0/W_N equals P_0/P_e above values of 2.

The constant P_c/P_e lines must intersect with the maximum flow line where $P_0/P_e = P_c/P_e$. There is a strong indication that supply flow is always cut off for a given P_c/P_0 ratio and therefore the line of

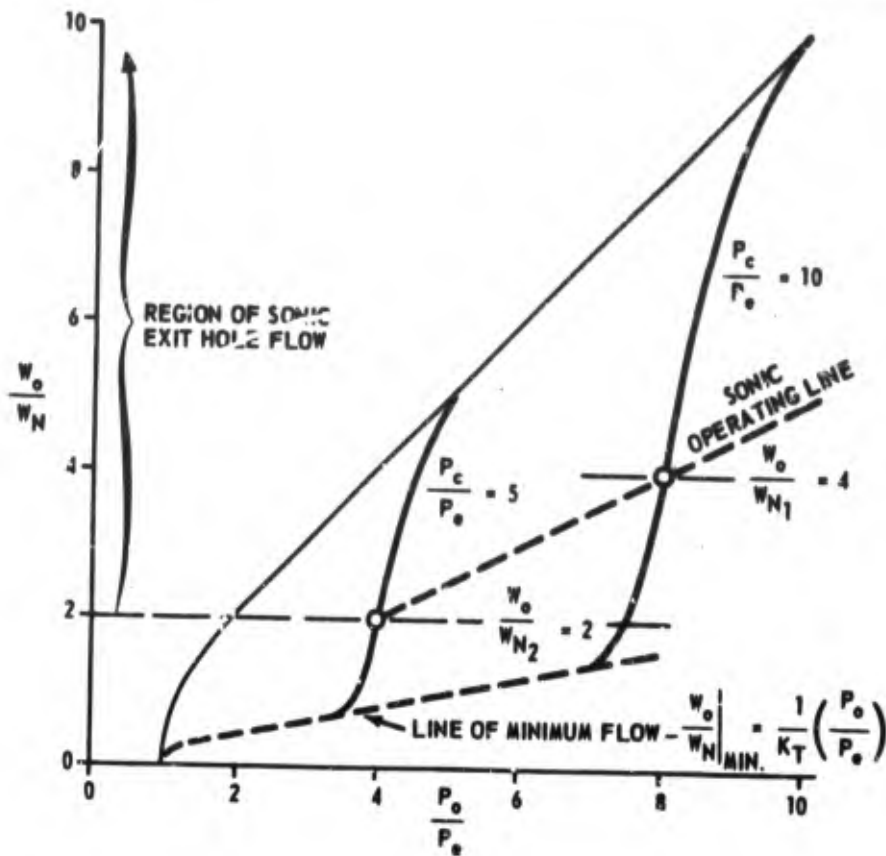


Figure B-7 - Operation of Vortex Valve with Exit Hole Flow Sonic

minimum flow (supply flow zero) is a straight line except at low values of P_0/P_e and has the equation:

$$\frac{P_c}{P_e} = K_T \left(\frac{W_0}{W_N} \right)$$

where K_T is the turndown ratio $W_0 \text{ max}/W_c$. There are some experimental discrepancies and theory does not as yet prove this point; but it is a reasonably good approximation as the values in general show the same turndown ratio above P_0/P_e pressure ratios of 2.

B.2 THEORETICAL FLOW AND PRESSURE CHARACTERISTICS

In order to determine the behavior of the flow through a vortex chamber it is first necessary to know the distribution of the tangential velocity as a function of chamber radius. This distribution of tangential velocity depends on chamber geometry, the magnitude of swirl and the

viscosity of the fluid. Where the viscosity is very low, conservation of angular momentum indicates that the tangential velocity must increase with decreasing radius; i.e., the tangential velocity, V_t , at any radius r is given by:

$$V_t = \frac{V_{to} r_o}{r} \quad (B-1)$$

where

V_{to} = tangential velocity at the outer wall - in/sec

r_o = maximum chamber radius - in.

As viscosity becomes very large, the fluid can rotate as a solid body and then the tangential velocity is given by:

$$V_t = \frac{V_{to} r}{r_o} \quad (B-2)$$

In general, the tangential velocity can be expressed as:

$$V_t = V_{to} \left(\frac{r}{r_o} \right)^n \quad (B-3)$$

where

$n = +1$ for a free vortex

$n = -1$ for solid body rotation.

A plot of these velocity distributions versus chamber radius, r , is shown in Figure B-8 for various values of n . In the case of the free vortex where the viscosity is low, the tangential velocity must eventually peak and then decrease and approach zero velocity at the center of the chamber since no fluid has completely zero viscosity. Also, for gases, a breakdown in tangential velocity must occur as chamber geometry cannot support supersonic flow. For gases, n can be taken as $+1$ until the velocity breaks down as indicated by the dashed curve in Figure B-8. Since we are interested in the pressure drop developed by the flow field, a suitable " n " value can be found for an experimental unit which gives some indication of the behavior of the tangential flow.

Bender

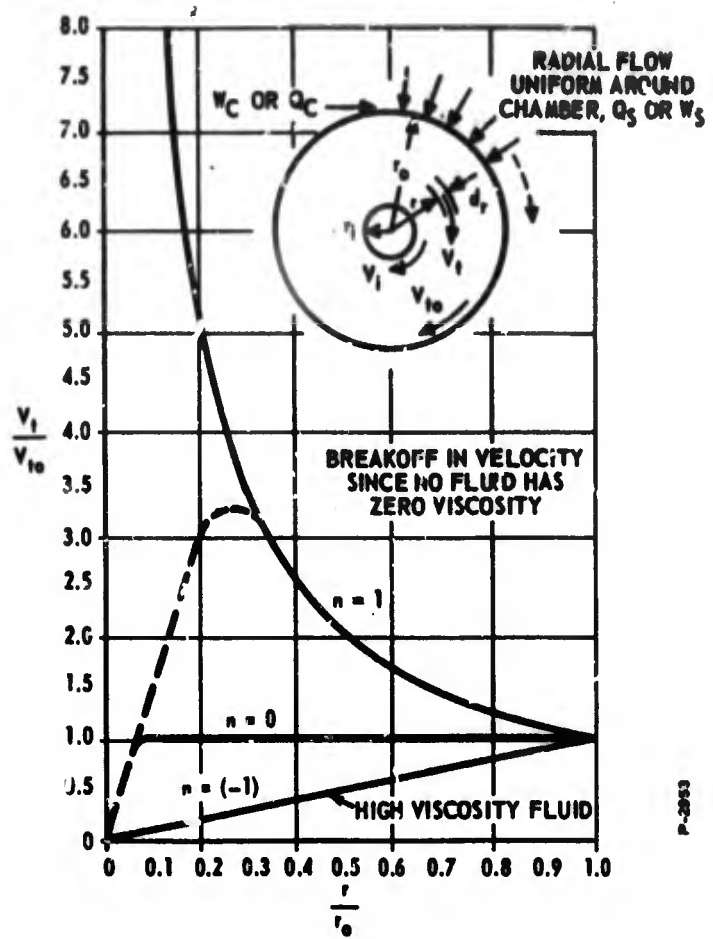


Figure B-8 - Vortex Tangential Velocity Distribution

The differential pressure developed across a differential radius dr is given by:

$$dP = \frac{\rho V_t^2 dr}{r} \quad (B-4)$$

where

- ρ = fluid mass density - lb./sec²/in⁴
- V_t = tangential velocity at radius r - in./sec
- r = chamber radius - in.
- dP = differential pressure across dr - psid

At this point some assumptions will be made:

- (a) Fluid temperature remains nearly constant.
- (b) The weight flow leaving the exit hole is very closely a function of P_i at radius r_i .
- (c) For gases $n = 1$, that is free vortex flow exists until a maximum tangential Mach number is reached, see Figure B-9.

As noted in Figure B-9, a higher initial outer wall velocity may cause a higher maximum tangential Mach number occurring at radius r_m . This maximum velocity is an unknown and will be found to be a variable depending on the operating pressure ratio across the chamber. Returning to equation (B-4), the density from the equation of state is $\rho = P/gRT$. Therefore:

$$\frac{dP}{P} = \frac{V_t^2}{gRT} \frac{dr}{r} \quad (B-5)$$

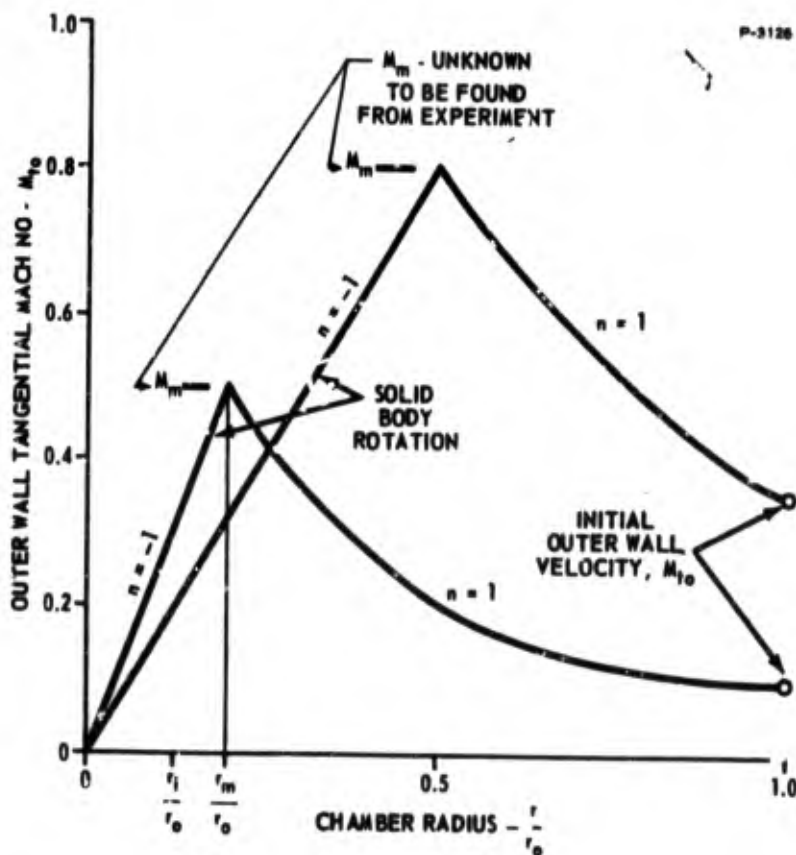


Figure B-9 - Assumed Tangential Velocity Profile for Gases

Bendix

Sonic velocity for a gas of temperature T is given by:

$$V_s = \sqrt{k g R T} \quad (\text{B-6})$$

therefore:

$$\frac{dP}{P} = k M_t^2 \frac{dr}{r} \quad (\text{B-7})$$

where

$$M_t = \frac{V_t}{V_s}$$

Using the velocity profiles of Figure B-9, equation (B-7) may be integrated from radius r_i to r_o for two different conditions. When $r_m < r_i$ or $M_{to} r_o / M_m r_i < 1$

$$\frac{P_o}{P_i} = \epsilon^{K M_{to}^2} \quad (\text{B-8})$$

where

$$K = \frac{k}{2} \left(\frac{r_o^2}{r_i^2} - 1 \right) \quad (\text{B-9})$$

and when $r_m > r_i$ or $\frac{M_{to} r_o}{M_m r_i} > 1$

$$\frac{P_o}{P_i} = \epsilon^{\frac{k}{2} \left[M_m^2 \left(2 - \frac{M_m^2 r_i^2}{M_{to}^2 r_o^2} \right) - M_{to}^2 \right]} \quad (\text{B-10})$$

It is to be noted that when $M_{to} r_o / M_m r_i = 1$, equations (B-8) and (B-10) are equal. At low values of M_{to} , the vortex flow behaves as a free vortex for all radii between r_o and r_i .

From conservation of angular momentum, the outer wall velocity is given by:

$$M_{to} = \frac{\eta W_c M_c}{W_c + W_s} = \frac{\eta \frac{W_c}{W_N} M_c}{\frac{W_o}{W_N}} \quad (B-11)$$

where

$$W_N = \frac{C_d C A_e P_e}{\sqrt{T}} \quad (B-12)$$

$$\frac{W_o}{W_N} = \frac{W_c}{W_N} + \frac{W_s}{W_N} \quad (B-13)$$

The expressions for weight flow as a function of pressures must now be developed. It will be recalled that orifice flow is given by:

$$W = \frac{C_d C A P_u}{\sqrt{T}} f_1 \left(\frac{P_d}{P_u} \right) \quad (B-14)$$

where

f_1 = ratio of subsonic to sonic flow, see Figure B-10.

For sonic flow

$$W = \frac{C_d C A P_u}{\sqrt{T}} \quad (B-15)$$

An elliptical approximation to the f_1 function is used in this analysis where:

$$f_1 \left(\frac{P_d}{P_u} \right) = \frac{2 P_d}{P_u} \sqrt{\frac{P_u}{P_d} - 1} \quad (B-16)$$

(See Figure B-10)

The maximum flow error occurs near $P_d/P_u = 0.8$ and is approximately 2.5 percent. Since the discharge coefficient is not known to this accuracy the approximation of f_1 is considered adequate for purposes of the

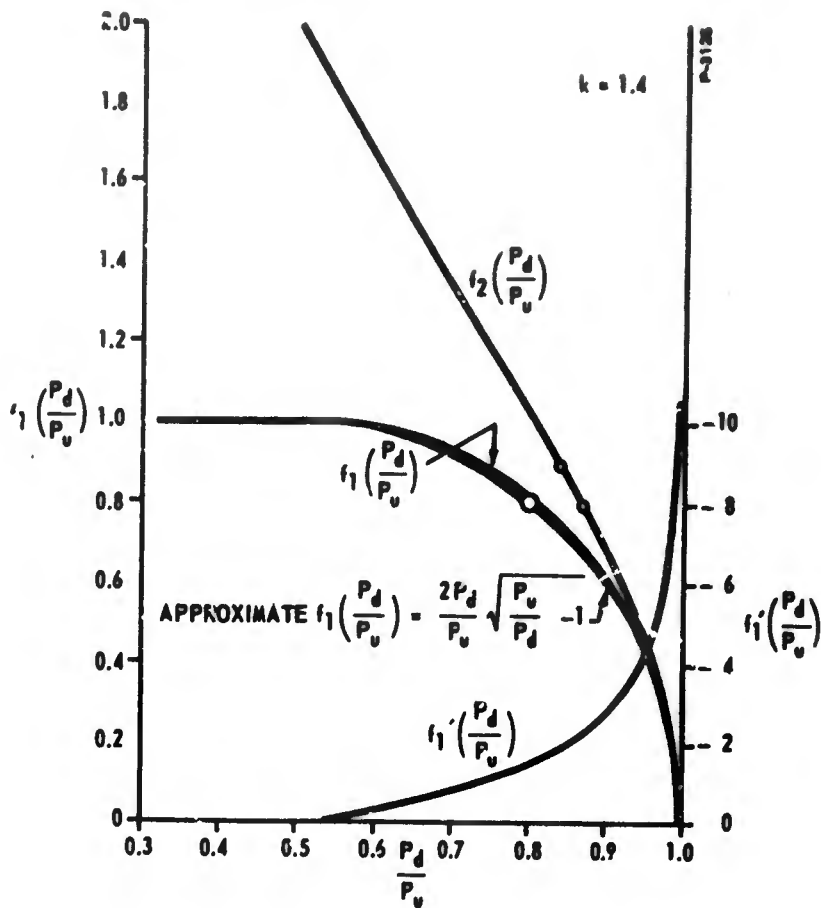


Figure B-10 - Gas Flow Functions

following analysis. Care must be used to remember that when $P_u/P_d \geq 2$, $f_1(P_d/P_u)$ remains unity.

The momentum expression $W_c M_c/W_N$ can be derived as follows:
For sonic flow with $k = 1.4$

$$\frac{W_c M_c}{W_N} = 0.915 \frac{C_{dc} A_c P_c}{C_d A_e P_e} \quad (B-17)$$

where $M_c = 0.915$, the Mach number at the orifice throat based on the upstream temperature.

For subsonic flow

$$\frac{W_c M_c}{W_N} = 0.915 \left(\frac{C_{dc} A_c P_c}{C_d A_e P_e} \right) f_3 \left(\frac{P_o}{P_c} \right) \quad (B-18)$$

where f_3 is plotted in Figure B-11.

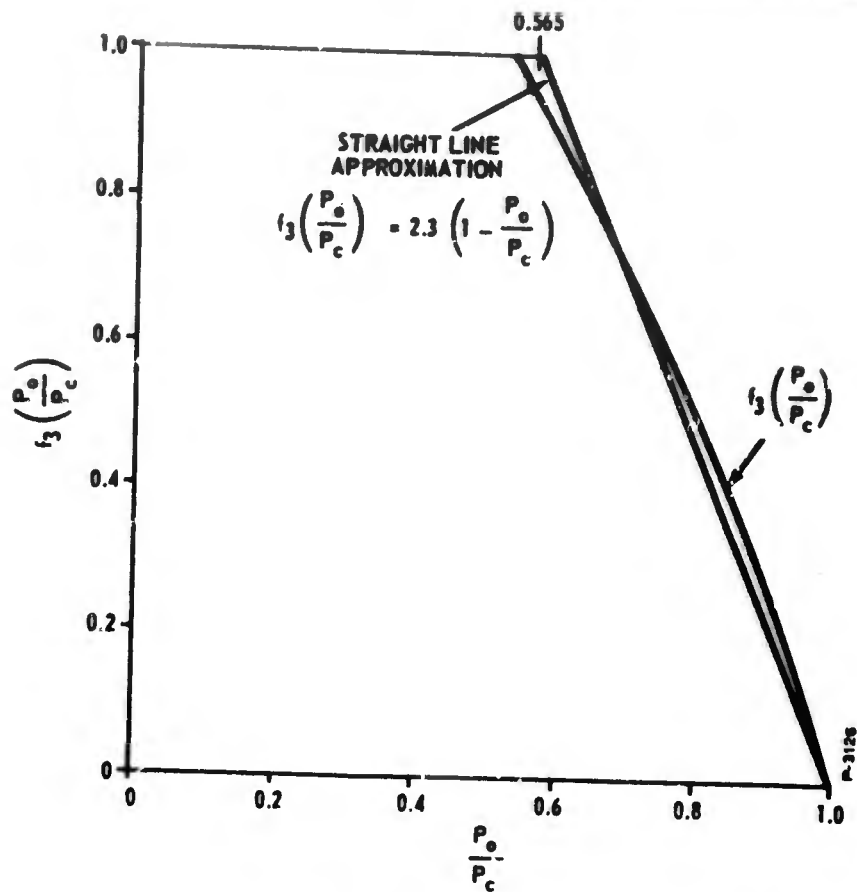


Figure B-11 - Momentum Function - $f_3 \frac{P_0}{P_c}$

A straight line approximation to this function as shown in Figure B-11 describes f_3 as follows:

$$f_3 \left(\frac{P_0}{P_c} \right) = 2.3 \left(1 - \frac{P_0}{P_c} \right) \quad (\text{B-19})$$

and introduces a maximum error of 10 percent in momentum. Even though this error is relatively large, it will be helpful to use the following approximate momentum expression for subsonic flow:

$$\frac{W_c M_c}{W_N} = \frac{2.1 C_{dc} A_c}{C_d A_e} \left(\frac{P_c}{P_e} - \frac{P_0}{P_e} \right) \quad (\text{B-20})$$

where it is seen that the momentum efflux at the throat of an orifice to a 10 percent maximum error is linearly related to the pressure drop across the orifice for subsonic throat velocities. Again care must be

used to remember that for $P_c/P_o > 2$, sonic conditions exist and equation (B-17) must be used. Most practical applications of vortex devices involve primarily subsonic flow at the control orifice. P_o is outer wall pressure in the vortex chamber which acts as a back pressure on the control jet orifice.

The flow leaving the exit hole using equation (B-16) is given by:

$$\frac{W_o}{W_N} = 2 \frac{P_i}{P_e} - 1 \quad \text{for subsonic flow } \frac{P_i}{P_e} < 2 \quad (\text{B-21})$$

The exit flow for sonic exit velocity is given by:

$$\frac{W_o}{W_N} = \frac{P_i}{P_e} \quad \text{for sonic flow } \frac{P_i}{P_e} \geq 2 \quad (\text{B-22})$$

Recapitulating:

$$\frac{P_c}{P_i} = \epsilon^{f(M_{to})} \quad (\text{B-23})$$

where

$$f(M_{to}) = \frac{k}{2} \left[\left(\frac{r_o}{r_i} \right)^2 - 1 \right] M_{to}^2 = K M_{to}^2 \quad \text{for } \frac{M_{to} r_o}{M_m r_i} < 1$$

or

$$f(M_{to}) = \frac{k}{2} \left[M_m^2 \left(2 - \frac{M_m^2 r_i^2}{M_{to}^2 r_o^2} \right) - M_{to}^2 \right] \quad \text{for } \frac{M_{to} r_o}{M_m r_i} > 1$$

$$M_{to} = \frac{2.1 \eta C_{dc} A_c}{C_d A_e} \left[\frac{P_c}{P_e} - \frac{P_o}{P_e} \right] \quad \text{for subsonic control flow, } \frac{P_o}{P_c} > 0.528 \quad (\text{B-24})$$

$$M_{to} = \frac{0.915 \eta C_{dc} A_c}{C_d A_e} \left(\frac{P_c}{P_e} \right) \quad \text{for subsonic control flow, } \frac{P_o}{P_c} < 0.528 \quad (\text{B-25})$$

$$\frac{W_o}{W_N} = 2 \sqrt{\frac{P_i}{P_e} - 1} \quad \text{subsonic exit flow, } \frac{P_i}{P_e} < 2 \quad (\text{B-26})$$

$$\frac{W_o}{W_N} = \frac{P_i}{P_e} \quad \text{for sonic exit flow, } \frac{P_i}{P_e} > 2 \quad (\text{B-27})$$

$$\frac{W_o}{W_N} = \frac{W_s}{W_N} + \frac{W_c}{W_N} \quad (\text{B-28})$$

$$W_N = \frac{C_{dc} A_e P_e}{\sqrt{T}} \quad (\text{B-29})$$

$$M_m = f \left(\frac{P_c}{P_e} \right) \quad (\text{B-30})$$

The maximum tangential Mach number given by equation (B-30) remains to be determined by using the experimental data. As indicated it is strongly related to the control pressure ratio used. If the assumed velocity profile model is reasonably correct, it can be expected that M_m should never exceed a value of one, as in reality, the vector sum of the tangential and radial velocities cannot exceed one.

Equations (B-23) through (B-30) can now be solved and the theoretical results compared with experimental results.

B-3 THEORETICAL - EXPERIMENTAL CORRELATION

In examining the equations it will be of interest to assume M_m so large that the vortex flow is considered to be that of a free vortex. The vortex chamber tested had a radius ratio, $r_o/r_i = 8$ and a control parameter, $2.1 \eta C_{dc} A_c / C_d A_e = 0.2$. The experimental data is plotted in Figure B-12 with the discharge coefficient C_d as given by Figure B-4 used for the maximum flow line; thus W_o/W_N for maximum flow follows exactly the theoretical form. Since the discharge coefficient for the control characteristic curves is unknown, an assumed value of 0.72 was used to normalize the experimental flow points. The normalizing flow

is given by equation (B-29). It was assumed that the momentum mixing efficiency was at least 90 percent in arriving at the control parameter given as 0.2 above.

Solving the theoretical equations for the values given produced theoretical results which plotted well to the left of the experimental points for all three control pressure ratios shown in Figure B-12. Two choices were now open to adjust parameters to effect a correlation. One choice was the reduction in η , the mixing efficiency, which would move the theoretical data points to the right (in the direction of increasing P_o/P_e). The other choice involved a reduction in radius ratio, below that of the theoretical value of 8. It will be noted that as long as M_m is large, the equations always use the parameter η^2 multiplied by $k/2 (r_o^2/r_i^2 - 1)$ and the choice in adjustment is arbitrary. However, for the lower flow portion of the characteristic curves this arbitrary product does not occur as $f(M_{to})$ involves the use of M_m . In order to get a satisfactory correlation at low flows, r_o/r_i had to be reduced to a value of 5.08 compared to the theoretical value of 8. It can be reasoned that a real fluid with viscosity could cause losses at the chamber walls which in effect reduce the apparent radius ratio.

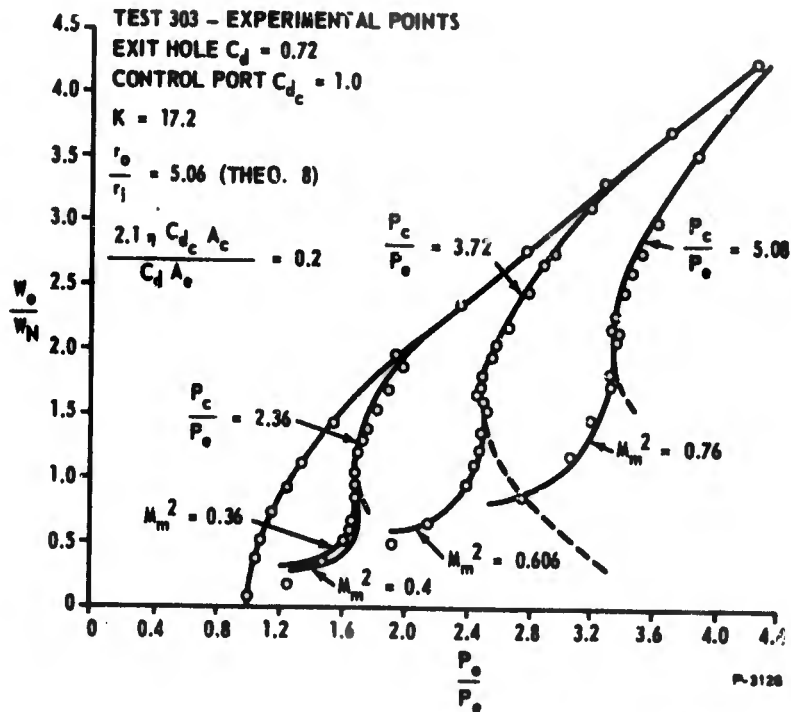


Figure B-12 - Theoretical-Experimental Correlation P_o/P_e

As a specific example, where M_m is assumed very large, the theoretical characteristic curve for $P_c/P_e = 3.72$ is shown in Figure B-12. The dashed portion indicates the solution if no maximum tangential velocity is reached. Here then, is theoretical behavior indicating the existence of a negative resistance characteristic. The pressure ratio P_o/P_i is strongly exponentially increasing with M_{t0}^2 and if no limit is reached on tangential velocity in the chamber, the centrifugal pressure buildup can increase so rapidly that P_o/P_e must be increased at lower flows to maintain the flow. Since only the slightest negative resistance is indicated by the particular experiment used, M_m must be nearly equal to $(r_o/r_i) M_{t0}$ taken at the point of curve verticality, $P_o/P_e \approx 2.47$. The value of M_m^2 determined in this manner was approximately 0.6. Since a slight negative resistance is involved a value of $M_m^2 = 0.606$ gave the best correlation. Using the same reduced, r_o/r_i , ($r_o/r_i = 5.06$), the other theoretical curves for $P_c/P_e = 2.36$ and 5.08 were constructed. Surprisingly, the fit was good indicating that whatever the loss mechanism is that effectively reduces r_o/r_i , it seems to hold for the range of pressure ratios, P_o/P_e , studied. Again, to get correlation at the low flows it was necessary to find the proper values of M_m . The interesting aspect of the theoretical model selected is that M_m seems to remain virtually constant for a given P_c/P_e but must be increased with increasing P_c/P_e as shown in Figure B-13. At this time

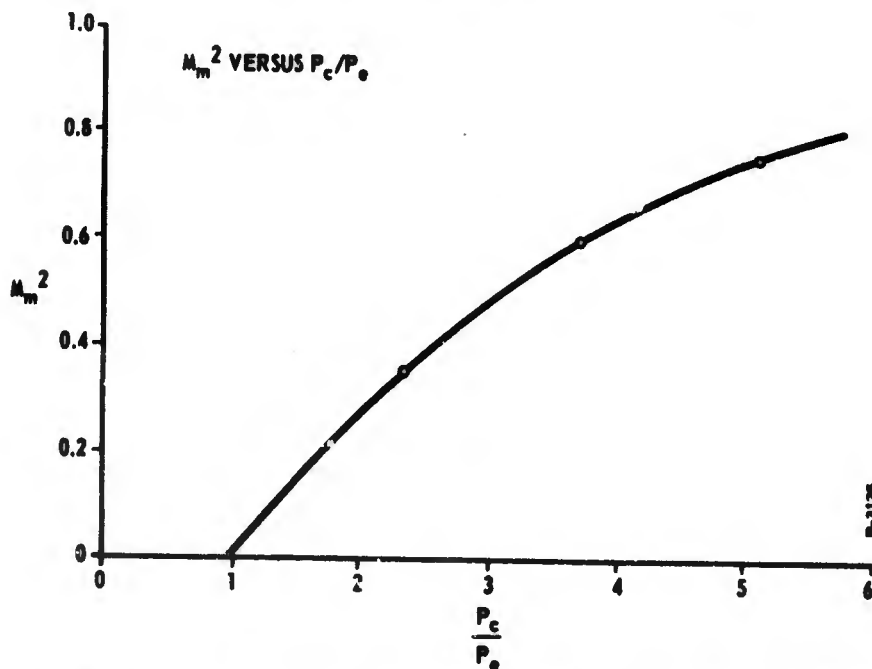


Figure B-13 - Maximum Tangential Mach Number Versus P_c/P_e

Bondin

it must be concluded that the velocity profile selected (see Figure B-9), has caused this empirical relationship between M_m and P_c/P_e and that some profile other than solid body rotation from the radius at which a maximum Mach number occurs could change this empirical relationship. However, the theoretical model may become more complex and less amenable to hand analysis should other profiles be used.

It is interesting to note the effect of increasing the maximum tangential Mach number. For the case of $P_c/P_e = 2.36$, M_m^2 was increased from 0.36 to 0.4 and the results are plotted in Figure B-12. As can be seen, a higher M_m causes more negative resistance and produces a better turndown ratio. The higher M_m , implies a chamber with less loss, and therefore better gain, turndown ratio, and negative resistance should result. If the losses are less, then the effective r_o/r_i should increase slightly, which will swing the upper portion of the weight flow curve (that portion above the point of verticality) to the left, thus further augmenting the negative resistance.

For the portion of the flow curves above the upper point of verticality, equations (B-8), (B-24), and (B-26) are again linearized to yield the following gain expressions:

$$\frac{\partial P_i}{\partial P_o} = \frac{\frac{P_{io}}{P_{oo}} + 2 K M_{to}^2 \left[\frac{P_{io}}{P_e} \right]}{1 - \frac{K M_{too}^2 \left[\frac{P_{io}}{P_e} \right]}{\frac{P_{io}}{P_e} - 1}} \quad (B-31)$$

$$\frac{\partial P_i}{\partial P_c} = \frac{-2 K M_{too}^2 \left[\frac{P_{io}}{P_e} \right] / \left[\frac{P_{co}}{P_e} - \frac{P_{oo}}{P_e} \right]}{1 - \frac{K M_{too}^2 \left[\frac{P_{io}}{P_e} \right]}{\frac{P_{io}}{P_e} - 1}} \quad (B-32)$$

$$\frac{\partial \left[\frac{W_o}{W_{oo}} \right]}{\partial \left[\frac{F_c}{P_e} \right]} = \frac{-1}{\left[\frac{P_{co}}{P_e} - \frac{P_{oo}}{P_e} \right]} \left[\frac{K M_{too}^2 \left[\frac{P_{io}}{P_{io} - P_e} \right]}{1 - \frac{K M_{too}^2 P_{io}}{P_{io} - P_e}} \right] \quad (B-33)$$

To find the flow gain $\partial W_o / \partial W_c$,

$$\frac{W_c}{W_N} = \frac{2 C_{dc} A_e P_o}{C_d A_e P_e} \sqrt{\frac{P_c}{P_o} - 1}$$

$$\frac{\partial \left[\frac{W_c}{W_{co}} \right]}{\partial \left[\frac{P_c}{P_e} \right]} = \frac{1}{2 \left[\frac{P_c}{P_e} - \frac{P_{oo}}{P_e} \right]} \quad (B-34)$$

$$\frac{\partial \left[\frac{W_o}{W_{oo}} \right]}{\partial \left[\frac{W_c}{W_{co}} \right]} = \frac{-2 K M_{too}^2 \left[\frac{P_{io}}{P_{io} - P_e} \right]}{1 - \frac{K M_{too}^2 P_{io}}{P_{io} - P_e}} \quad (B-35)$$

It is, of course, interesting to note the denominator in each gain expression. When $K M_{too}^2 P_{io} / (P_{io} - P_e)$ equals unity, all gains are infinite which indicates, of course, that the quiescent operating point is at the point of verticality on the characteristic curve. The denominator can be thought of as a regenerative effect which becomes more dominant as M_{to} or bias control is increased.

Bendix

B-4 NOMENCLATURE FOR APPENDIX B

- A_c = control jet area - in²
- A_e = exit hole area - in²
- C = gas constant - °R^{1/2}/sec
- C_d = exit hole discharge coefficient
- C_{dc} = control jet discharge coefficient
- K = vortex sensitivity constant
- K_T = vortex chamber turndown ratio
- M_c = control jet Mach number
- M_m = maximum tangential velocity Mach number
- M_t = tangential Mach number of flow field
- M_{to} = outer wall Mach number
- P_c = control jet pressure - psia
- P_d = pressure downstream of an orifice - psia
- P_e = back pressure on vortex chamber - psia
- P_i = vortex static pressure at radius r_i - psia
- P_o = vortex chamber - outer wall pressure - psia
- P_s = supply pressure - psia
- P_u = pressure upstream of an orifice - psia
- R = gas constant - in.-lbf/lbm - °R
- T = gas temperature - °R

V_c = control jet velocity entering chamber - in/sec
 V_s = sonic velocity of gas at temperature, T - in/sec
 V_t = tangential velocity of vortex flow field at radius r - in/sec

V_{to} = outer wall tangential velocity of vortex flow field - in/sec

W_c = control flow to vortex chamber - lbm/sec

W_N = normalizing weight flow

W_o = total flow leaving vortex chamber - lbm/sec

W_s = supply flow to vortex chamber - lbm/sec

$f_1 \left(\frac{P_d}{P_u} \right)$ = see Figure B-10

$f_3 \left(\frac{P_o}{P_c} \right)$ = see Figure B-11

g = local acceleration of gravity - in/sec²

k = ratio of gas specific heats

l = chamber thickness or length - in.

n = vortex tangential velocity characteristic exponent

r = vortex chamber radius - in

r_o = vortex chamber outer radius - in.

r_m = radius at which M_m occurs - in.

η = momentum mixing efficiency

ρ = fluid density - lbm/in³

Note: Additional subscript zeros indicate quiescent value of variables.

Bendix

APPENDIX C
BREADBOARD COMPONENTS

The following breadboard components have been designed for "building block" assembly to provide flexibility in the investigation of alternative circuit concepts.

<u>Quantity</u>	<u>Component Designation</u>	<u>BRLD Drawing No(s).</u>
8	MB1-6, Manifold Blocks	2157627; 2157664 2157626; 2157663 2157670; 2157672
1	Cover, MB1	2157652
2	Injector Plate (0.625 Dia.)	2157625
3	Injector Plate (1.0 Dia.)	2157624
5	Injector Manifold	2157620
5	Injector Cover	2157619
5	Button	2157621-1,2; 2157687
5	Receiver	2157623-1,2
2	Receiver, long	2157654-1,2
2	Pick-off	2157653-1,2
1	Space (blank)	2157675
1	Cover	2157673
2	Plate, nut	2157721
5	Sleeve	2157674
6	Orifice, supply	2157677
10	Housing, needle valve	2157622

The vortex valves are assembled by sandwiching a button, injector manifold, injector plate, injector cover, and receiver between

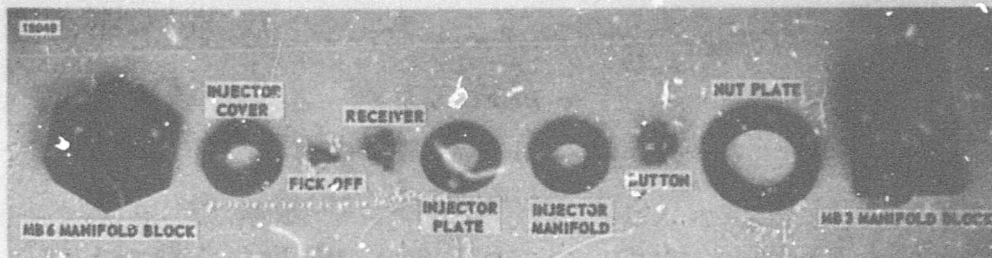


Figure C-1 - Typical Vortex Valve Components

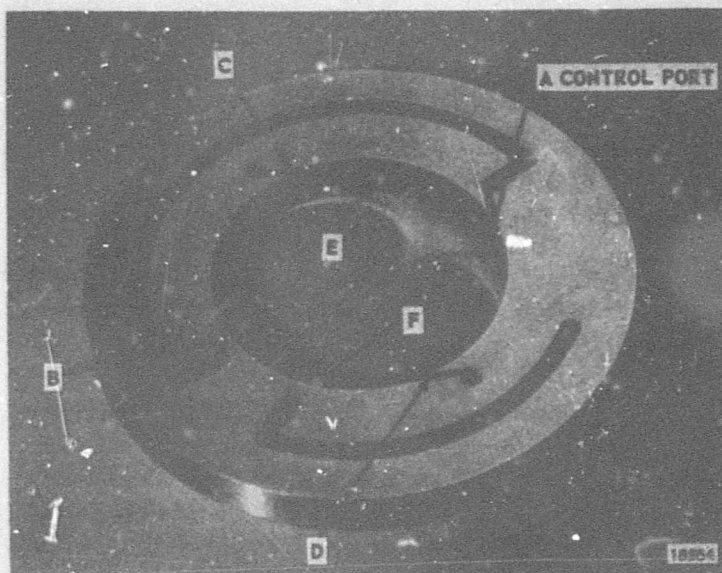


Figure C-2 - Control Injector Plate

manifold blocks (Figure C-1). These components can be replaced or modified individually.

The injector plate design is shown in the close-up Figure C-2. When placed between the injector manifold and injector cover and over the button, the injector plate forms the outside wall of the vortex chamber. Control ports A and B are common as are control ports C and D. Control ports A, B, C, and D are on one side of the injector plate and are additive in the sense that they induce control swirl in the vortex chamber in the same direction. Control ports E and F (F is not visible in Figure 3) are located on the opposite side of the injector plate; they are common and induce swirl in opposition to control ports

A, B, C, and D. By choice of angular location of the injector plate, the vortex valve may be assembled with two sets of control ports that induce swirl in either the same or opposite directions. A thin (approximately 0.005 inch) teflon gasket bonded to the injector manifold and injector cover seals the communicating passage between control ports.

The vortex valves may be close coupled for either pilot cascade operation or cascade connections with external control. An assembly of three vortex valves in Figure C-3 illustrates this capability.

Components of a confined-jet amplifier are shown in Figure C-4. The positions of the body and cover are interchanged in this photograph.

Bendix

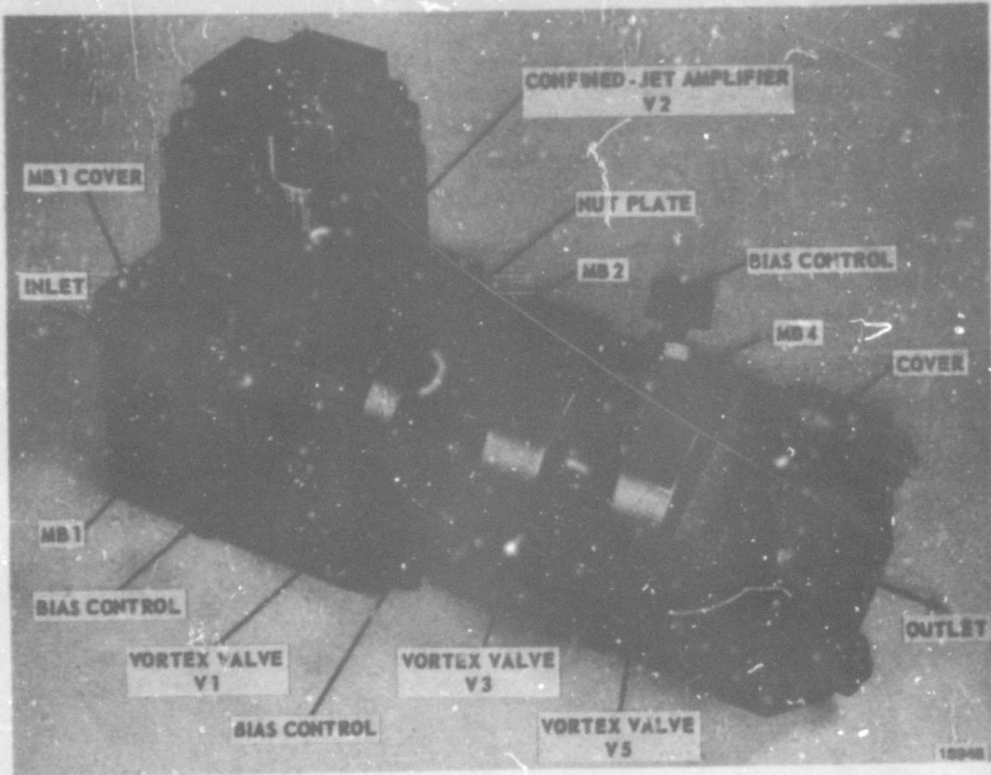


Figure C-3 - Throttling Circuit Assembly

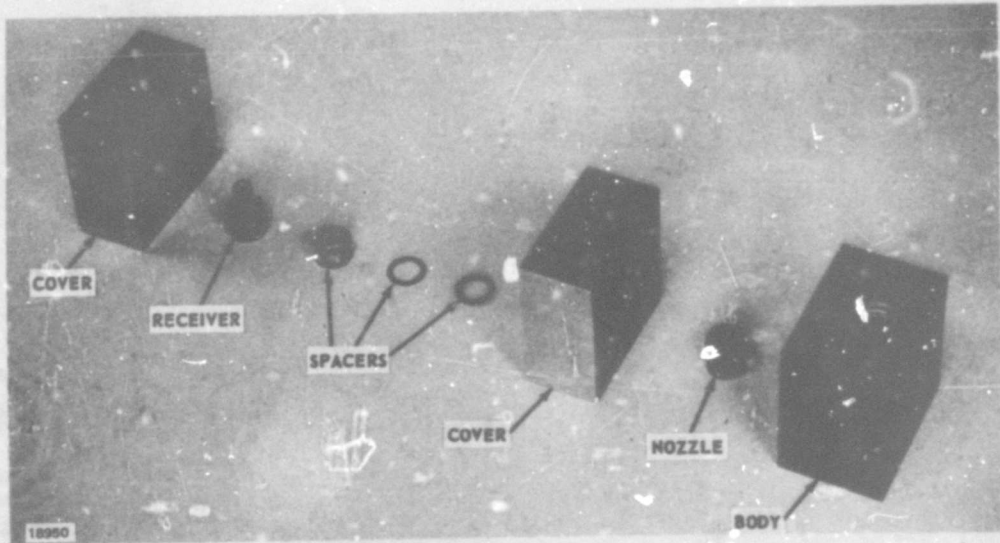


Figure C-4 - Confined-Jet Amplifier Components

APPENDIX D

FLOW CHARACTERISTICS OF n ORIFICES IN SERIES

D.1 ANALYTICAL BASIS

Consider n orifices in series as indicated in Figure D-1. Here the orifices are counted from the upstream side so that the n th orifice is at the outlet. The inlet pressure may be denoted P_0 ; the outlet pressure of the first orifice, P_1 ; and so on to the outlet pressure of the downstream orifice, which is denoted P_n . The "P's" are all measured in absolute units so that the pressure ratio across the overall array of orifices is P_n/P_0 .

For the unchoked condition, the flow of an ideal gas through a single orifice is given by:

$$\dot{w} = C_d A \sqrt{\frac{2gk}{R(k-1)}} \frac{P_u}{\sqrt{T}} \left(\frac{P_d}{P_u}\right)^{1/k} \sqrt{1 - \left(\frac{P_d}{P_u}\right)^{(k-1)/k}} \quad (D-1)$$

Given a series of orifices, the weight flow of gas through any orifice must be equal to the weight flow through any other orifice. For a given orifice we can write from equation (D-1) where $2 \leq j \leq n$.

$$\dot{w}_{j-1} = C_d A_{j-1} \sqrt{\frac{2gk}{R(k-1)}} \frac{P_{j-2}}{\sqrt{T}} \left(\frac{P_{j-1}}{P_{j-2}}\right)^{1/k} \sqrt{1 - \left(\frac{P_{j-1}}{P_{j-2}}\right)^{(k-1)/k}} \quad (D-2)$$

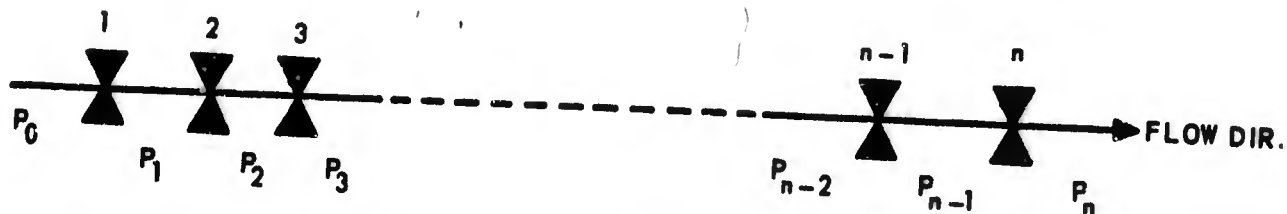


Figure D-1-Orifice and Pressure Notation

For the next orifice:

$$\dot{w}_j = C_d A_j \sqrt{\frac{2gk}{R(k-1)}} \frac{P_{j-1}}{\sqrt{T}} \left(\frac{P_j}{P_{j-1}}\right)^{1/k} \sqrt{1 - \left(\frac{P_j}{P_{j-1}}\right)^{(k-1)/k}} \quad (D-3)$$

Since $\dot{w}_{j-1} = \dot{w}_j$, we can combine equations (D-2) and (D-3) to obtain:

$$\left(\frac{A_{j-1}}{A_j}\right) \left(\frac{P_{j-2}}{P_{j-1}}\right) \left(\frac{P_{j-1}}{P_{j-2}}\right)^{1/k} \sqrt{1 - \left(\frac{P_{j-1}}{P_{j-2}}\right)^{(k-1)/k}} = \left(\frac{P_j}{P_{j-1}}\right)^{1/k} \sqrt{1 - \left(\frac{P_j}{P_{j-1}}\right)^{(k-1)/k}} \quad (D-4)$$

Equation (D-4) shows that for fixed areas, defining the pressure ratio across either orifice defines the pressure ratio across the other. This may be generalized to the statement that defining the pressure ratio across any orifice defines the pressure ratio across any adjacent orifice. The corollary conclusion is that setting the pressure across any single orifice in the series defines the pressure ratio across every other orifice in the series and since:

$$\frac{P_n}{P_o} = \left(\frac{P_n}{P_{n-1}}\right) \left(\frac{P_{n-1}}{P_{n-2}}\right) \dots \left(\frac{P_3}{P_2}\right) \left(\frac{P_2}{P_1}\right) \left(\frac{P_1}{P_o}\right) \quad (D-5)$$

the overall pressure ratio is also defined.

The effective area of a series of n orifices may be defined as:

$$A_{ni} = \frac{\dot{w}}{C_d \sqrt{\frac{2gk}{R(k-1)}} \frac{P_o}{\sqrt{T}} \left(\frac{P_n}{P_o}\right)^{1/k} \sqrt{1 - \left(\frac{P_n}{P_o}\right)^{(k-1)/k}}} \quad (D-6)$$

with the restriction that

$$\left(\frac{P_n}{P_o}\right)^{1/k} \sqrt{1 - \left(\frac{P_n}{P_o}\right)^{(k-1)/k}} = 0.2588 \text{ for } \frac{P_n}{P_o} < 0.528 \text{ and } k = 1.4$$

The area of the first orifice is given by:

$$A_1 = \frac{\dot{w}}{C_d \sqrt{\frac{2gk}{R(k-1)}} \frac{P_o}{\sqrt{T}} \left(\frac{P_1}{P_o}\right)^{1/k} \sqrt{1 - \left(\frac{P_1}{P_o}\right)^{(k-1)/k}}} \quad (D-7)$$

We can divide equation (D-6) by (D-7) to obtain:

$$\frac{A_m}{A_1} = \frac{\left(\frac{P_1}{P_o}\right)^{1/k} \sqrt{1 - \left(\frac{P_1}{P_o}\right)^{(k-1)/k}}}{\left(\frac{P_n}{P_o}\right)^{1/k} \sqrt{1 - \left(\frac{P_n}{P_o}\right)^{(k-1)/k}}} \quad (D-8)$$

D.2 RESULTS

Equations (D-4), (D-5), and (D-8) have been used to calculate the significant pressure flow characteristics of n orifices in series. Since the equations are not suited for hand computation, the calculations were performed using a digital computer.

In many of the applications involving the use of a series of orifices, the primary interest is in obtaining the maximum change in effective area as pressure ratio changes. Therefore the first set of computations was used to determine the distribution of individual orifice areas in a series string which gives the greatest change in ratio A_m/A_1 as P_n/P_o changes. For this set of computations $n = 5$ and A_5/A_1 ranged from 0.1 to 10 with areas A_2 , A_3 , and A_4 varying in both arithmetic and geometric progressions.

The results of the first set of calculations shows that the greatest change in the ratio A_m/A_1 for a given change in P_n/P_o occurs when all orifices in the series have the same area. All other calculations were performed in this case.

Examination of equation (D-4) shows that for the case in which adjacent orifice areas are equal, the downstream orifice will have the pressure ratio closest to the critical value. Thus as the overall pressure ratio P_n/P_o is decreased, the first orifice to choke will be the downstream orifice. Once the downstream orifice has choked, its effective pressure ratio will remain fixed at the critical value as the ratio P_n/P_o decreases further. Since fixing one pressure ratio fixes all others in the series string, the pressure ratios across all orifices in the string are invariant once the downstream orifice has choked and the weight flow of gas is a function of the upstream conditions only.

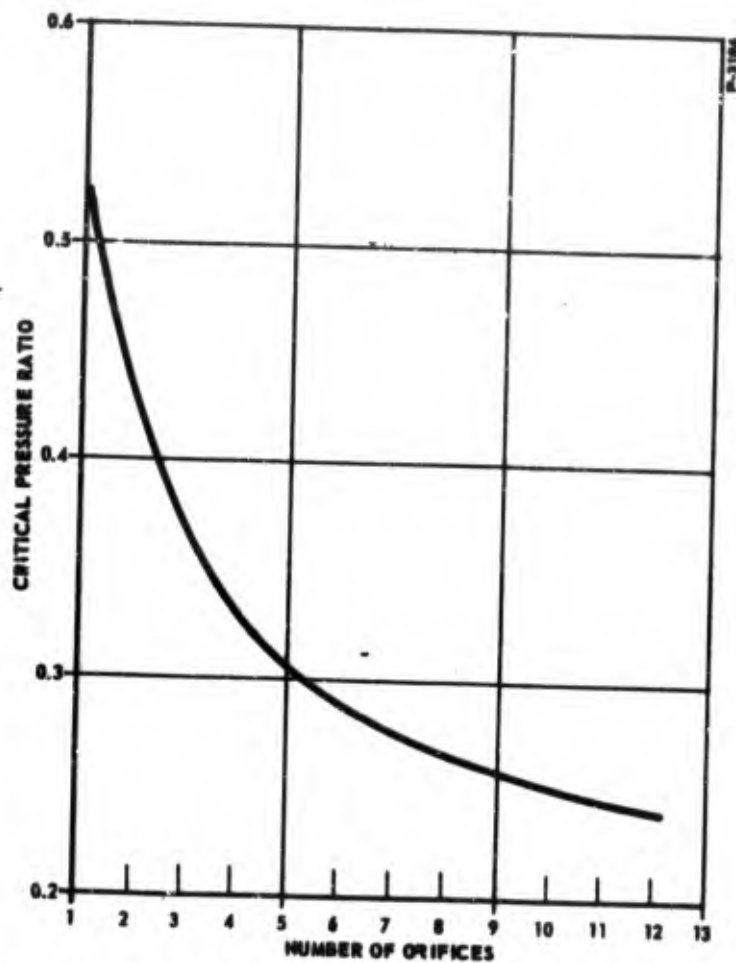


Figure D-2 - Critical Pressure Ratio for Equal Orifices in Series as a Function of the Number of Orifices $k = 1.4$

Since the overall pressure ratio across a string of orifices is always smaller than the pressure ratio across any individual orifice, the critical pressure ratio of a series of orifices is less than that of a single orifice. This is a highly useful property. Figure D-2 shows the critical pressure ratio as a function of the number of orifices for a diatomic gas ($k=1.4$). This has been plotted from a curve given in the reference.

The flow through a series of equal orifices may be computed by means of an effective area which is a function of the pressure ratio. Table D-1 gives the values of the effective areas for values of $n = 2, 5,$ and 10 at pressure ratios with increments of 0.05 . The table has been computed from the simultaneous solution of the system of equations (D-4), (D-5) and (D-8).

The nondimensional effective areas given in the table may be used to compute the flow of a diatomic gas through a series string of equal area orifices by means of the following equation:

$$\dot{w} = C_d A_1 \left(\frac{A_m}{A_1} \right) \sqrt{\frac{2 g k}{R(k-1)}} \left(\frac{P_o}{\sqrt{T}} \right) \left(\frac{P_n}{P_o} \right)^{1/k} \sqrt{1 - \left(\frac{P_n}{P_o} \right)^{(k-1)/k}} \quad (D-9)$$

Table D-1 - Nondimensional Effective Areas of Equal Orifices in Series for Various Pressure Ratios

Press Ratio	Number of Orifices		
	2	5	10
0.95	0.7124	0.4526	0.3205
0.90	0.7183	0.4585	0.3252
0.85	0.7249	0.4651	0.3304
0.80	0.7322	0.4724	0.3363
0.75	0.7404	0.4807	0.3428
0.70	0.7497	0.4900	0.3502
0.65	0.7601	0.5006	0.3586
0.60	0.7720	0.5128	0.3682
0.55	0.7854	0.5269	0.3794
0.50	0.7991	0.5425	0.3918
0.45	0.8064	0.5553	0.4026
0.40	---	0.5651	0.4119
0.35	---	0.5715	0.4189
0.30	---	---	0.4243

Bender

where values of A_m/A_1 for a given pressure ratio are obtained from Table D-1 and using

$$\left(\frac{P_n}{P_o}\right)^{1/k} \sqrt{1 - \left(\frac{P_n}{P_o}\right)^{(k-1)/k}} = 0.2588 \text{ for } \frac{P_n}{P_o} < 0.528$$

REFERENCE

Robinson, C. S. L., "Flow of a Compressible Fluid through a Series of Identical Orifices," Journal of Applied Mechanics Vol. 15 n 4 December 1948 pp. 308-10.